Factors influencing plastic settlement cracks in concrete and the corresponding influence on concrete durability.

By:

Gabriel Brits

Thesis presented in fulfilment of the requirements for the degree of Master of Engineering in Civil Engineering in the Faculty of Engineering at Stellenbosch University

Supervisor: Dr. Riaan Combrinck

March 2021

Declaration

By submitting this thesis electronically, I declare that the entirety of the work contained therein is my own, original work, that I am the sole author thereof (save to the extent explicitly otherwise stated), that reproduction and publication thereof by Stellenbosch University will not infringe any third-party rights and that I have not previously in its entirety or in part submitted it for obtaining any qualification.

March 2021

Abstract

Plastic settlement cracking occurs as a result of differential settlement during the plastic state of concrete. Differential settlement is always caused by a restraining factor, such as steel reinforcement or a varying concrete section depth. Concrete settles due to the influence of gravitational forces. Since plastic settlement cracks occur at the object of restraint, and form from the bottom upwards, it may not be visible at the surface of the concrete, even though they are present below the concrete surface. This has resulted in plastic settlement cracking being overlooked as the source or start of durability related issues.

Any form of cracking is likely to increase the permeability of the concrete, or act as a weak point that allow other, more severe cracks to form. These cracks permit the ingress of aggressive agents that accelerate the deterioration of the concrete structure. Steel reinforced concrete durability is mostly affected by the corrosion of its steel reinforcement; therefore, the quality of the concrete plays a large role in its durability. If the concrete is very permeable and of low quality, it would provide easy access for aggressive agents to the steel reinforcement which may compromise the structural integrity of the structure.

This study investigates the behaviour of plastic settlement cracking in concrete and the factors influencing it, namely cover depth, re-vibration, viscosity, and plastic shrinkage cracking. Practical measures were developed to study this behaviour more closely and durability index tests were performed on the concrete. The crack severity of the plastic settlement cracks was also investigated. All these results were compared to determine the influence of these cracks on the durability of the concrete, depending on the factor being tested. CT scans were also taken to get a visual representation of the cracks present in the concrete.

The results show that a smaller concrete cover result in more severe plastic settlement cracking. It also indicated that higher strength concrete typically has less severe plastic settlement cracks. Re-vibration or a lower plastic viscosity does not necessarily decrease the severity of plastic settlement cracks, but it does improve the concrete permeability. Plastic shrinkage cracks are likely to amplify the plastic settlement cracks and make it more severe. It was concluded that plastic settlement crack severity does not directly influence the durability parameters of the concrete. The main durability parameters considered for this study was the permeability, sorptivity, porosity and crack severity of the concrete. These factors interacted inconsistently, and it was therefore determined that more durability tests are needed to draw final conclusions.

Other aspects also need further investigation, such as the influence of high strength concrete, the influence of higher plastic viscosity, the effect of a different method of re-vibration, and the influence of plastic settlement cracks induced by a varying concrete section depth.

Acknowledgements

I would first like to thank my Thesis supervisor, Dr. Riaan Combrinck from the Civil Engineering department of Stellenbosch University. He is an excellent mentor and he continually guided me in the right direction throughout the duration of the project, but also allowed this project to be my own work.

I would also like to thank everyone from the structure's laboratory, in the Civil Engineering department of Stellenbosch University. I spent a lot of time in the laboratory and they were always willing to help whenever I ran into a problem or needed a helping hand.

Finally, I would like to thank my parents who provided me with unfailing support throughout my six years of studying. And for the amount of time, effort and sacrifice they gave to provide me with the opportunity to complete my degree. I would not have been able to do this without them.

Table of Contents

Table of figures

Table of tables

List of Symbols

ER	Evaporation rate [kg/m^2/h]
η_{pl}	plastic viscosity
p	Capillary pressure value
r	Relative humidity percentage
R_1	minimum radius of water surface curvature
R_2	maximum radius of water surface curvature
T_a	Air temperature [^{o}C]
T_c	Concrete temperature [^{o}C]
τ	shear stress
τ_0	yield stress
V	Wind velocity
$\dot{y}$	shear rate
γ	surface tension of the pore liquid

1 Introduction

1.1 Background

After water, concrete is the second-most consumed material in the world. Around three tonnes per year is used for every person on earth. It is used more than any other engineering or construction material, including steel and timber (Gagg, 2014).

Plastic settlement cracking in concrete occurs as a result of differential concrete settlement during the plastic state. The plastic state of concrete is typically the first 3 – 8 hours after being cast (Kayondo, Combrinck and Boshoff, 2019). Differential settlement is caused by an object of restraint, such as steel reinforcement or varying section depth. As the concrete settles the restraining factor prevents settlement in one area of the concrete compared to another. This causes the development of tensile stresses. If the tensile stresses are larger than the attraction forces between the concrete particles, cracks are likely to form (Slowik, Schmidt and Fritzsch, 2008).

Factors that may influence plastic settlement cracking are the depth of the concrete section, cover depth of the steel reinforcement, fines content in the concrete, w/c ratio, aggregate size and distribution, and capillary pressure. Any factor that increases the amount and degree of concrete settlement is likely to increase the risk of plastic settlement cracking (Kayondo, Combrinck and Boshoff, 2019).

Plastic settlement cracking is often unavoidable, but there are methods to reduce the likelihood and severity of these cracks. Re-vibration of concrete is a method used to salvage the concrete from already formed plastic settlement cracks (Permana *et al.*, 2017). Any method that reduces the amount and degree of settlement is also likely to reduce the risk of plastic settlement cracking.

Plastic shrinkage cracking is another important cracking behaviour that occurs during the plastic state. It occurs due to the evaporation of the bleed water on the surface of the concrete. If the evaporation rate of the bleed water is higher than the bleed rate, cracks are likely to form. Plastic shrinkage cracks are usually visible at the concrete surface and allows corroding agents to penetrate the concrete, which can accelerate the corrosion of the steel reinforcement (Wittmann, 1976), (Kayondo, Combrinck and Boshoff, 2019). According to Ghourchian *et al.*, (2019) around 80% of cracks that occur in concrete during its early age, is as a result of plastic shrinkage.

The durability of concrete is the most affected by the corrosion of the steel reinforcement. Therefore, the quality of the cover concrete plays a large role in the durability. If the concrete cover has a high permeability, corrosive agents can easily reach the steel reinforcement and cause corrosion. The corrosion of the steel will lead to a lower structural integrity and cause the deterioration of the concrete structure. Therefore, permeability along with concrete strength are key factors to consider when determining the durability of concrete (Mackechnie and Alexander, 2002).

1.2 Problem statement

Plastic settlement cracking occurs at the object of restraint, therefore, the cracks form from the bottom upward and may not be visible at the surface of the concrete, often causing their presence to be overlooked.

Any form of crack is likely to increase the permeability of the concrete, allowing the ingress of aggressive agents, accelerating the deterioration of the concrete structure. Plastic shrinkage cracks are known to have a negative influence on the long-term durability of the concrete, however, the effect of plastic settlement cracks on the concrete durability is still somewhat unfamiliar. Therefore, this study sets out to determine how plastic settlement cracks influences the durability of the concrete.

1.3 Objectives

The objectives of this study are as follows:

- To provide a fundamental understanding of the behaviour of plastic settlement cracking.
- To determine the influence of different factors, namely reinforcement cover depth, concrete strength and viscosity, re-vibration of concrete, and plastic shrinkage cracking on the formation and severity of plastic settlement cracking.
- To relate how the severity of plastic settlement cracking and each specific factor influences the durability of the concrete.

1.4 Methodology

The approach followed to achieve the objectives of this study was in the form of practical experiments where concrete beams were placed under the conditions necessary to induce plastic settlement cracking or any other phenomenon necessary. Various physical tests were conducted to determine the crack severity caused by the settlement cracks, as well as the possible influence on durability. Each of these experiments isolated and focused on a different aspect of settlement cracking.

1.5 Significance

The motivation behind the study is to compliment research in the field of plastic settlement cracking in concrete. The problem with plastic settlement cracking is they are mostly not visible and primarily occur under the surface of the concrete at the object of restrain. Even when concrete is cut and examined at the restraint, plastic settlement cracks are barely visible.

However, plastic settlement cracks can act as a weak point for the formation of more severe types of cracks, such as plastic shrinkage cracks, or cracks that form during the hardened state of concrete. Therefore, these cracks are assumed to influence the concrete durability in some way, and it is possible that the influence is larger than expected.

The significance of this study is to determine the severity of plastic settlement cracks and its impact on concrete durability. This is an important subject to consider, because if these cracks are determined to have a major impact on concrete durability, this study would shed light on this and motivate further research on this topic.

1.6 Report layout

This thesis consists of the following chapters:

- *Chapter 1*: The introduction, which gives a brief discussion of the topic and the objectives of the study.
- *Chapter 2*: A literature study discussing the research available on the topic to provide the necessary insights and background on plastic settlement cracking and its influence on concrete durability, and where further research is needed.
- *Chapter 3*: The experimental framework which describes the physical experiments and processes undertaken to achieve the said objectives of the study.
- *Chapter 4*: The results and discussion of the experimental process conducted and explained in Chapter 3.
- *Chapter 5*: Conclusion of the results achieved through the experimental process and recommendations of areas where further study is needed.

2 Literature study

2.1 Concrete

Concrete is a mixture between aggregates (sand, gravel or crushed stone) and paste (water and cement). The water and cement combination hardens and bind the aggregates into a rocklike mass, through the process of hydration. This process will continue with time, causing concrete to get stronger as it gets older (Gagg, 2014).

Concrete is made up of binder, water, coarse and fine aggregates, whereas reinforced concrete is typically a combination of concrete and steel rebar, however, other forms of reinforcement can also be used, such as glass or steel fibres, pre- or post-tensioning, PC strand etc. Concrete has a very high resistance to compression, but moderate tensile forces will cause it to crack. Without the steel rebar, concrete will act as a relatively brittle material. The steel rebar acts as a resistance to the tensile stresses concrete may experience. This combination allows the concrete to have the tensile strength of steel, as well as the compressive strength of the concrete, which creates a durable and inexpensive structural material that is capable of withstanding bending, tensile and shear loading (Gagg, 2014).

Concrete is so widely used around the world because of the various advantages associated with it. It is mouldable into any shape, varying from simple beams or slabs, to more advanced architectural features, such as domes or shells. This is possible due to the workable state of concrete before it hardens. The materials used to create concrete, such as sand, gravel/stone, and water, are widely available and relatively inexpensive. Binder and reinforcing steel, only make up about 20% and 2-4% of the weight and volume of concrete, respectively (Narayanan, 2013).

There are some disadvantages to concrete. As mentioned, concrete needs steel to resist tensile stresses. If not constructed and cured properly, cracks may occur in the concrete, which could lead to the corrosion of the steel reinforcement and lower the tensile capacity of the concrete structure. Construction of cast in situ concrete also requires formwork, which must be constructed before and removed after the concrete is cast. This is not needed with the construction of steel structures (Narayanan, 2013).

However, the most negatively associated aspect of concrete is the CO_2 emissions associated with the manufacturing of cement. Cement is produced by heating limestone and other ingredients to about 1480^{o}C by burning fossil fuels. This phenomenon accounts for 5-7% of the global CO_2 emissions. Approximately one ton of CO_2 is produced with the production of one ton of cement. Other materials such as fly ash can be used with cement which will reduce the CO_2 emissions and also improve some properties, such as reduction in heat of hydration, enhancement of strength and/or workability and the durability of the concrete (Narayanan, 2013).

Concrete goes through three different states during its lifetime: the plastic state, setting state and the hardening state. In this chapter only the plastic state is discussed in further detail. The first 3-8 hours after concrete is cast is generally known as the 'plastic state'. This is when the concrete has not yet hardened and is still relatively mouldable. However, during this state, concrete bleeding and segregation may occur, which may cause several problems with regards to the concrete aesthetics, durability, and other properties (Barlow *et al.*, 1998).

Cracking in concrete does not generally result in the failure of a concrete structure, but it can cause accelerated deterioration to occur. The significance of a crack depends on the type of structure and the nature of the crack. There are many different types of cracks that can form in a concrete structure during its lifetime. Most cracks typically occur in one of two states. Cracking during the plastic state, namely plastic shrinkage and -settlement cracking, and cracking during the hardened state, caused by drying shrinkage, thermal stresses, chemical reactions, weathering, corrosion of reinforcement, poor construction practices, construction overloads and error in design and detailing (Barlow *et al.*, 1998).

2.1.1 Cracking during the plastic state

Cracking during the plastic state, especially plastic settlement cracking, is the focus of this research study, thus it is also discussed in further detail later in Section 2.2.

2.1.1.1 Plastic shrinkage cracking

Plastic shrinkage cracking might occur when concrete is exposed to conditions that cause a rapid loss of moisture on the concrete surface. This can be caused by a combination of factors, such as air temperature, wind speed and relative humidity. When the evaporation rate of the surface/bleed water is higher than the bleed rate of the freshly placed concrete, it causes the concrete to shrink. The concrete below the drying surface, steel rebar and formwork shape provide a restraint that causes tensile stresses to develop in the stiffening plastic concrete. This results in cracks that appear on the surface, usually with varying depths (Barlow *et al.*, 1998).

2.1.1.2 Plastic settlement cracking

After the placement of concrete, it continues to settle and consolidate vertically, due to gravitational forces. If any form of restraint, such as reinforcing steel, formwork, or older placed concrete, are present it will cause differential settlement to occur which may induce voids and cracks. Typically, the degree of plastic settlement cracking depends on the size of the reinforcing bar, cover depth of the reinforcement and the slump of the mix (Barlow *et al.*, 1998).

2.1.2 Cracking during the hardened state

2.1.2.1 Drying shrinkage cracking

Drying shrinkage occurs when hardened concrete contracts/shrinks, due to a loss of capillary water. If this shrinkage is restrained in any way tensile stresses develops in the concrete. If the tensile stresses

exceed the tensile forces between the concrete particles, it will cause cracks to form. If drying shrinkage could take place without any form of restraint, cracks would not occur in the concrete, however, shrinkage combined with restraint is likely to induce cracks (Barlow *et al.*, 1998).

2.1.2.2 Thermal stresses cracking

Internal or external temperature differences in a concrete structure result in differential volume changes in the concrete. This happens because the cooler part of the concrete contracts more than the warmer parts, which will inevitably act as a restraint against the contraction. When the tensile stresses, induced by the differential volume changes, exceed the tensile capacity of the concrete, it will crack (Barlow *et al.*, 1998).

2.1.2.3 Chemical reactions cracking

Chemical reactions in concrete may cause cracks to form. When the aggregates react with the alkalis in the cement paste the alkali-silica reaction result in the formation of a swelling gel, which absorbs water from other areas of the concrete and causes an expansive chemical reaction. The expansion induced tensile stresses in the concrete which may lead to cracking (Barlow *et al.*, 1998).

2.1.2.4 Weathering cracking

Weathering can influence concrete and cause cracking. This includes processes such as wetting and drying, heating, and cooling, and freezing and thawing. The most common weathering occurrence that cause deterioration is freezing and thawing. With freezing and thawing, the water in the concrete paste or aggregate freeze when subjected to freezing temperatures, which cause it to expand. The stresses induced by the expansion may cause cracks to form. After the water unfreezes and cracks formed, it allows more water to enter the concrete through the cracks, which increases the potential damage of this effect (Barlow *et al.*, 1998).

2.1.2.5 Corrosion of reinforcement

The corrosion of steel reinforcement in concrete is an electrochemical reaction that requires an oxidizing agent, moisture, and electron flow within the metal. However, the corrosion of steel in concrete is not a very common occurrence, because of passive protection of the steel, which is a protective layer that forms around the steel in a tightly alkaline environment. The steel may corrode if carbonation reduced the alkalinity of the concrete, or if the passivity of the steel is destroyed by chlorides or other aggressive ions. If the steel corrodes it produces iron oxides and hydroxides, which has a much greater volume than the original metallic iron. This increase in volume results in radial cracks around the reinforcement (Barlow *et al.*, 1998).

2.1.3 Early age of concrete

The early age of concrete is generally known as the first 1 – 2 days after concrete was cast, however, there is no exact time duration which signifies the early age of concrete. According to S.G. Bergstrom

of the Swedish Cement and Concrete Research Institute, the early age of concrete depends on the time it takes to achieve the property you are interested in, which means it all depends on how the concrete will be used (Mehta and Monteiro, 2006).

Early age covers a very insignificant amount of time during the total life span of concrete, but during this period numerous operations are performed, such as mixing, transport, placement, consolidation, finishing and curing of the concrete, which has a large influence on the behaviour of the concrete. Therefore, these operations should be performed with control to ensure the concrete is adequate for the intended purpose (Mehta and Monteiro, 2006).

Concrete has a relatively low strength at an early age; thus, any induced tensile stresses could cause cracks to form, be it microscopic or large. If the tensile stresses are larger than the internal tensile strength of the concrete, cracks are likely to form. The cracks that may form can have a large impact on the concrete at later stages in its life (Nehdi and Soliman, 2011).

There are different types of early age cracks in concrete, however, the grouping of the cracks may vary depending on the literature discussed. Some researchers group early age cracks according to the cause of the cracking, such as settlement cracks and drying shrinkage cracks, whereas others group the cracks according to the characteristics of the cracking, such as random, map, transverse, longitudinal, corner and re-entrant cracks (Safiuddin *et al.*, 2018).

There are many ways to compensate for the shrinkage of concrete, but it is nearly impossible to completely avoid concrete shrinkage. Depending on the driving forces behind the early age shrinkage behaviour, according to Nehdi and Soliman (2011) it is typically affected by one of the following:

a) The binder type, content, and rate of hydration.
b) The aggregate content.
c) The water contents.
d) Admixtures.
e) Pozzolanic materials.
f) Curing conditions.

The early age properties and behaviour of concrete has a large effect on the long-term performance thereof. The coupling between thermal characteristics, such as hydration, and mechanical characteristics, such as compressive strength, for early age concrete is more critical compared to that of mature concrete (Nehdi and Soliman, 2011).

2.1.4 Hydration

Hydration in concrete is the chemical reaction between Portland cement and water. As soon as the cement encounters water, a gel layer forms on the surface of the cement grains, which contains amounts of sulphate and calcium. About 30% of the cement reacts during the middle period of hydration, where

calcium silicate hydrate (C-S-H) and calcium hydroxide (C-H) forms and is accompanied by a significant development of heat. Cement hydration proceeds more rapidly with increasing temperature (Helmuth and Detwiler, 2006).

The heat of hydration plays a significant role during the early age of concrete. Hydration of cement is a highly exothermic reaction (Nehdi and Soliman, 2011). The heat generated by cement hydration is an important parameter for predicting the temperature development within a concrete member. At early age, the rate and total heat generated during hydration are influenced by the chemical composition and amount of the cement, the types of admixtures used, section thickness, as well as the ambient temperature.

Cements with high tricalcium silicate (C_3S) as well as tricalcium aluminate (C_3A) typically demonstrate high heat discharge, whereas a high dicalcium silicate (C_2S) and/or tetra-calcium aluminoferrite (C_4AF) content are considered low-heat cements (Nehdi and Soliman, 2011).

The hydration process is somewhat complex due to the collection of chemical processes each of which occurs at a rate that is determined both by the nature of the process and the state of the system (Bullard *et al.*, 2011).

2.1.4.1 Stiffening

Stiffening is the first state of hydration and occurs directly after the concrete is cast. It is the loss of consistency and slump of the concrete over time, resulting in the loss of workability and plasticity. Free water gives concrete its plasticity, however, it is gradually lost during the hydration process, because of the formation of hydration products, surface absorption by unsaturated aggregates and evaporation, which cause the paste to stiffen, set and harden (Mehta and Monteiro, 2006).

2.1.4.2 Solidification

Setting refers to the solidification of the plastic cement paste. The initial set marks the beginning of solidification and is the point in time where the cement paste becomes unworkable. Therefore, the placement, compaction and finishing operations of concrete is difficult from this state onwards. However, the solidification process happens over a period of time, and does not occur instantly. This period of time is known as the final set. At this time the concrete has solidified, but has not yet hardened, and only marks the beginning of the hydration of tricalcium silicate (C_3S) therefore, it has little to no strength (Mehta and Monteiro, 2006).

2.1.4.3 Hardening

After the start of the C_3S hydration process, the concrete starts to harden. This includes the progressive filling of void spaces in the cement paste, a decrease in the porosity and permeability of the concrete and finally an increase in the concrete strength over time (Mehta and Monteiro, 2006).

2.1.5 Curing

Curing of concrete is the process where an adequate amount of moisture and temperature is contained on the surface of concrete after being cast to prevent it from drying out too fast. It plays an important role in strength development and the durability of concrete (Zemajtis, 2019).

Proper curing of concrete after placement is a crucial step to prevent unnecessary cracks to occur, such as plastic shrinkage cracks. It is necessary during the early age of concrete to maintain acceptable moisture content and temperature around the concrete to allow the desired properties to develop sufficiently (Nehdi and Soliman, 2011).

The aim of curing concrete is to eliminate or reduce the evaporation of surface water. This can be achieved by covering the concrete with a plastic sheet, spraying it with aliphatic alcohols or replacing the evaporated surface water by rewetting the surface. Rewetting reduces the evaporation rate through increasing the ambient relative humidity and also by replacing the lost water on the surface, due to evaporation (Sayahi, Hedlund and Emborg, 2016).

The application of curing methods is important since it allows the concrete to develop strength and reduce its porosity. A proper curing procedure will allow full hydration of the cement where many of the pores are filled in order to decrease the porosity. It also results in a reduction of the permeability and therefore increases the durability of the concrete (Gjørv, 2011). An adequate amount of moisture allows hydration to continue and strength to develop (Zemajtis, 2019).

2.1.6 Rheology

Rheology is the science of the deformation and the flow of matter. Typically, the attention paid to concrete during its plastic period is small, despite the large influence this state can have on the long-term durability of the concrete. Pumping, spreading, moulding and compaction of concrete all depend on the rheology (Banfill, 2006).

Rheology is the flow behaviour of concrete and can be described by the Bingham Model (Faleschini *et al.*, 2014); (Banfill, 2006); (Leemann and Winnefeld, 2007); (Kolawole, Combrinck and Boshoff, 2019). The flow of fresh concrete can be described by at least two parameters, namely yield stress and plastic viscosity. The Bingham model, Equation 2.1, is the most used out of the other models since the parameters can be measured independently and it predicts the flow of concrete accurately.

$$\tau = \tau_0 + \eta_{pl} \cdot \dot{y} \tag{2.1}$$

Where, τ is the shear stress, τ_0 is the yield stress, η_{pl} is the plastic viscosity and $\dot{y}$ is the shear rate. Typically, in Newtonian fluids, the shear stress and shear rate are directly proportional; however, a minimum stress – the yield stress – is needed for flow to initiate. The plastic viscosity is the constant slope of the shear stress vs. shear rate curve, above the yield stress (Leemann and Winnefeld, 2007).

Parameters often used to characterise concrete rheology are slump, static yield stress, dynamic yield stress and plastic viscosity. However, these parameters can be altered using rheology modifiers such as superplasticisers (SP), viscosity modifying agents (VMA) and the water content (Kolawole, Combrinck and Boshoff, 2019).

A study conducted by Leemann and Winnefeld, (2007) determined the effect of VMA on mortar and concrete. They tested different types of VMA's, namely inorganic VMA microsilica and nanosilica slurry and organic VMA were used, and also combined it with SP. They discovered that at a constant w/c ratio, the addition of VMA decreases the mortar flow, while the flow time is increased, causing an increase of yield stress and plastic viscosity. This same effect can also be achieved with a reduction in w/c ratio; however, the effect is much stronger with the addition of VMA.

In a study conducted by Kolawole, Combrinck and Boshoff, (2019) they used five different mixes, each with varying parameters to determine the effect of VMA on thixotropy. One of which contained VMA, one contained SP, one mix where SP and VMA were combined, one where the water content alone is increased and a control mix. Through conducting rheology tests, it was discovered that the plastic viscosity of concrete was increased but other rheological and thixotropic properties were not significantly impacted by the inclusion of VMA. Inclusion of SP alone, both SP and VMA, as well as increased water content influenced the thixotropy and rheology properties, by reducing them in a similar manner.

2.1.7 Setting time

The setting time of cement gives an indication of how long it remains workable when used in a concrete mix. It is known as the transition of concrete from a liquid phase to a solid phase. There are two main setting times that are considered, namely: initial setting time and final setting time. As mentioned in Section 2.1.4.2 the initial set marks the beginning of solidification and is the point in time where the cement paste becomes unworkable. Therefore, the placement, compaction and finishing operations of concrete is difficult from this state onwards. However, the solidification process happens over a period of time, and does not occur instantly. This period of time is known as the final set (Mehta and Monteiro, 2006). At final setting time, the concrete has hardened enough so that a 5 mm round needle no longer penetrates the surface (Piyasena *et al.*, 2013), (American Society for Testing and Materials, 2008).

The standard practice to determine the setting times are based on ASTM C 403. Test are conducted on the cement paste from a concrete mix. The initial setting time is then based on the needle penetration measured on the paste and defined as the time taken to achieve a penetration depth of 6 ± 3 mm from the bottom of the paste (Piyasena *et al.*, 2013). The apparatus used to conduct the penetration resistance test is the Vicat apparatus, shown in Figure 2.1 (American Society for Testing and Materials, 2008). The exact procedure used to determine the initial setting time is discussed in Section 3.5.

The final setting time can be determined using a circular shaped point, instead of a needle. The same test procedure is used as with the initial setting time. The final setting time is taken when the circular ring does not leave an impression on the concrete anymore.

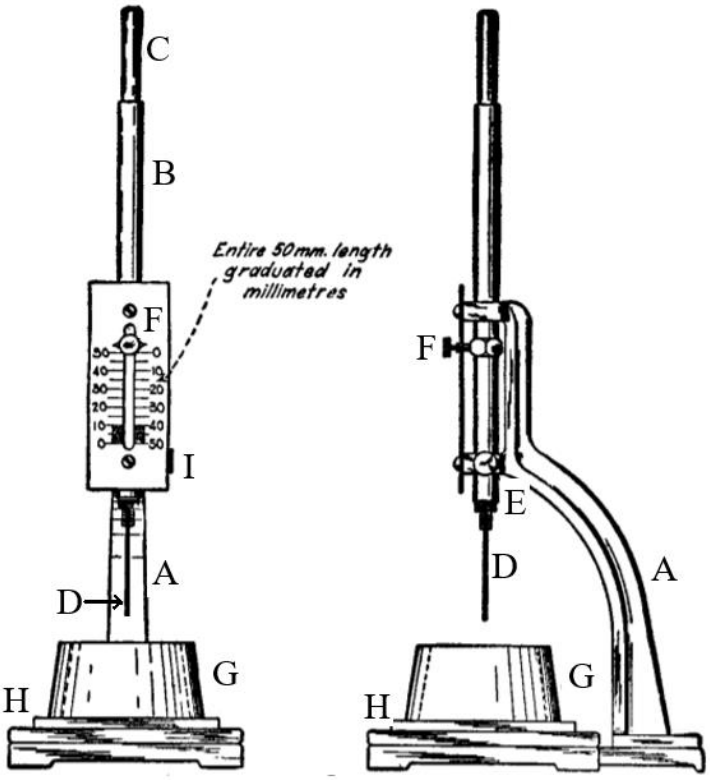

Figure 2.1 Vicat apparatus

2.1.8 Bleeding

Concrete bleeding occurs in fresh concrete and is the process where free water within the concrete mix migrates toward the top surface of the concrete, due to the heavier aggregate or solid particles settling downwards as a result of gravity, thus, bleeding is a direct result of concrete settlement. Plastic cracking of concrete, namely, plastic shrinkage cracking is directly related to concrete bleeding. Initially the bleeding rate can be rapid, but it slows down with time. It can occur for up to two hours after concrete is cast (Ravindrarajah, 2003).

The bleed mechanism is driven by consolidating particles, due to free settlement, which displaces water to the surface of the concrete where there forms a free layer of bleed water. The spaces between the solid particles of concrete facilitates the bleeding by creating a system of pores through which water can travel to the surface. Evaporation of the bleed water on the concrete surface can also have an influence on the capillary pore pressure causing a suction effect which also causes bleeding (Kayondo, Combrinck and Boshoff, 2019).

Bleeding is generally terminated by the end of particle consolidation, the end of concrete settlement or the end of the hydration process. This also indicates the initial setting time of concrete. Bleeding is

dependent on the w/c ratio, fines content, viscosity of the mix and the hydration rate, as well as the dimensions of the section. Generally, the more fines and the less water a concrete mix contains, the less the bleeding (Kayondo, Combrinck and Boshoff, 2019).

2.1.9 Evaporation

Evaporation is when the surface water on the concrete is converted into a gaseous state (Kayondo, Combrinck and Boshoff, 2019). This happens when heat energy is absorbed into the liquid e.g. through solar radiation or when there is a pressure difference above and below the liquid surface, allowing the active water molecules to escape from the liquid as vapor. If other environmental factors are present, such as wind, it accelerates the process (Uno, 1998).

One of the main reason's plastic cracking occur, especially plastic shrinkage cracking, is the rapid and excessive evaporation of surface water during the plastic state of concrete (Sayahi, Hedlund and Emborg, 2016).

Evaporation rate is influenced by various factors such as: temperature of the air and concrete, temperature difference between the air and concrete, wind speed, relative humidity, and solar radiation. Generally, a higher evaporation rate is achieved when there are higher wind speed, solar radiation, concrete temperature and lower relative humidity (Hasanain, Khallaf and Mahmood, 1989) (Kayondo, Combrinck and Boshoff, 2019).

Studies done by Hasanain, Khallaf and Mahmood, (1989) reported that besides weather conditions, the time of casting, difference in concrete and air temperatures as well as moisture conditions of the concrete surface also has an influence on the evaporation rate.

(Uno, 1998) developed a simplified evaporation rate equation, based on Menzel's formula, to estimate the evaporation rate of a fresh concrete surface as shown in Equation 2.2.

$$ER = 5 \times 10^{-6}(V + 4)[(T_c + 18)^{2.5} - r(T_a + 18)^{2.5}] \quad (2.2)$$

Where, ER is the evaporation rate, T_c is the concrete temperature, T_a is the air temperature, r is the relative humidity percentage and V is the wind velocity.

2.1.10 Capillary action

The moment the surface bleed water start to evaporate, up to the point where it exposes the solid concrete surface, a system of menisci is formed, as seen in Figure 2.2 (Kayondo, Combrinck and Boshoff, 2019). The menisci are a system of interconnected pores, formed by the spaces between the solid cement particles, aggregates and the additives in the concrete, which is mostly completely filled with water (Slowik, Schmidt and Fritzsch, 2008).

Eventually, the surface particles are no longer covered with water, causing a negative pressure to build up in the capillary water. More water is drawn to the concrete surface which cause the solid particles to draw closer to each other. The surface water, as a result of the negative pressure, is also able to evaporate, which reduces the radii of the menisci to a point where a shrinkage strain is possibly induced. Cracking may then occur if this shrinkage strain is not counteracted by the tensile response of the plastic concrete (Kayondo, Combrinck and Boshoff, 2019).

The negative pore pressure due to meniscus curvature is represented by the Gauss-Laplace equation, Equation 2.3 (Kayondo, Combrinck and Boshoff, 2019), (Slowik, Schmidt and Fritzsch, 2008):

$$p = -\gamma\left(\frac{1}{R_1} + \frac{1}{R_2}\right) \tag{2.3}$$

Where, p is the capillary pressure value, γ is the surface tension of the pore liquid, R1 and R2 are the minimum and maximum radius of water surface curvature, as seen in Figure 2.2.

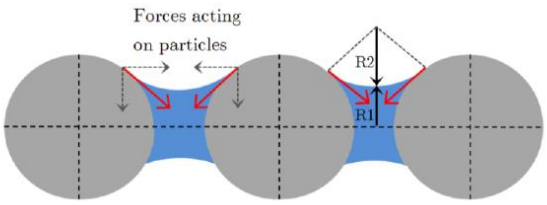

Figure 2.2 Illustration of the forces caused by menisci forming in capillary pores.

It was stated by Wittmann, (1976) that capillary pressure is the cause of plastic shrinkage. Wittmann clearly discussed the action of capillary pressure in fresh concrete and simultaneously measured capillary pressure and plastic shrinkage to find the exact correlation between these two phenomena. During the early 2000's capillary pressure was confirmed to be the main mechanism responsible for plastic shrinkage cracking of concrete. From this realisation most of the research was built on that understanding. Other factors, such as additives, w/c ratio etc. were also shown to have an influence on the capillary pressure in concrete. Therefore, these other factors may indirectly influence the plastic cracking, by influencing the capillary action in the concrete (Kayondo, Combrinck and Boshoff, 2019).

2.1.11 Concrete settlement

Free settlement in fresh concrete is the vertical volume reduction of concrete due to gravitational forces and cause the denser packing of solid particles. When solid particles settle, it essentially displaces water upwards which causes an upward buoyancy force and viscous drag of the flowing water, as seen in Figure 2.3. The water that accumulates on the surface of the concrete as a result of settlement is the bleeding water (Kayondo, Combrinck and Boshoff, 2019).

Settlement of concrete is what causes the vertical volume change of plastic concrete, called plastic settlement. Plastic settlement is one of the main driving forces behind plastic cracking, since concrete settles in a fresh state. Between uniform settlement and non-uniform or differential settlement, non-uniform settlement is of greater cause for concern since it may lead to tensile stress development and cracking. Settlement and its role in plastic cracking have been studied for decades, and the main results show that w/c ratio, specimen height and the consistency of the concrete is the major influencers of settlement of fresh concrete (Slowik, Schmidt and Fritzsch, 2008).

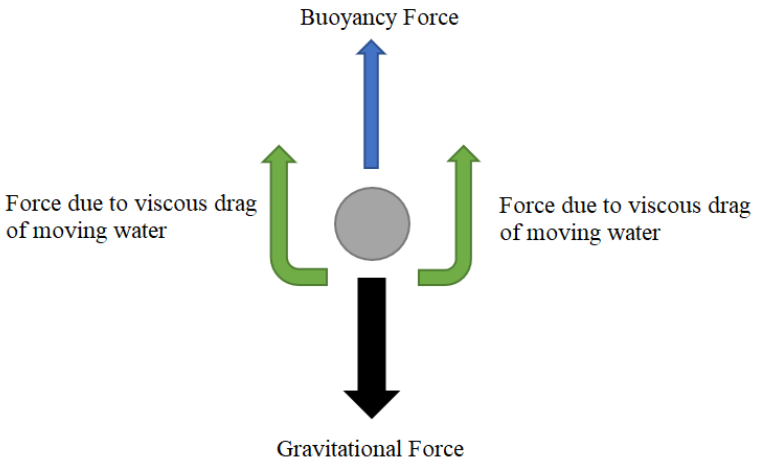

Figure 2.3 The basic mechanism of settlement (Kayondo, Combrinck and Boshoff, 2019)

2.2 Plastic settlement cracking

During the plastic state of concrete, a vertical volume reduction occurs due to the settlement of the solid particles in the fresh concrete mixture. Settlement cracking is caused by differential settlement, which is when the concrete in one area settles more than the concrete in an adjacent area, typically caused by a form of restraint or a change in section depth, as seen in Figure 2.4. For instance, the concrete on the top of a reinforcing bar settles less than the concrete on the sides or bottom of the bar. This causes tensile or shear stresses to occur in the concrete which may lead to cracks or voids, since the concrete has not yet gained sufficient tensile strength to counteract these stresses (Kayondo, Combrinck and Boshoff, 2019).

This process is due to the differential movement of particles and is influenced by poor grading, excessive bleeding, a lack of consistency in the mix, a lack of cohesiveness, low concrete cover above the bar, larger reinforcing bar sizes and closer reinforcing bar spacing (Slowik, Schmidt and Fritzsch, 2008).

Figure 2.4 shows the different forms of plastic settlement cracking, namely differential settlement, due to a varying section depth as well as differential settlement due to the presence of steel reinforcement (Kayondo, Combrinck and Boshoff, 2019). Figure 2.5 indicates the phenomenon of shear cracks, also

caused by steel reinforcement. The main type of restraint responsible for plastic settlement cracking is steel reinforcement (Combrinck, Steyl and Boshoff, 2019). As the solids settles to the bottom, the steel reinforcement obstructs this movement. This prevents some particles to settle and cause it to break away from the other moving particles which leads to fine cracks to form in the mortar. If cracking occurs, the cracking pattern typically aligns with the layout of the steel reinforcement (Combrinck and Boshoff, 2018).

Plastic settlement cracking occurs within the first few hours after concrete is cast, during the plastic state of concrete, and is one of the earliest forms of cracking. The settlement cracks may become visible early on or may only be noticed a couple of hours after being cast (Combrinck and Boshoff, 2018).

Combrinck, Steyl and Boshoff, (2018) concluded that with settlement cracking two distinct types of cracks occur, cracks at the surface, namely tensile cracks, and cracks below the surface near the restraint, namely shear induced cracks. It was also concluded that even if settlement cracking may not be visible at the surface of the concrete, it can still be present in the concrete underneath the surface. Cracking may also occur, even if the sample was placed in perfectly controlled climate conditions with no evaporation.

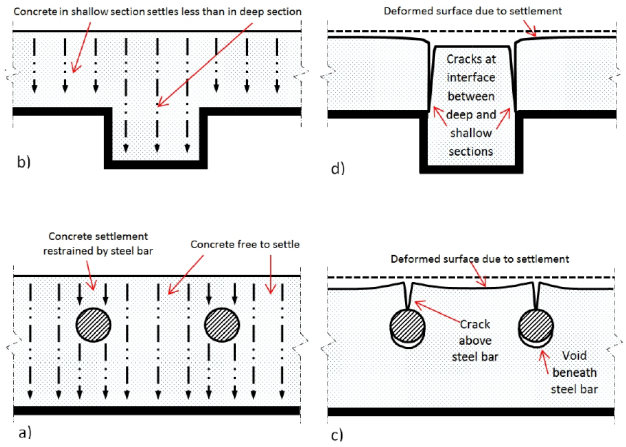

Figure 2.4 Demonstration of plastic settlement cracking in a slab and T-beam due to the presence of steel reinforcement (a&c) and a change in section depth (b&d) (Kayondo, Combrinck and Boshoff, 2019)

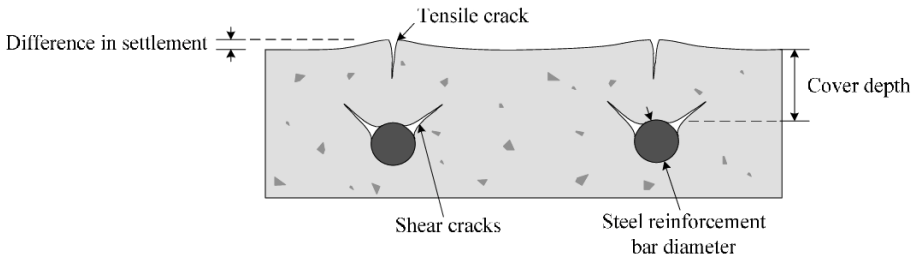

Figure 2.5 Demonstration of shear cracks and tensile cracks in concrete due to plastic settlement (Combrinck and Boshoff, 2014)

Although a lot is already known regarding plastic settlement cracking, the behaviour of pure plastic settlement cracking without the influence of plastic shrinkage cracking is still relatively unfamiliar. After conducting experiments, Combrinck and Boshoff, (2018) found that the majority of cracks occurred around 1 hour and 20 minutes after the concrete was cast. It was also discovered that plastic settlement cracks form from the bottom upwards and not from the surface down. That is why even though cracks are not visible on the surface of concrete structures it does not mean that plastic settlement cracks are not present.

Combrinck, Steyl and Boshoff, (2018) discovered that the surface plastic settlement cracks have a multiple crack pattern and not a single isolated crack. It was also found that pure plastic shrinkage cracks have a single well-defined crack pattern, which forms throughout the entire depth of the concrete section and not from the top to the bottom. Plastic shrinkage cracks do not have a multiple crack pattern, as with plastic settlement cracks. The difference in cracks patterns enables easy identification of the cracks after it has formed.

2.2.1 Main factors influencing plastic settlement cracking

There are many factors that influence the development of plastic settlement cracking of concrete. These factors are related to two aspects, namely the degree of differential settlement, as well as the rate and amount of differential settlement.

The factors affecting the amount and rate of differential settlement are the depth of the concrete, capillary pressure, setting times, the wall effect, water content, fines content and the aggregate dispersion. Whereas the factors affecting the degree of differential settlement are all the factors mentioned that affect the amount and rate of differential settlement, as well as concrete cover and formwork geometry (Kayondo, Combrinck and Boshoff, 2019).

These factors mentioned do not directly cause plastic settlement cracking to occur but has an influence on the degree/amount of concrete settlement and therefore an influence on the degree/amount of differential settlement, if restrained. Typically, a higher degree/amount of differential settlement lead to a higher chance of- or more severe plastic settlement cracking.

All these factors also relate to the bleeding of concrete. A higher amount of concrete settlement leads to higher amounts of bleeding. Thus, if these factors increase the amount of settlement, it will also cause an increase in the amount of bleeding.

2.2.1.1 Concrete section depth

The depth of a section determines the amount of solid materials present in the section. A deeper section contains more solids to settle, and correspondingly more bleed water to form. The higher amount of settlement allows a higher probability of plastic settlement cracking to occur. Thus, deeper sections are more prone to plastic settlement cracking (Uno, 1998).

2.2.1.2 Rebar cover depth

The cover depth of the rebar further influences the settlement of the concrete. A smaller cover depth allows less settlement above the reinforcement. This cause higher degrees of differential settlement and increases the tensile stresses that develop, which improve the likelihood and degree of plastic settlement cracking. Thus, a smaller cover depth increases the risk of plastic settlement cracking (Kwak *et al.*, 2010).

2.2.1.3 Capillary pressure

Once the bleed water at the concrete surface has evaporated, it triggers the build-up of capillary pressure. As mentioned in Section 2.1.10, once this happens more water is drawn to the concrete surface through the menisci which cause the solid particles to draw closer to each other. The additional surface water, as a result of the negative pressure of the menisci forces, is also able to evaporate, which reduces the radii of the menisci to a point where a shrinkage strain is possibly induced. This causes more settlement and bleeding to occur. This additional settlement increases the risk of plastic settlement cracking (Combrinck, 2012).

2.2.1.4 Water content

Higher w/c ratio allows more water to move to the surface during bleeding. More bleeding water prolongs the hydration process, and it takes longer for the surface water to disappear, which delays the capillary pressure build up and prolongs the plastic state, which gives the concrete more time to settle (Sayahi, 2016). This may increase the risk of plastic settlement cracking.

The w/c ratio also plays an important role on the strength of the concrete. Typically, a lower w/c ratio indicates a higher strength concrete, which is usually considered to have less cracking. However, very low w/c ratios may negatively affect the plastic settlement cracking due to the lack of workability of the concrete. Thus, the w/c ratio requires a fine balance that determines its effect on plastic settlement cracking, and it is not always that less water equals less plastic settlement cracks.

2.2.1.5 Fines content

An increase in fines decreases the rate of settlement in the concrete, due to the smaller amount of gravitational force that act on fines compared to more solid aggregates. A higher fine content also causes a lower bleeding rate. Thus, more fines decrease the risk of plastic settlement cracking. However, this is only true if no plastic shrinkage cracking is present (Suhr and Schoner, 1990).

2.2.1.6 Aggregate

The aggregate size and quantity as well as the degree of aggregate dispersion effects concrete settlement. Aggregate has a high density compared to the other materials in the concrete, therefore, larger aggregates, or a higher quantity of aggregates experiences stronger gravitational forces, which causes a higher amount of settlement, thus, increasing the risk of plastic settlement cracking (Combrinck, 2012).

Uniformly and high dispersed aggregate allow higher amounts of settlement, since the aggregate is not easily hindered by other pieces of aggregate which allow sufficient space to settle, whereas, aggregate with lower degrees of dispersion hinder the settlement (Combrinck, 2012).

2.2.1.7 Formwork geometry

Restraints such as steel reinforcements or section depth are forms of internal restraints. External restraints also have an impact on concrete, such as formwork that is irregular or has a rough surface finish, or the sub-grade on which the concrete is cast, increases the restraint against the concrete. The restrained concrete surface would settle less than the internal parts of the concrete. This can potentially lead to cracking in the concrete (Combrinck, 2012).

2.2.2 Testing methods

As mentioned, there are mainly two types of plastic settlement cracks, one is due to reinforcement and the other is due to a change in depths throughout the section of the concrete sample, as seen in Figure 2.6 and Figure 2.7.

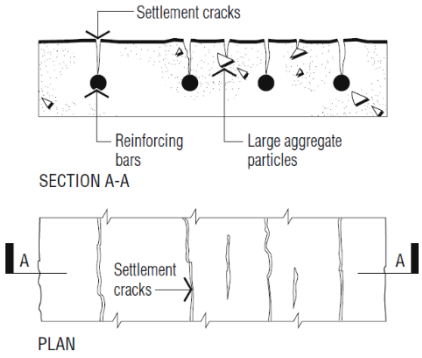

Figure 2.6 Settlement cracks due to steel reinforcement

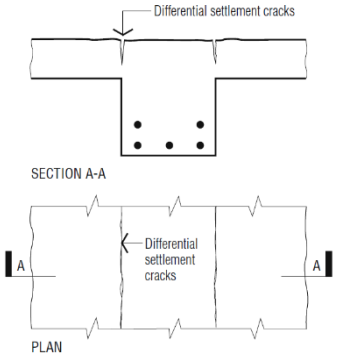

Figure 2.7 Settlement cracks due to differential settlement

Plastic settlement cracking only occurs when there is a difference in settlement in the concrete. The fundamental characteristics of plastic settlement cracking was tested by (Combrinck, Steyl and Boshoff, 2018) through the construction of different moulds, which simulated the behaviour of both these types of settlements. To test plastic settlement cracking due to reinforcement, a steel bar mould was

constructed, as seen in Figure 2.8. The mould had a depth of around 200 mm, and contained rods placed throughout the length at a specific cover depth to simulate the placement of reinforcement in a concrete slab or beam. This mould allowed the study of how restraints influence plastic settlement cracking.

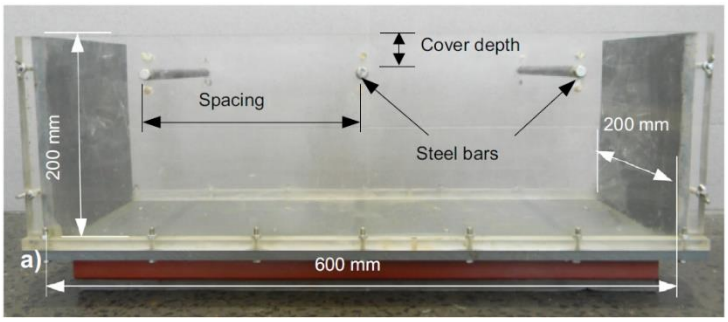

Figure 2.8 Reinforcement settlement mould

The tests were done in a climate-controlled room to ensure low evaporation rates. This ensured that there was a sustained layer of bleeding water present on the concrete surface to prevent plastic shrinkage cracking and therefore only study plastic settlement cracking.

To test the effect of a varying section, Combrinck, Steyl and Boshoff, (2018) constructed a mould which had two different depths throughout its length, as seen in Figure 2.9.

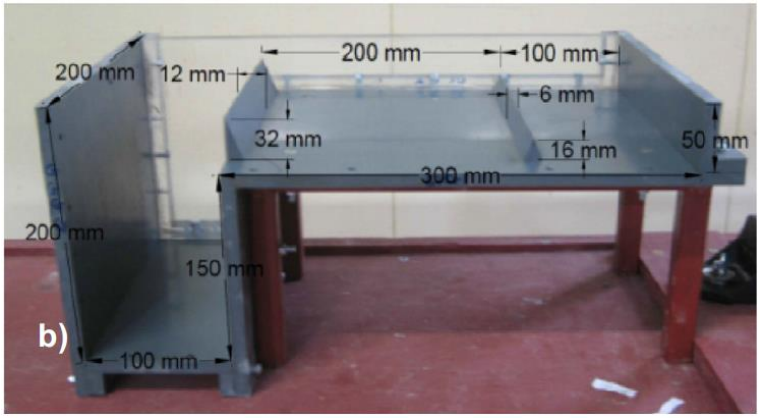

Figure 2.9 Differential settlement mould

Both testing methods were observed with the eye, as well as with high-resolution imagery. In both cases surface cracks as well as interior cracks were observed.

2.2.3 Mitigation of plastic settlement cracks

Cracking in concrete, be it plastic settlement-, shrinkage- or any other type of cracking, is inevitable. However, there are methods, such as re-vibration of concrete, that may lessen the effect of plastic settlement cracks. Re-vibration presumably removes some of the settlement cracks, as well as increase the strength of the concrete, if applied within the initial setting time (Combrinck and Boshoff, 2018); (Permana *et al.*, 2017).

Combrinck and Boshoff, (2009) conducted experiments to determine the effects or re-vibration of concrete on pure plastic settlement cracking. Pure plastic settlement cracking was achieved by preventing capillary build-up and evaporation to occur in the concrete, by constantly keeping the concrete wet.

They found that when re-vibration is applied at the initial setting time, there is a noticeable increase in the strength of the concrete. This may be due to a lowered w/c ratio, because of the excessive bleeding water that flowed to the surface after re-vibration. It was also found that if re-vibration is applied at the final setting time, it significantly reduces the strength of the concrete.

Plastic settlement cracking is a result of differential settlement. Therefore, any method that reduces the amount of settlement and the degree of differential settlement can minimise plastic settlement cracking, such as increasing the cover depth above the reinforcement, decreasing the section depth, limiting the use of varying sections, and adjusting the mix design to lower the amount of settlement. This includes having a lower w/c ratio, increasing the amount of fines material, such as fly ash, and using smaller or less aggregate. However, when adjusting the mix design, it should not be adjusted as to favour the prevention of plastic settlement cracking at the cost of having acceptable concrete strength and structural integrity.

2.3 Plastic shrinkage cracking

The rapid evaporation of the water from inside the concrete pores (after surface water has evaporated), while in the plastic state causes negative pressure in the pore system of concrete. This pressure, known as capillary pressure, is the main mechanism or cause of plastic shrinkage (Wittmann, 1976).

It is presumed that once the tensile capillary pressure reaches a level beyond the material's tensile capacity, plastic shrinkage cracking takes place (Kayondo, Combrinck and Boshoff, 2019). Plastic shrinkage cracking occurs while concrete is in its plastic state and is one of the earliest forms of cracking in concrete. Various factors influence the formation of plastic shrinkage cracking, especially environmental conditions, such as temperature, humidity, wind and solar radiation. The cracking severity depends on the capillary pressure and maximum shrinkage strain as well as the level of restraint (Wittmann, 1976).

Plastic shrinkage cracking is often associated with hot and dry weather conditions. It is caused when the concrete surface dries and shrinks so fast that the tensile strains induced exceed the strain capacity of the fresh concrete (Sayahi, 2016). High evaporation causes a rapid loss of moisture which dries the concrete surface so excessively that it shrinks and causes cracks while it has a poorly developed strength and stiffness. Plastic shrinkage cracking is mainly a problem with large, exposed surfaces, such as bridge decks, building slabs, parking areas, etc. where the concrete is placed in an area with a high evaporation rate (Combrinck, 2012).

At the initial setting time, concrete reaches its lowest strain capacity. Any restraint present in the concrete while setting may cause tensile stresses within or at the surface of the concrete, which in turn can cause cracking if it exceeds the low strain capacity. Restraints can include anything such as, the mould itself, any form of reinforcement, the lower levels of the concrete etc. (Sayahi, 2016).

According to Ghourchian *et al.*, (2019) around 80% of cracks that occur in concrete during its early age, is as a result of plastic shrinkage.

It was determined by Wittmann, (1976) that chemical shrinkage is not a major contributor to plastic shrinkage, since not much hydration takes place during the first two hours. Wittmann also found that as soon as the concrete surface becomes dry, plastic shrinkage cracking occurs. Thus, the evaporation of bleed/surface water of concrete is a very important factor to consider.

2.3.1 Main factors influencing plastic shrinkage cracking

Sayahi, (2016) investigated the different causes of plastic shrinkage cracking, and the main factors influencing it, such as the w/c ratio, additives, fibres, fines content and the depth of the concrete section.

2.3.1.1 Evaporation

Evaporation is the process where a liquid is converted into a vapor or gas. As previously stated, evaporation rate is one of the main causes of plastic shrinkage cracking. As long as the evaporation rate of the surface water is higher than the rate at which the concrete can replace the surface water through bleeding, there is a high risk of plastic shrinkage cracking. The evaporation rate is dependent on environmental factors, such as concrete temperature, air temperature, relative humidity, solar radiation, and wind speed. A higher evaporation rate, which is typically caused by high concrete- and air temperature, high wind speeds and solar radiation, and low relative humidity, leads to a higher degree or likelihood of plastic shrinkage cracking (Uno, 1998).

2.3.1.2 Concrete strength (water/cement ratio)

Since it has a significant effect on the tendency of plastic shrinkage cracking, the w/c ratio is very important. Higher w/c ratio may cause more bleeding and lower w/c ratios may cause less bleeding, in conventional concrete. Therefore, an optimised w/c ratio is preferred to reduce the risk of cracking, but also maintain optimal strength in the concrete. The ideal water/cement ratio, according to Sayahi, (2016) is 0.55, or somewhere between 0.45 and 0.55.

High strength concrete mixes contain high amounts of cement, and lower amounts of water, which produces a lower bleed rate. This makes higher strength concrete more susceptible to plastic shrinkage cracking (Uno, 1998).

2.3.1.3 Admixtures

Admixtures may influence the plastic shrinkage of concrete and may be practical to reduce the evaporation rate of the concrete, as well as the settlement, capillary pressure and plastic shrinkage formation (Sayahi, 2016).

Admixtures such as water reducers, superplasticisers, accelerators, and retarders all have an effect on the plastic state of the concrete. In general, it was found that superplasticisers prolong the forming of plastic shrinkage cracks, even if the bleeding is less. This is because of the modification in surface tension of the concrete. A lower surface tension reduces the capillary pressure in the concrete, and thereby lowering the potential of plastic shrinkage cracking. Retarding admixtures, if used in excess, can make concrete more susceptible to plastic shrinkage cracks, because of the slower set and strength gain of the mix. Accelerators hasten the setting process and thereby decreases the probability of plastic shrinkage cracks (Uno, 1998).

2.3.1.4 Section depth

Section depth also has an impact on plastic settlement cracking. The depth of a section usually indicated the bleed capacity of the concrete. In a deeper section, there are more solids to settle, causing more bleed water to rise to the surface. Therefore, if a section is deeper, it will produce more bleed water, over a longer period of time, making the concrete less prone to plastic shrinkage cracking, however, more prone to plastic settlement cracking (Uno, 1998).

2.3.1.5 Fibres

The addition of fibres, such as micro polypropylene fibres, is regularly used in concrete to reduce the width of the potential plastic shrinkage cracks that may form (Sayahi, 2016). It holds/stitches the plastic concrete together, thereby minimising the formation of early microcracks (Uno, 1998).

Hybrid fibres (which is a combination between steel and polypropylene fibres) is shown to reduce plastic shrinkage crack widths by up to 55%. It does however cause the formation of parallel cracks in the concrete (Sayahi, 2016).

2.3.1.6 Fines content

Fines typically lead to a larger total specific surface area of the binder and also leads to narrower pores. This higher surface area leads to higher tensile capillary pressure, which ultimately leads to a higher probability of plastic shrinkage cracking. The larger surface area presented to the water volume may also lead to less bleeding. Therefore, if fines such as fly ash, silica fume, slag, fine portion of sand etc. are included in a mix there is a higher chance of plastic shrinkage cracking (Sayahi, 2016), (Uno, 1998).

2.3.2 Testing methods

Due to the nature of plastic shrinkage cracking, it would be easy to test the behaviour of concrete under certain conditions that induce the effect. Various test methods were developed throughout the last few decades to test plastic shrinkage cracking.

Combrinck, Steyl and Boshoff, (2018) were able to successfully test the behaviour of concrete subjected to plastic shrinkage and the cracking that follows. They constructed two moulds to induce plastic shrinkage cracking which was observed using high resolution imagery. Additional 300 x 300 x 100 mm moulds were built to measure horizontal shrinkage, vertical settlement and unrestrained capillary pressure.

Most tests on plastic shrinkage cracking is based on the ASTM 1579 (2013) code standard (ASTM, 2013). Both moulds were constructed to specifically induce plastic shrinkage cracking. With the first mould, based on the ASTM 1579 (2013) standard, as seen in Figure 2.10, three triangular inserts were used. However, it was discovered that this mould did not allow pure plastic shrinkage cracking to occur, since there were signs of settlement cracking as well.

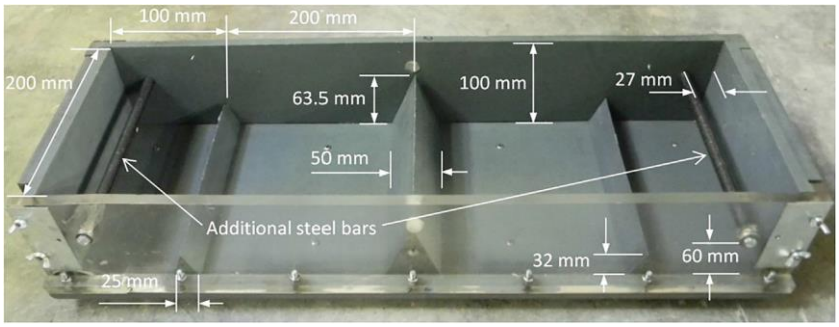

Figure 2.10 Mould used for testing plastic shrinkage cracking, based on ASTM 1579 (2013) Standard

Combrinck, Steyl and Boshoff, (2018) built a dog-bone mould that allowed pure plastic shrinkage cracking to occur, as seen in Figure 2.11. The triangular prisms restrained the concrete shrinkage to form a crack at the centre of the concrete. To prevent plastic settlement cracking to occur, no inserts were present in the mould that restraint vertical settlement.

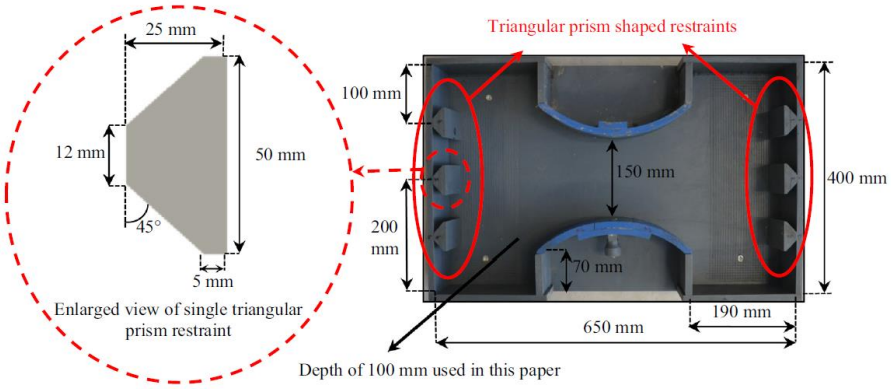

Figure 2.11 Dog-Bone concrete mould

After testing the mould, it was found that multiple cracks were not present, such as in the first mould, but only a single crack, thus it confirmed that the mould only allowed plastic shrinkage cracking to occur.

It was concluded that the ASTM mould resulted in both plastic shrinkage and settlement cracking. However, the dog-bone mould did induce pure plastic shrinkage cracking to occur, with no sign of settlement cracking. A single crack was observed through the concrete.

The Ring test method is another test method used by Sayahi, Emborg and Hedlund, (2017) to test plastic shrinkage cracking. The method was developed by R. Johansen and P. Dahl in 1993. It is designed to achieve similar outcomes to the ASTM 1579 method.

It consists of a mould with two concentric steel rings, with diameters of 300 and 600 mm, respectively. The rings formed the bottom part of the mould and had a depth of 80 mm. They also contained steel raisers all around the circumference which acted as crack initiation points. A transparent air funnel was placed over the mould which had a fan at the end, as seen in Figure 2.12. The fan generated 4.5 m/s wind across the surface of the concrete to increase the risk of plastic shrinkage cracking.

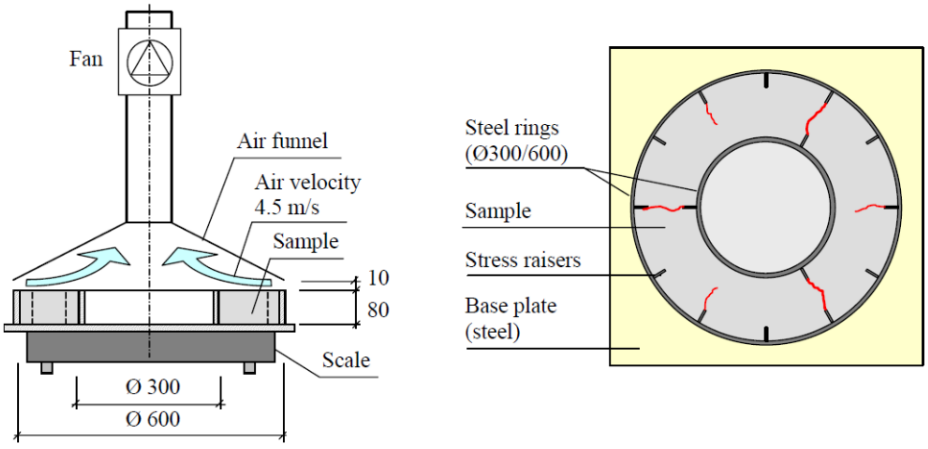

Figure 2.12 Ring Test method setup

2.3.3 Preventative Measures

Since plastic shrinkage cracking is mainly caused by the rapid evaporation of surface water of concrete, one of the main ways to prevent plastic shrinkage cracking is by proper curing measures, as described in Section 2.1.5. Maintaining a sufficient amount of moisture on the concrete surface will prevent the high evaporation rate from drying out the concrete surface and causing shrinkage cracks (Nehdi and Soliman, 2011) and (Sayahi, 2016).

Another preventive measure is the use of fibres, specifically polypropylene fibres. As stated in Section 2.3.1.5, the fibres holds/stitches the plastic concrete together, thereby minimising the formation of early microcracks. Thus, if fibres are used sufficiently it can minimise the potential of plastic shrinkage cracking (Uno, 1998).

2.4 Interaction between plastic settlement and plastic shrinkage cracking

It is rare that pure plastic settlement or pure plastic shrinkage cracking occurs in a real-life concrete structure. There is usually a combination of the two factors. When the two cracks occur at the same time, plastic settlement cracks are amplified by plastic shrinkage cracks, thus having a more severe impact on the concrete than pure plastic shrinkage – or settlement cracking. Combrinck, Steyl and Boshoff, (2018) conducted experiments to determine the interaction between plastic settlement and plastic shrinkage cracking. Their results were summarised as shown in Figure 2.13.

To achieve no or minor cracking, the conditions had to be close to perfect, where there was no potential for evaporation and no significant differential concrete settlement taking place. It was also discovered that pure plastic settlement- or pure plastic shrinkage cracking occurred, without any interaction, only if the conditions were optimal. A low potential for evaporation, with a high potential for differential concrete settlement, would allow pure plastic settlement cracking to take place, and vice-versa for pure plastic shrinkage cracking.

Combrinck, Steyl and Boshoff, (2018) also discovered the crack behaviour can differ significantly if both types of cracks are present, compared to the individual behaviour of pure plastic shrinkage- or settlement cracking. For conditions with moderate to high potential for both types of cracks, plastic shrinkage cracks amplify plastic settlement cracks. In the test, the plastic settlement crack occurred prior to plastic shrinkage cracks, as indicated by the lack of capillary build-up. Therefore, the start time and severity of the plastic shrinkage cracks are highly dependent on the severity of the plastic settlement cracks. In the case of high potential for both plastic shrinkage and plastic settlement cracking, significant cracking can occur early, referred to as crack jumping.

As seen in Figure 2.14, the early formed plastic settlement crack acts as a weak spot in the concrete. The weak spot relieves capillary pressure in that area through air entry. As evaporation and shrinkage

continues, the particles are pulled closer, which cause the settlement crack to widen further through the influence of the shrinkage crack (Le Roux, 2016).

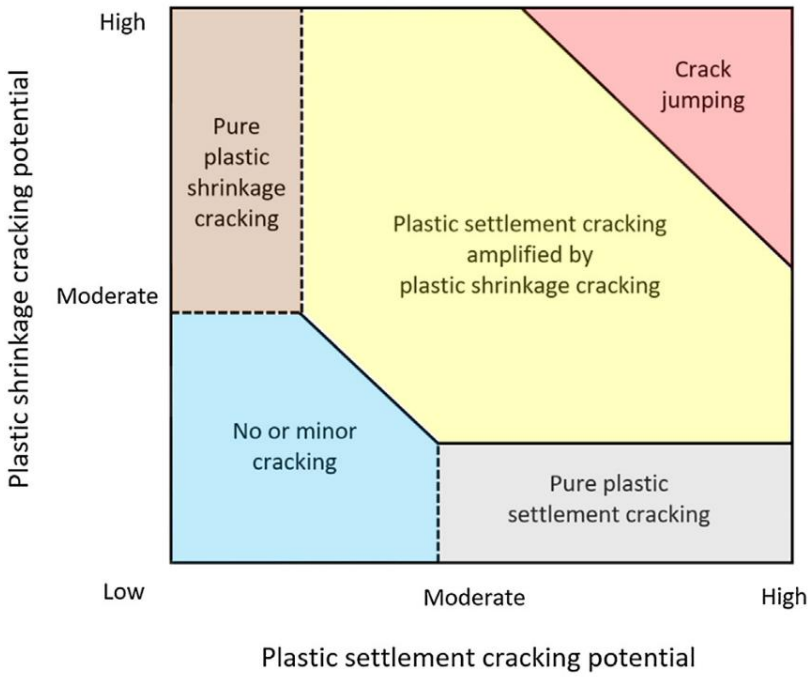

Figure 2.13 Diagram that illustrates the interaction between plastic settlement and plastic shrinkage cracking

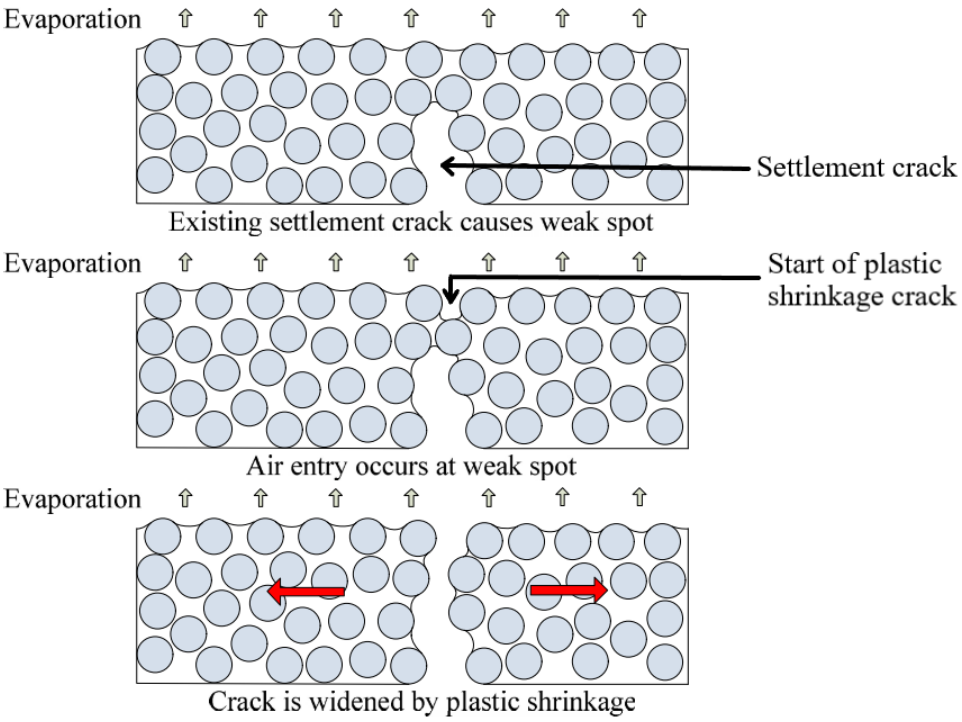

Figure 2.14 Representation of how plastic shrinkage cracks amplifies plastic settlement cracks

2.5 Concrete durability

Durability is an important aspect of concrete. However, due to all the factors influencing the behaviour of concrete it is difficult to predict the long-term durability thereof (Nehdi and Soliman, 2011). The corrosion of steel is a much greater problem to the durability of reinforced concrete than the deterioration of the concrete itself. It is important to ensure that the cover layer of concrete between the steel and the environment does not allow any corrosive agents from the surrounding environment to enter the concrete structure and cause steel corrosion (Mackechnie and Alexander, 2002).

Concrete structures are typically designed according to the strength characteristics of the material, however, it is not the only factor that should be considered (Mehta and Monteiro, 2006). It was determined by Armaghani, Larsen and Romano, (1992) that different concrete samples/structures with equal compressive strength does not necessarily have the same levels of durability. In general, it is assumed if a specific target strength is achieved in concrete it implies a certain level of durability. Durability is not determined by the concrete's compressive strength, but rather by its permeability, combined with its strength. Today it is known that permeability governs concrete durability and is a very important aspect to consider. Thus, to accurately determine the durability of concrete, strength tests, along with permeability tests should be performed.

The interaction between water and the permeability of concrete is the key to the service life and durability of the structure. Water is an essential element needed to create concrete. It starts the hydration process with cement and contributes to the strength of the concrete. It also allows the concrete to be workable and mouldable. However, water is the centre of most durability problems in concrete and cause many types of physical degradation as well as chemical degradation. It acts as a transport medium for aggressive agents and the source of degradation through chemical processes and reactions. The deterioration rate of a solid depends on the type and concentration of ions in the water. The alkaline nature of concrete is vulnerable to acidic waters (Mehta and Monteiro, 2006).

Permeability governs the rate of flow of a fluid into a porous solid, such as concrete. Water molecules are small and are able to penetrate into extremely fine pores and cavities. If a porous material such as concrete has a high permeability, it allows more water to travel through the concrete and deteriorate the structure and reach the steel reinforcement. Many variables determine the water permeability of the concrete, namely the water-cement ratio, aggregate content, aggregate size, and pore characteristics. A lower water-cement ratio reduces permeability. The addition of aggregate into a cement paste, or the use of larger aggregate size increases the permeability. Concrete permeability and strength are related to each other through the capillary porosity of the concrete, therefore the factors that influence the concrete strength also has an influence on the permeability (Mehta and Monteiro, 2006).

Cracking in concrete can also significantly increase the permeability, which may lead to less durable concrete. Low permeability protects against the ingress of agents that reach the steel reinforcement which can cause corrosion (Dhawan, Bhalla and Bhattacharjee, 2003).

There are a few basic transport mechanisms for the movement of fluids and ions through concrete, namely: permeation, sorption/capillary suction, and diffusion. Permeation occurs due to pressure gradients or pressure differences in the concrete. Sorption refers to the transport of liquids into a soil through the process of capillary suction, which occurs due to capillary action in the cement paste. Diffusion occurs due to concentration gradients or concentration differences between the concrete surface and the interior zones of the concrete (Bertolini *et al.*, 2004).

Various parameters, such as pozzolanic materials, namely fly ash, blast-furnace slag, and silica fume, as well as a low w/c ratio can contribute to improve the strength and long-term performance of concrete.

Early age cracking in concrete is another common issue faced regularly in concrete construction. Even though technology has advanced tremendously over the past few decades, the prevention of early-age cracking in concrete still remains a problem in practice. The early age properties and behaviour of concrete may influence the long-term durability thereof in a large extent. Therefore, to ensure the safety and long-term durability of concrete structures it is important to understand the early age behaviour of concrete (Nehdi and Soliman, 2011).

Cracks, especially early age cracks, are influenced by various factors and it is difficult to isolate the contribution of each factor. Some of these factors include tensile strength of the concrete, temperature change, environmental conditions, and the restraint to movement. A summary of the factors that affect early age cracking are summarised in Figure 2.15 (Safiuddin *et al.*, 2018).

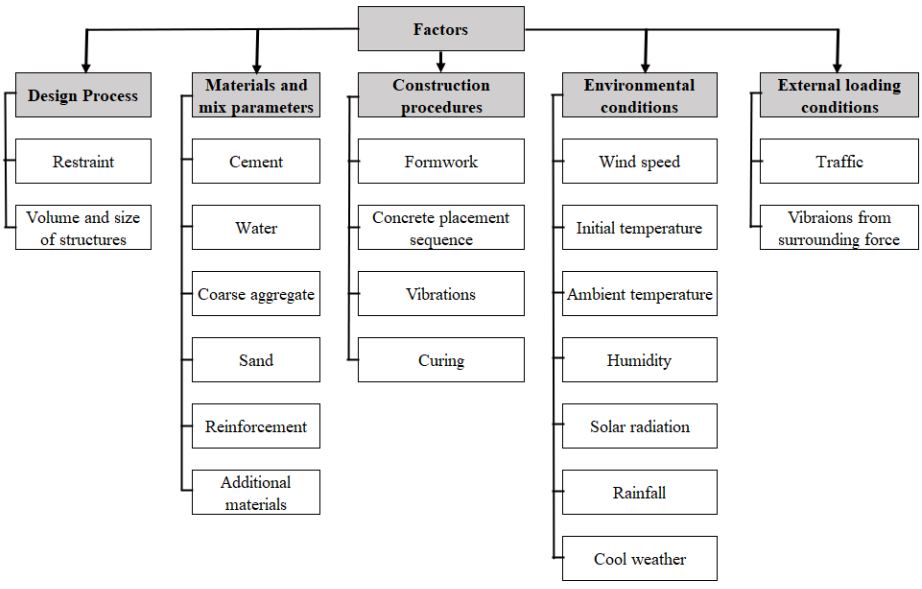

Figure 2.15 Various factors which influence cracking of hardened concrete.

Typically, during the first 3 hours after concrete is cast it has a low tensile strength, therefore it is easy for cracks to form during this stage of the concrete's setting time. Cracks created during the early-age of concrete can have a lasting effect on the aesthetical appearance, safety and durability of the concrete (Safiuddin *et al.*, 2018).

2.5.1 Effects of plastic settlement cracking on concrete durability

The exact impact of plastic settlement cracks on the durability of concrete is still somewhat unfamiliar. It is assumed that these types of cracks, and any other form of cracks, has a negative impact on the concrete structure, however, no actual physical testing or experimental results could be found in literature. Although plastic settlement cracking occurs at the object of restraint and does not usually reach the surface of the concrete, it can still act as a weak point for further crack development. These are typically induced by loading or ingress of external materials which can cause corrosion of the steel reinforcement. As discussed in Section 2.4, plastic shrinkage cracking amplifies plastic settlement cracks. Thus, the plastic settlement cracks may not directly affect concrete durability, but the presence of the crack can increase the severity and likelihood of other, more detrimental cracks to form.

2.5.2 Corrosion of steel in concrete structures

The corrosion of reinforcing steel in concrete structures is one of the main causes of deterioration of the structure and a major durability problem. Once the concrete reinforcement starts to corrode, the service life of the structure is shortened through crack initiation, propagation and subsequent spalling of the concrete cover, caused by the expansion of the corroding steel (Marques and Costa, 2010), (Dhawan, Bhalla and Bhattacharjee, 2003).

There are two main parameters affecting corrosion, namely, the breakdown of the protective film on the reinforcing bar, by a lowering pH level, through the ingress of aggressive agents, such as chlorides or through carbonation, and the amount of said agents needed to do so (Hansson, Poursaee and Jaffer, 2012). The corrosion rate is affected by the availability of oxygen and capillary water, as well as the concentration of Fe^{2+} in the concrete near the reinforcement (Dhawan, Bhalla and Bhattacharjee, 2003).

In reinforced concrete, the concrete forms a protective layer around the steel, limiting the access of water and oxygen to the steel surface. It also provides high levels of alkalinity through the solution of the pores in the cement paste, which starts when cement hydration starts. This provides a passive layer around the steel and pH levels in the concrete that protects the steel from corrosion products, or at least limits the metal loss to about 0.1 – 1.0 µm/year (Hansson, Poursaee and Jaffer, 2012).

However, the passive layer is not stable at pH levels below 9 or in solutions containing chloride ions. Due to the permeability of concrete it allows the ingress of chlorides, especially in a marine atmosphere, or from de-icing salts. The reactive nature of concrete allows CO_2 to neutralise the pore solution of the cement paste. Through the ingress of chlorides and carbonation the pH levels in the concrete lowers

below stable levels which causes the passive/protective layer around the steel to be destroyed and for corrosion rates to increases significantly, as high as several mm/year, and cause noticeable degradation in the reinforced concrete (Hansson, Poursaee and Jaffer, 2012).

The corrosion mechanism in a reinforced concrete member takes place after the steel passive layer is destroyed, however, only if the steel has large electrical potential difference, as well as sufficient oxygen and moisture present (Marques and Costa, 2010).

Steel corrosion in concrete is an electrochemical process. An anode and cathode are formed by the surface of the corroding steel, acting as a mixed electrode, where “half-cell”- or anodic and cathodic reactions take place. Through the reduction process, the cathodic reaction results in a reduction of dissolved oxygen, which forms hydroxyl ions. The anodic reaction results in a loss of metal through the oxidation process (Dhawan, Bhalla and Bhattacharjee, 2003). Figure 2.16 shows the corrosion cells that form in cracked concrete (Uddin and Shaikh, 2018).

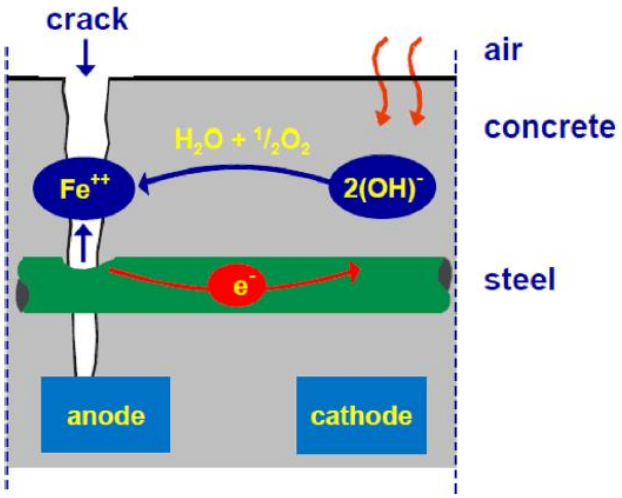

Figure 2.16 Corrosion cells that form in cracked concrete (Uddin and Shaikh, 2018)

The influence of oxygen permeability depends on the concrete cover present. The concrete cover generally reduce the availability of oxygen on the steel surface (Uddin and Shaikh, 2018). Concrete members with cracks results in a higher oxygen permeability than a member without cracks.

Crack formation affects the durability properties of concrete severely. Cracks formed in concrete shortens the corrosion initiation rate of the steel. The corroded steel also loses its high tensile characteristics and thereby lowers the tensile strength of the concrete. Unfortunately, the formation of cracks in concrete is almost unavoidable, because concrete has a very low tensile strength (Uddin and Shaikh, 2018). Some of the characteristics of cracks and the influence on durability is discussed in the following sections.

2.5.2.1 Crack widths

One of the most important factors that determine the severity of a crack is the crack width. Two types of cracks occur in a concrete structure, namely, transverse cracks (perpendicular to steel reinforcement) and longitudinal cracks (parallel to reinforcement). Longitudinal cracks are more dangerous, in regards with corrosion of steel, than transverse cracks (Uddin and Shaikh, 2018).

Although it is generally assumed that the width of cracks may accordingly influence/accelerate the corrosion initiation, the data that establishes a direct relationship between cracks width and corrosion of steel are limited. It has, however, been established that crack widths up to 0.3 mm is linked with an increasing trend of corrosion of steel, with a scatter of results at 0.5 and 0.7 mm crack width, as seen in Figure 2.17 (Uddin and Shaikh, 2018).

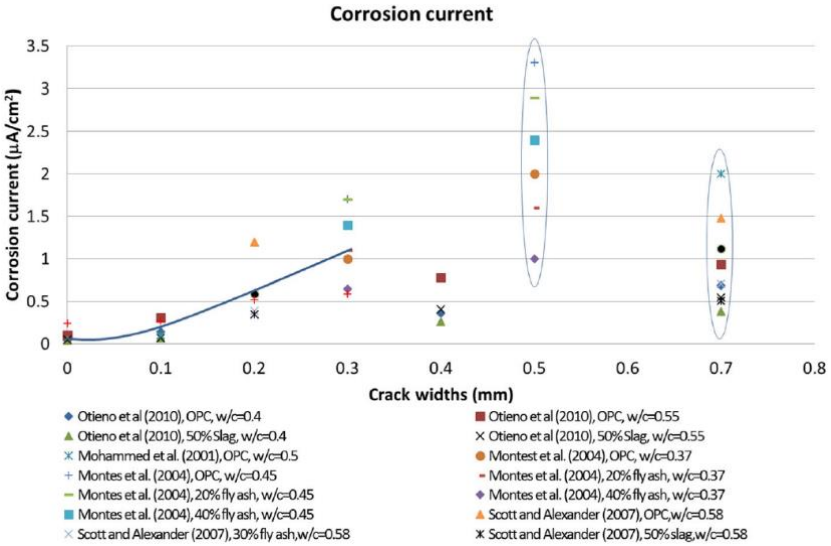

Figure 2.17 Effect of transverse crack widths (Uddin and Shaikh, 2018)

2.5.2.2 Longitudinal cracks

Longitudinal cracks are considered more dangerous since they provide easier access of environmental agents, such as moistures, chlorides and oxygen to the steel reinforcement, since the cracks are formed along the lengths of the reinforcement, and therefore exposes a larger area thereof. This can possibly accelerate the corrosion of steel further than the influence of transverse cracks. Longitudinal cracks can also be formed as a result of plastic settlement and shrinkage cracking (Uddin and Shaikh, 2018).

2.5.2.3 Crack frequency

The number of cracks per specific length is defined as the crack frequency. It is stated by Uddin and Shaikh, (2018) that the frequency of transverse and longitudinal cracks both affects the corrosion of steel. An increase in crack frequency causes a significant increase in the corrosion of steel.

2.5.2.4 Crack depth

The depth of cracks accordingly affects the chloride penetration depths. Thus, in terms of corrosion the crack depth is also a key parameter, especially if loading is applied where crack depth increases during the life of the concrete structure. This affects the chloride ion penetration depth. However, there are still limited research available that thoroughly explains the exact influence of crack depths on the corrosion of steel (Uddin and Shaikh, 2018).

2.6 Testing and prediction methods

Durability index testing can be used to provide means that are more practical for the characterisation of the durability potential of concrete. Many concrete durability tests have been developed in order to test the rate of fluid and ion transport through concrete, by utilising the three transport mechanisms namely, permeation, diffusion and sorption (Mackechnie and Alexander, 2002).

2.6.1 Prediction of corrosion rates

Corrosion rate allows for reliable and accurate prediction of the severity of damage to the structure. However, it is fairly underutilised in practice today (Otieno, Beushausen and Alexander, 2011). Existing corrosion rate prediction models:

1. *Alonso et al.'s model (1988)*
2. *Yalcyn and Ergun's model (1996)*
3. *Katwan et al.'s model (1996)*
4. *Liu and Weyers' model (1998)*
5. *Duracrete model (1998)*
6. *Vu and Stewart's model (2000)*
7. *Scott's model (2004)*
8. *Martinez and Andrade's model (2009)*

Aspects to consider when creating a corrosion rate model:

1. Time-variant nature of corrosion rate
2. Influence of cover cracking on corrosion rate
3. Corrosion rate measurement techniques
4. Validation of models
5. Accounting for variability

Otieno, Beushausen and Alexander, (2011) concluded that with corrosion induced damage prediction models, corrosion rate is the most important factor to consider, however, it is still necessary to take other corrosion-influencing factors, such as concrete quality, cover depth, cover cracking etc. into consideration. It is also important to account for the inherent variability of corrosion rate and the influencing factors thereof.

2.6.2 Durability Index testing

Typically, the transportation of aggressive agents into concrete is caused by one of the following transport types: absorption, permeation, and diffusion. The material properties and environmental conditions has an influence on each transport type (Mackechnie and Alexander, 2002).

Concrete allows, to a certain degree, the transportation of fluids or ions through it, and durability of concrete is considered as the resistance of these processes. South African researchers has developed three durability index testing methods that can be used to determine an index that relates to the durability of the concrete that takes into account the different transportation methods of these agents through the concrete (Gouws, Alexander and Maritz, 2001).

These tests are:

- Oxygen Permeability Test
- Water Sorptivity Test
- Chloride Conductivity Test

2.6.2.1 Oxygen Permeability Index test

The capacity of a material to transfer fluids under the action of an externally applied pressure is known as permeability. The concrete microstructure, as well as the moisture condition of the material and the permeating fluid characteristics, determines the permeability of concrete (Mackechnie and Alexander, 2002).

To perform an oxygen permeability test, 70 ± 2 mm in diameter and 30 ± 2 mm thick concrete samples are used, which were core drilled from larger beams or other specimens. After extraction, the samples are oven-dried at ±50ºC for 7 days and then exposed to 100 kPa pressure over an extended period, at least 6 hours, to determine oxygen permeability index (OPI). The OPI is determined using the pressure decay over time through the concrete samples and performing various calculations. The apparatus, as seen in Figure 2.18 to Figure 2.20, is used for this test. An OPI test uses the negative log of the coefficient of permeability where a value between 8.5 to 10.5 is determined. A value below 9.0 is considered poor, and may indicate a concrete with high permeability, where a value above 10.0 is considered excellent and indicates a well-developed concrete with low permeability (Mackechnie and Alexander, 2002). This test is highly sensitive to the presence of voids and cracks in the concrete which acts as pathways for the permeating gas.

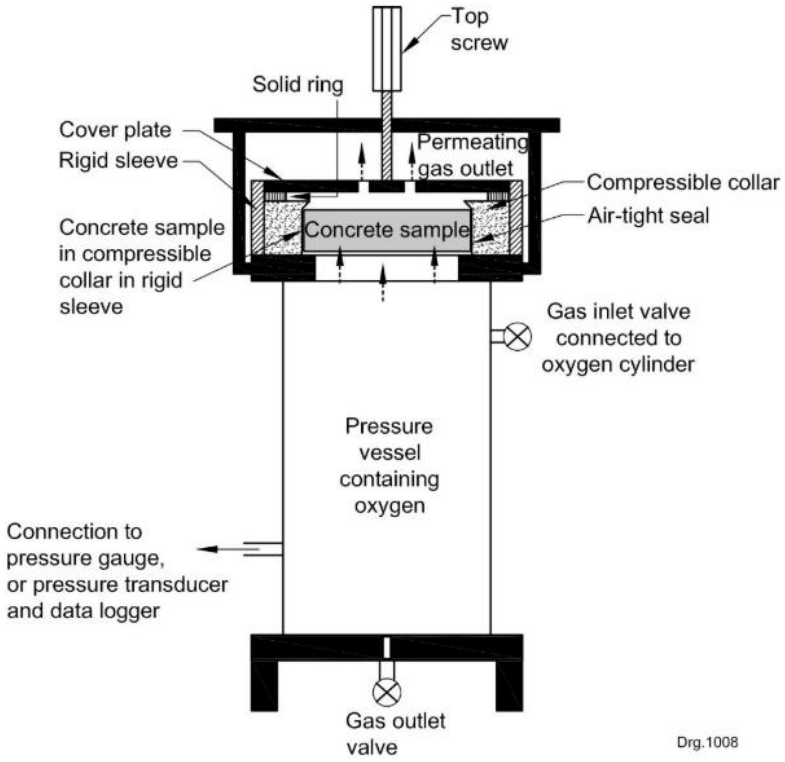

Figure 2.18 Permeability cell arrangement

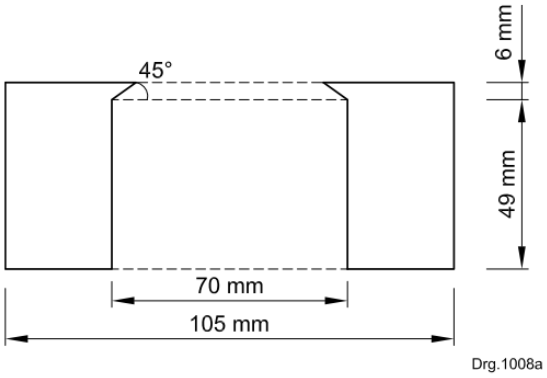

Figure 2.19 Compressible collar section to house the concrete samples

Figure 2.20 Picture of a permeability cell

2.6.2.2 Water Sorptivity test

Sorptivity is the tendency of a material to absorb and transmit water and other liquids through capillary action. It can also be described as the rate at which a wetting front moves through a porous material. The sorptivity test measures the absorption of water in a uni-directional way into a concrete sample of around 70 ± 2 mm in diameter and 30 ± 2 mm thick, where water is absorbed from one face of a concrete sample to the other. The samples are places in a container, filled 5 mm with water, on small lifts, such as 2 mm rods or ten layers of paper towel, as seen in Figure 2.21. Only one face is exposed to the water, as seen in Figure 2.22. The sides are sealed with silicon, epoxy, or packaging tape to prevent the water from entering the samples through its side and only from the bottom (Gouws, Alexander and Maritz, 2001), (UCT, 2017).

Weight measurements are then taken at predetermined time increments to determine the mass of water absorbed. The mass is then again determined after the sample is vacuum-saturated. The water sorptivity index is determined using the mass of the water absorbed plotted versus the square root of time. A lower index typically relates to a higher durability of the sample. The sorptivity test is sensitive to early-age drying effects, which influence the microstructural porosity gradients, as well as sensitive to the degradation of concrete quality with depth from the surface (Gouws, Alexander and Maritz, 2001).

Figure 2.21 Examples of the sorptivity test being conducted (UCT, 2017)

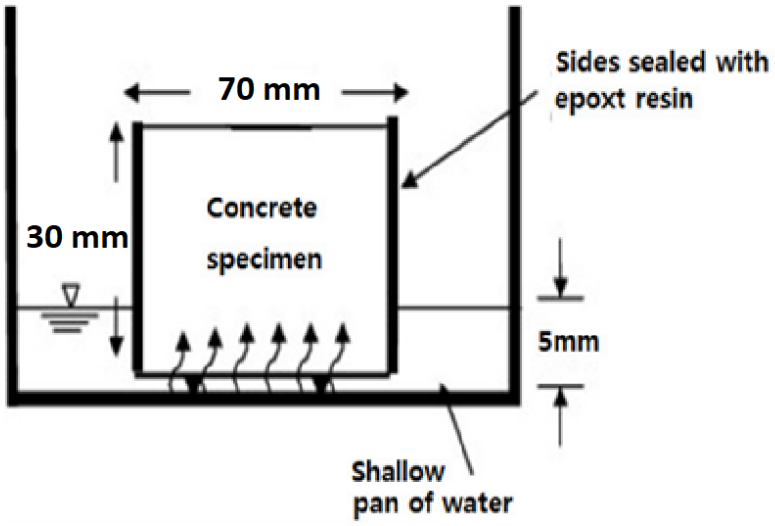

Figure 2.22 Schematic presentation of sorptivity test (Saraswathy, Karthick and Kwon, 2014)

2.6.2.3 Chloride conductivity test

Diffusion is when a substance moves from an area of high concentration to an area of low concentration. Chloride enters concrete through the process of diffusion, specifically in a marine environment. The chloride conductivity test allows you to test how a concrete sample reacts when subjected to chloride from the flat sides of the sample. This method does not favour large pores over smaller ones, as with the permeation process, but moves through all pores of a sufficient size, providing a good indication of the overall diffusivity of the material (Gouws, Alexander and Maritz, 2001).

The chloride conductivity cell layout used is shown in Figure 2.23 to Figure 2.26. It consists of a collar, luggins and a connection point. The specimen is placed in the collar. Test specimens consist of concrete samples that are 70 ± 2 mm in diameter and 30 ± 2 mm thick. The specimens are oven-dried at 50^{o}C for 7 days before testing to ensure no moisture is present in the samples. The mass is determined before the testing starts. The samples are placed in a vacuum saturated facility, where a NaCl solution is allowed to flow in and cover the specimens, with a water level of 40 mm above the top face. After a period in the vacuum saturation tank, with and without the vacuum applied, the mass is taken again. The samples are then placed in conduction cells, as seen in Figure 2.25 (UCT, 2017).

The sides are then screwed into the central portion, as seen in Figure 2.26, and the rig is made to stand upright. The sides, anode, and cathode compartments are then filled with NaCl solution, through the holes, and sealed afterwards. The ammeter and voltmeter are then connected and a voltage of 10V is applied through a DC power supply. The current and voltage is then recorded from the ammeter and voltmeter, after which the chloride conductivity index is determined (UCT, 2017).

Chloride conductivity values typically range from >3 mS/cm to <0.75 mS/cm. The lower the index, the better the potential durability of the concrete (Gouws, Alexander and Maritz, 2001).

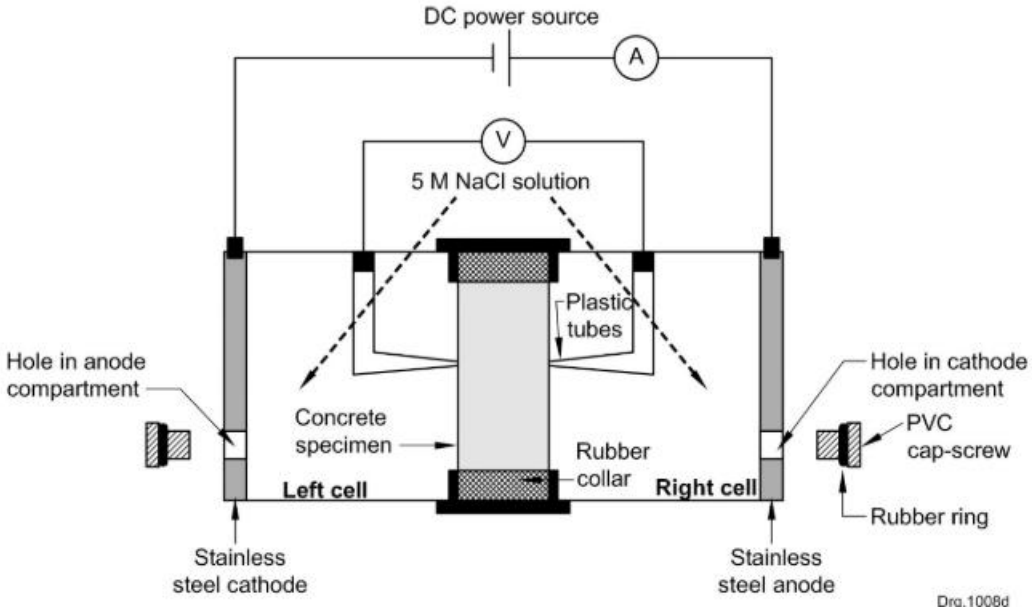

Figure 2.23 Schematic presentation of a conductivity cell arrangement (UCT, 2017)

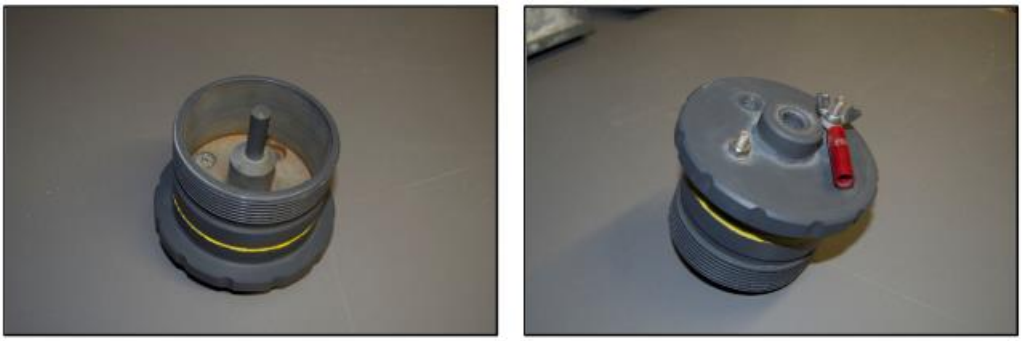

Figure 2.24 Luggin (left) and connection point (right) of chloride conductivity cell (UCT, 2017)

Figure 2.25 Properly placed specimen in collar (UCT, 2017)

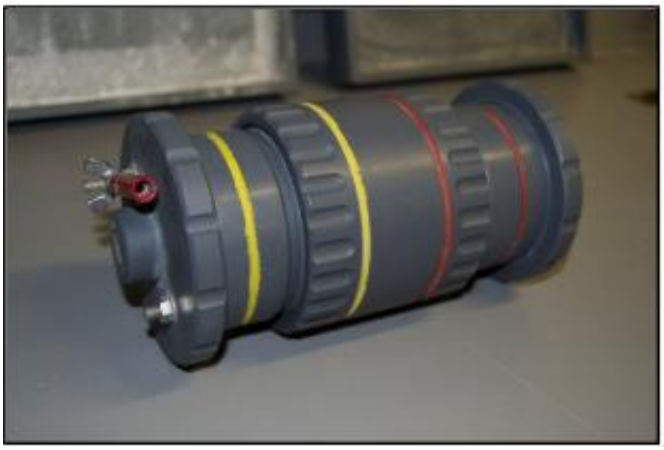

Figure 2.26 Assembled chloride conductivity cell (UCT, 2017)

2.7 Concluding summary

In this chapter, a general background is given on concrete. Different mechanisms of concrete are discussed, and it is found that bleeding, evaporation, and capillary action are major factors that influence plastic shrinkage cracking. The amount and degree of settlement, section depth and concrete cover is found to have a major impact on plastic settlement cracking.

The cracking mechanisms during the plastic and hardened state are discussed, as well as during the early age of concrete. The plastic state of concrete is shown to be important, since the short period of time can have a major effect on the long-term behaviour of the concrete. Plastic shrinkage and -settlement cracking is discussed as well as the interaction between the two types of cracks.

The durability of concrete is an important section in this chapter. It is found that water permeability is a major aspect of durability, as well as the three transport mechanisms of concrete and how it influences corrosion of steel reinforcement. Three durability index tests are discussed which were performed for the practical section of this study.

The literature study indicated an absence in information regarding the specific effect of plastic settlement cracking on concrete durability. The section on the interaction between plastic shrinkage and -settlement cracking, along with the factors that affect concrete durability, indicated that plastic settlement cracking may act as initiation points for more severe cracking to form. However, this study aims to test the factors that affect plastic settlement cracking, and how these factors specifically influence the concrete durability.

3 Experimental Framework

Plastic settlement cracks typically occur at the object of restraint and is not always visible at the surface of the concrete. Therefore, it is important to determine the effects of plastic settlement cracking on concrete durability.

To determine this, plastic settlement cracking was induced in a controlled manner that enabled experimental tests to be performed on the concrete. The crack severity and its durability on the concrete was tested. It is also important to note that only pure plastic settlement cracks occurred and not any other form of cracks, such as plastic shrinkage cracking, except during Experiment 7.

Several experiments were conducted to determine what factors affects plastic settlement cracking most severely and how it influences the durability of the concrete.

The preliminary- and main experiments conducted were as follows:

1. Cylindrical concrete moulds.
2. The influence of cover depth on plastic settlement cracking.
3. The effect of different types reinforcing rods on plastic settlement cracking.
4. The influence of cover depth and concrete strength on plastic settlement cracking.
5. The influence of re-vibration of concrete on plastic settlement cracking.
6. The influence of plastic viscosity of concrete on plastic settlement cracking.
7. The influence of plastic shrinkage cracks on plastic settlement cracking.

CT Scans were also performed on the concrete samples to visualise the crack layout of the plastic settlement cracks and compare the cracks between different cover depths and beams.

3.1 Materials and mix proportions

For Experiments 1 to 3, a set of three mixes were used, each with a different design strength, as shown in Table 3.1. However, only Experiment 2 made use of all three mixes, whereas Experiment 1 and 3 used Mix A. The mixes were designed to be 15 MPa, 30 MPa and 45 MPa, respectively, and are named Mix A to Mix C.

Table 3.1 Preliminary experiment mix designs

Amount (kg/m^3)			
Component	**Mix A**	**Mix B**	**Mix C**
Water	190	205	205
Cement	262	383	487
Stone	840	940	940
Sand	1075	852	764
Slump (mm)	97	105	111
Design Strength	15 MPa	30 MPa	45 MPa

For the main Experiments, 4 to 7, two new mixes were used. The first mix, Mix 1, was designed to be around 20 MPa with a w/c ratio of 0.76, whereas the second mix, Mix 2, was designed to be around 35 MPa in strength with a w/c ratio of 0.52. The proportions of both these mixes were optimised in trial mixes to ensure no segregation, good workability, and a slump value between 100 – 110 mm. These parameters allowed testing the concrete with the ICAR rheology meter, as discussed later in this section. Mix 3 was designed to test the influence of viscosity on plastic settlement cracking. A liquid viscosity modifying agent (VMA) was added to Mix 2, to form Mix 3. The CHRYSO quad 20 VMA was used, with a dosage of 0.23 kg VMA per 100 kg of cement, or, 1.035 kg/m^3.

The mix proportions of each mix are given in Table 3.2. The mixes consist of CEM III A-S 42.5 N Surebuild cement, natural pit sand known locally as Malmesbury sand and Greywacke aggregate/stone with a nominal size of 13.2 mm.

Table 3.2 Mix designs

	Amount (kg/m^3)		
Component	**Mix 1**	**Mix 2**	**Mix 3**
Water	230	235	235
Cement	300	450	450
Stone	900	850	850
Sand	926	832	832
VMA	0	0	1.035
Slump (mm)	108	110	145

3.2 Mould Design

The experiments in this study were done using two mould designs. The first mould, Figure 3.1, was smaller and mainly used to conduct the preliminary experiment before using the larger mould. The larger beam mould, Figure 3.2, was also firstly used for a preliminary experiment, Experiment 2. The cover depths of the reinforcing rods were adjusted to create the beam mould for the main experiments, as seen in Figure 3.3 and Figure 3.4.

To investigate the behaviour of plastic settlement cracks the mould needed to fulfil the following requirements:

- The length of the mould should be adequate to ensure that the rods does not influence each other.
- The moulds should be strong enough to handle the amount of concrete when filled up, without negatively impacting the structural integrity of the mould.
- It must have adequate depth to simulate real-life beam thickness and enable the use of different cover depths for the reinforcing rods.
- Must be reusable and easily deconstructed and reconstructed after every use.

Since the main topic of this study is to test plastic settlement cracking, the mould was designed to induce pure plastic settlement cracks. With both moulds, only single rods were placed throughout its length to concentrate and isolate the settlement effect as much as possible.

The preliminary mould dimensions were 300x300x200 mm, whereas the larger beam mould dimensions were 200x1200x200 mm, as shown in Figure 3.1 to Figure 3.3.

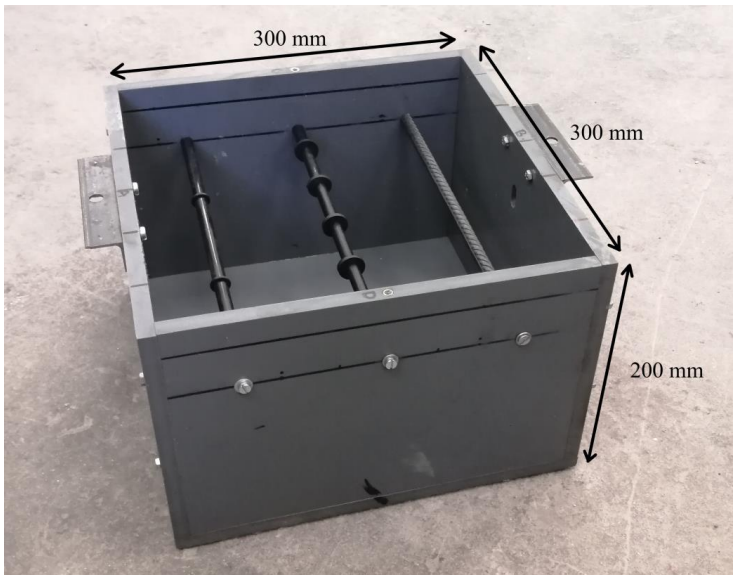

Figure 3.1 Preliminary testing mould with dimensions

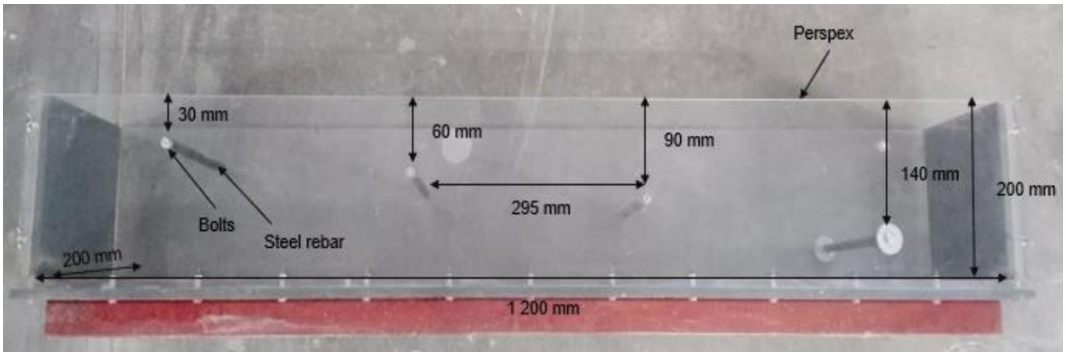

Figure 3.2 Beam mould used for preliminary experiment, with dimensions

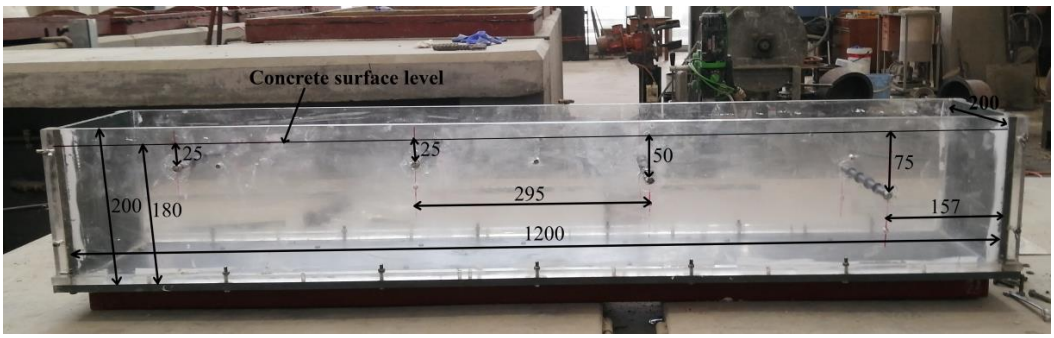

Figure 3.3 Beam mould with dimensions in mm

Figure 3.4 Beam mould

For the main experiments, four different reinforcing rods (10 mm diameter) were placed throughout its length, spaced 295 mm apart, at various depths. The first two rods were at the same depth since one of these rods were used for the traditional OPI test procedure, as discussed in Section 3.7, and the other one was used to test the crack severity from the side, as discussed in Section 3.8. The third and fourth rod were also used to perform the crack severity tests. The first two rods had a cover depth of 25 mm, the third 50 mm and the fourth 75 mm, as shown in Figure 3.3.

3.3 Mould preparation and finishing (Pre-cast procedure)

Every experiment needed to undergo the same preparation and finishing procedure to ensure consistency throughout the experiments and prevent any unwanted external factors to influence the results. Therefore, a strict procedure was followed before, during and after casting each beam.

For each of the main experiments, namely Experiments 4 to 7, the same beam moulds were used, as shown in Figure 3.4. Plastic rods were used, as discussed in Experiment 3, Section 4.2.3. Rubber O-rings were equally spaced on the rods. For the preliminary experiments, Experiment 2 and 3, the same pre-cast procedure was followed. However, the cover depths of the rods were different, and steel rods were used. Also, for Experiment 3, the preliminary test mould was used, as shown in Figure 3.1.

Before concrete was cast, the mould parts were cleaned thoroughly to make sure no liquids, dirt or remaining concrete was present. The mould was then assembled completely, with the sides added and screwed in place. The rods were then prepared. Each rod was cut to the appropriate length and a 6 mm hole was drilled in on their sides. This allowed the rods to be attached from the outside using a 5 mm bolt. The bolt only provided support and was not screwed into the rod. This allowed the bolts to be easily removed after the 6-hour period, as discussed in the next section. After the mould was fully assembled and the rods prepared, it was placed at the specific depths throughout the mould, as seen in Figure 3.3 and Figure 3.4.

The bottom of the mould, as well as a radius around area where the rods were placed, was covered in a thin layer of grease. A thin layer of oil was also placed on all the areas inside the mould, to prevent the concrete from sticking to it and allow the beams to be easily removed from the mould. The concrete could now be cast into the respective moulds.

3.4 Specimen extraction and preparation (Post-cast procedure)

After the beams were cast, it was vibrated for 1 minute on a vibrating table to ensure that the concrete compacted sufficiently, and most entrapped air was removed. The beams were then placed in a temperature-controlled room at 23^{o}C and 60% relative humidity to prevent any effects that a change in temperature or humidity might have on the beams. The concrete surface was then hand-floated with a steel trowel to ensure a smooth and constant surface finish.

It was important to keep all exposed sides, in this case only the top, sufficiently moist to prevent plastic shrinkage cracking to occur. This was achieved by covering the top of the concrete with a thin layer of moisture for the first 6-8 hours after being cast, as seen in Figure 3.5. After six hours the bolts that supported the rods in the beam were removed from the sides of the mould using a pair of pliers. The beam was then covered with a moist cloth or blanket, as seen in Figure 3.6. After 24 hours, the sides of the moulds were removed, thus exposing the sides of the beam, as seen in Figure 3.7. The blanket was again placed over the beam and kept moist for the following 28-days.

Figure 3.5 Beam after being cast, with thin layer of moisture on exposed surface

Figure 3.6 Beam covered with moist blanket

Figure 3.7 Side panels of the mould removed

After a period of 28 days, the beams were carefully removed from the mould, and cores were drilled in the appropriate places, as seen in Figure 3.8 to Figure 3.11. The first two reinforcements were at the same cover depth of 25 mm; therefore, one was drilled from the side/parallel to the reinforcement, and the other one was drilled from the top, as seen in Figure 3.12 and Figure 3.13. Two cores were obtained by drilling from the top in this case, but each core only produced one sample, since the reinforcement was needed in the centre of the sample, as seen in Figure 3.14. The remaining two rods, at 50- and 75 mm cover depths were also drilled from the side. Reference cores were drilled in each direction to be compared to the durability and crack severity samples. After the cores were obtained, the 30 mm thick specimens were cut from the cores using a concrete cutting table saw. Four 30 mm thick specimens

were cut from the reference and crack severity cores, whereas only one specimen could be cut from the top drilled OPI cores. The crack severity and OPI specimens used is shown in Figure 3.14 and Figure 3.15, respectively.

After the samples were obtained, they were tested as described later in Sections 3.7, 3.8 and 3.9.

Figure 3.8 Beam being core-drilled

Figure 3.9 Beam being core-drilled, close-up

Figure 3.10 Concrete cores from beam

Figure 3.11 Cores extracted from a beam

Figure 3.12 Top view of crack severity core, with the rod in the centre

Figure 3.13 Durability core, drilled through the top of the rod

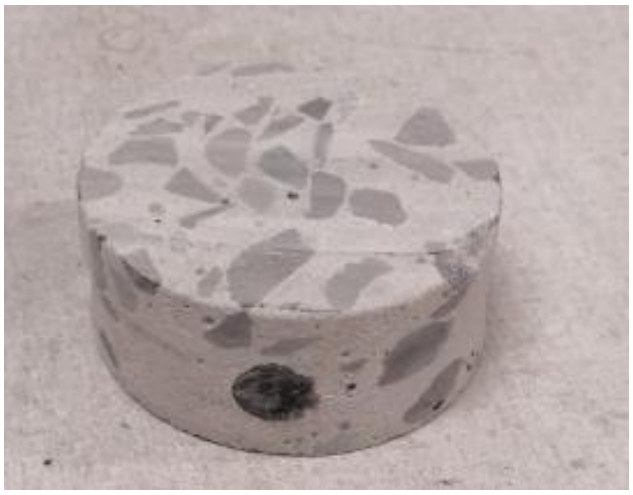

Figure 3.14 Concrete OPI sample

Figure 3.15 Concrete crack severity sample

3.5 Initial setting times test

The initial and final set times test was briefly discussed in Section 2.1.7. However, for this study only the initial setting times were tested since it was used to determine the time to apply the re-vibration to the concrete during the re-vibration experiment. The initial setting times were tested according to the ASTM C 403 (2008) manual, using the Vicat, as seen in Figure 3.16 and Figure 3.17.

3.5.1 Apparatus

A sieve was needed to sieve the concrete and obtain cement paste from the mix. A container was needed that could hold the cement paste after being sieved. A vibrating table was also needed to vibrate the cement paste in the conical ring container before performing the test. The vibrating table was also used to speed up the sieve process, alternatively, a manual method could be used, but it would take significantly longer.

The apparatus used to perform the tests was a Vicat, as seen in Figure 3.16, which consisted of parts labelled from A – F. This included the frame, A, holding a movable rod, B, which has a mass, C, which allowed the rod to have a specific weight to perform the penetration. The other end of the rod, D, holds the removable needle that penetrates the cement paste. This needle can be changed depending on the test performed. The rod is held in place by a setscrew, E, which must be loosened to perform the penetration. The Vicat also has an adjustable indicator, F, graduated in millimetres, to the nearest 1 mm. This was used to measure the penetration depth. The conical ring and bottom flat piece are indicated with G and H, respectively. A real-life representation of the apparatus is shown in Figure 3.17.

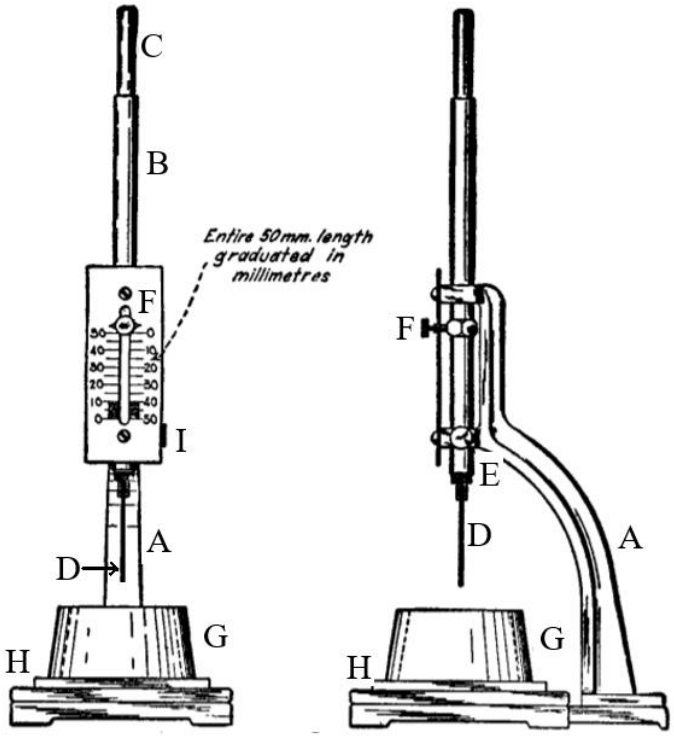

Figure 3.16 Vicat apparatus sketch (ASTM C 403, 2008)

Figure 3.17 Vicat apparatus with conical ring

The conical ring was used to hold the cement paste when performing the test. A top and bottom flat piece was used to support the cement paste in the ring from the bottom and cover the cement paste and ring between performing the penetration tests.

A temperature-controlled room was used to perform the test. Preferably controlled at 23ºC and 60% relative humidity. A stopwatch was used to time the duration of the test from the moment of mixing until the setting time was determined.

3.5.2 Test procedure

After the concrete was mixed, the timer was started and the concrete was scooped onto the sieve, which was placed in a steel container. The container and sieve were then placed on the vibrating table and vibrated until there was mainly aggregate left in the sieve. During the vibrating period, the concrete was mixed around with a trowel. This procedure was repeated until enough cement paste was collected to fill three separate conical rings. After the rings were filled with cement paste it was vibrated for 30 seconds and levelled with a trowel.

The three rings filled with cement paste was placed in a temperature-controlled room and covered with a plastic flat piece. The specimens were left undisturbed for 30 minutes after moulding. After the initial 30 minutes the Vicat test was performed every 15 minutes to measure the distance of penetration of the 1 mm Vicat needle, until a penetration of 25 mm or less was obtained. This was performed by lowering the movable rod where the point of the needle barely touches the surface of the cement paste and

releasing the rod quickly. It was important to clean the needle after every drop to keep it clean and preventing it from influencing the results.

The initial setting time was the time from the first contact of water and cement, until the penetration of the needle reached 6 ± 3 mm from the bottom.

3.6 ICAR Rheometer test

One of the factors considered in this study is the viscosity of the concrete and its effect on plastic settlement cracking. Therefore, a rheometer was utilised to measure the plastic viscosity of the concrete and relate the viscosity to the crack severity to find a correlation between the two factors. To perform the viscosity tests an ICAR rheometer was used on Mix 1, Mix 2, and Mix 3. The rheometer tests were conducted as described in the ICAR Rheometer Manual, by Germann Instruments (GI, 2016).

3.6.1 Apparatus

To perform a standard rheology test using the ICAR rheometer, the following apparatus, as seen in Figure 3.18 and Figure 3.19, were used: a laptop or computer with the necessary installed software, ICAR concrete container, ICAR Rheometer, the vane and the frame which hosts all the components and the necessary power and LAN cables.

The container has a volume of 20 litres. To prevent the concrete from slipping on the container wall it has vertical strips along the side. The vane is centred into the container through the frame. It consists of four blades each of equal size (127x63.5 mm) (GI, 2016).

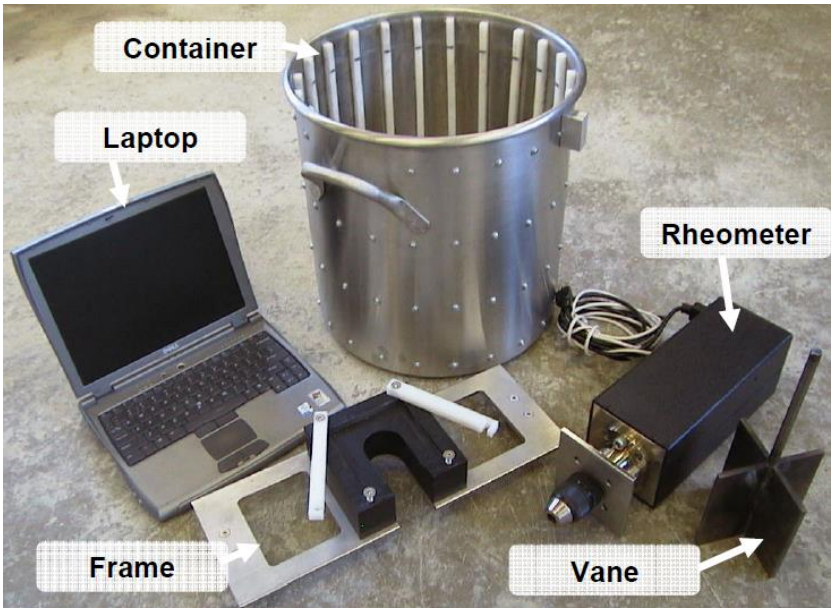

Figure 3.18 ICAR Rheometer components (GI, 2016)

Figure 3.19 ICAR Rheometer components assembled (GI, 2016)

3.6.2 Concrete conditions

All the components of the concrete mix were placed in a temperature-controlled room, at 23 ± 2ºC and 60% relative humidity, at least 24 hours before mixing occurred. This was done to keep the results as consistent as possible.

It was also important that the tests were performed as soon as possible after the concrete was mixed, to ensure the most accurate results.

3.6.3 Test procedure

The ICAR rheometer can perform a flow curve test and a stress growth test. However, in this study only the flow curve test was performed. The flow curve test is used to compute the Bingham parameters of yield stress and plastic viscosity by measuring the relationship between shear stress and shear rate.

A 25-litre concrete mix was made, and the container was filled with the concrete to the top of the vertical strips, directly after being mixed. Due to the high slump of the mixes, no additional compaction was needed. The container was just lightly tapped on the side to let the concrete set evenly.

The vane, frame and rheometer were then assembled and placed on the container with the vane into the concrete, as seen in Figure 3.20. The frame was latched onto the blocks on the side of the container as seen in Figure 3.21.

The input parameters required to perform the flow curve tests and obtain the Bingham parameters were breakdown speed and time, number of points, time per point, initial speed, and final speed, as seen in Table 3.3. The test ran for about one minute.

Figure 3.20 Assembled rheometer placed into concrete

Figure 3.21 Frame attached to the container

Table 3.3 Flow curve test input parameters

Parameter	Value
Breakdown Time	25 s
Breakdown Speed	0.20 rps
Number of Points	7
Time per Point	5 s
Initial Speed	0.20 rps
Final Speed	0.05 rps

3.7 Oxygen Permeability Index (OPI) test

The OPI test was briefly mentioned in Section 2.6.2.1. The standard OPI testing procedure is described as follows. The permeability of the concrete samples was measured in permeability cells as shown in Figure 3.22, where the rate of pressure decay was determined. This was conducted 28 days after casting since the concrete age can have a significant effect on the results. The OPI tests were conducted as described in the Durability Index Testing Procedure Manual, by the University of Cape Town (UCT, 2017).

3.7.1 Apparatus

The apparatus used to perform a standard OPI test were four permeability cells of 5 litre each, shown in Figure 3.22. Each cell held a rigid sleeve on the top of the cell. The rigid sleeve hosted a rubber collar in which the concrete specimen was placed. The rubber collar allows a tight seal to the specimen. On top of the collar, it fits a plastic ring and a cover plate that tightens everything together. These apparatuses are shown in Figure 3.23 to Figure 3.29.

Figure 3.22 Full permeability cell setup

On each of the permeability cells there were pressure gauges and transducers, which provide the pressure reading to an accuracy of at least 0.5 kPa. The oxygen, which has a purity of at least 99.8%, was supplied through a pipe system connected to the permeability cells. The whole system was also connected to a computer that takes readings electronically. The electronic readings were found to be more accurate than eyeballing the readings from the gauges. Another PC was connected to the OPI computer using a LAN cable. It was able to log and store the data electronically and used to export the data after the experiments. A Vernier calliper, capable of reading 0.01 mm was also used to measure the thickness of the samples (UCT, 2017).

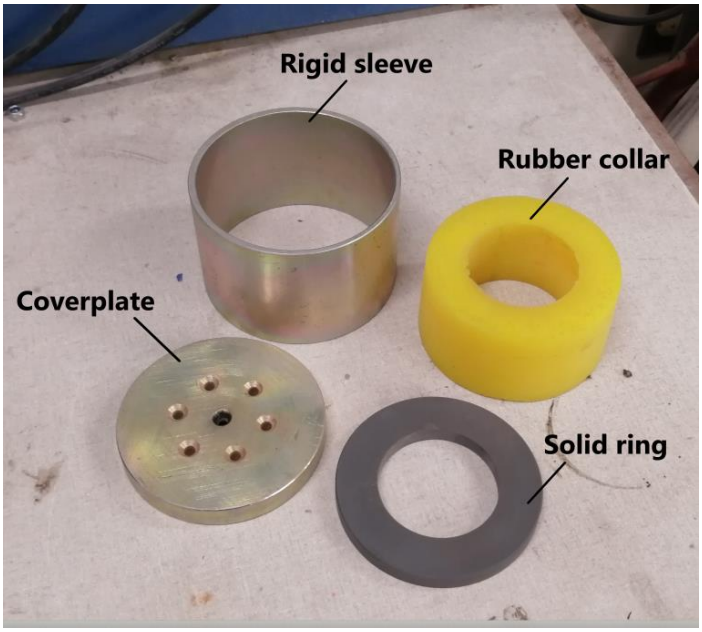

Figure 3.23 Apparatus used to hold the concrete specimen for the OPI test

3.7.2 Specimen conditions

For the standard OPI test, the concrete was core-drilled from the top, through the plastic rod, to obtain the concrete specimens, as seen in Figure 3.26. A visual representation of the drilling direction is shown in Figure 3.24 and Figure 3.25. The cores were then cut into a 30 mm disc, as seen in Figure 3.27, with the rod in the centre of the specimen. The thickness and diameter of the specimens were measured with a vernier calliper to the nearest 0.01 mm. The thickness was measured at four different points, equally spaced around the perimeter of the specimen, and the average was used. The specimens were oven-dried at 50 ± 2°C for seven days.

After the drying period, the specimens were placed in a temperature-controlled room, controlled at 23 ± 2°C and 60% relative humidity, to cool down for 2 to 4 hours. After the cooling period the testing was started. For the OPI test two specimens were tested for each beam, which was extracted from the 25 mm cover rod.

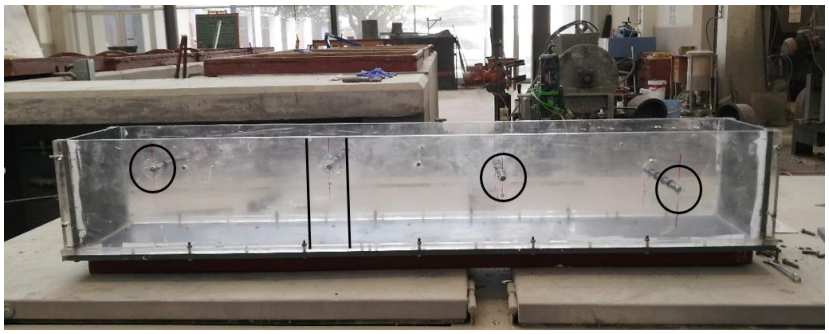

Figure 3.24 OPI cores drilled from the top, represented by the vertical straight lines

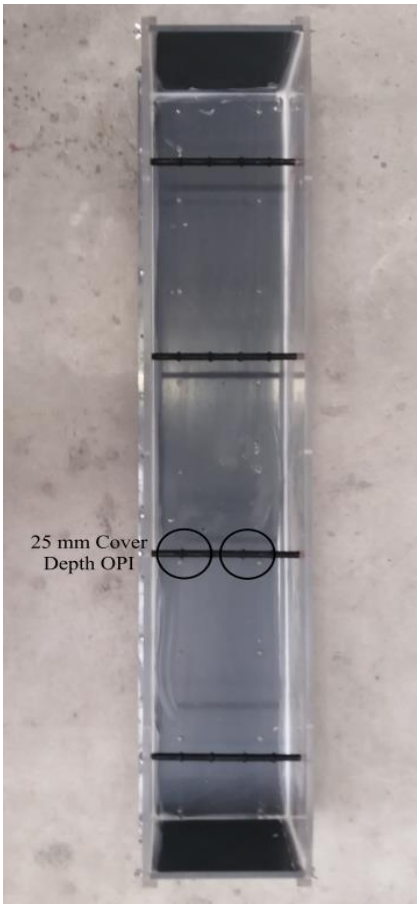

Figure 3.25 OPI cores drilled from the top, through the rod

Figure 3.26 Concrete core drilled from the top

Figure 3.27 Durability concrete specimen

3.7.3 Testing procedure

After samples were obtained and oven-dried, it was tested using the OPI test procedure. The 70 ± 2 mm Dia. x 30 ± 2 mm thick specimens were placed in the compressible rubber collar. The compressible collar was then placed in a rigid sleeve and covered with a solid ring and cover plate, as seen in Figure 3.28 and Figure 3.29. The specimen, collar and rigid sleeve were placed on top of the permeability cell and slid into the circular groove around the hole on the top of the cell. The top screw was then tightened on top of the cover plate to seal it and hold it in place, as seen in Figure 3.30 and Figure 3.22.

The oxygen inlet was opened, and the pressure gauge was set to 100 ± 1 kPa. The initial time was recorded to allow data extraction from the computer after the tests were completed. The pressure after 5 minutes was also recorded to the nearest 0.5 kPa. For the durability samples, the standard OPI procedure was followed, where the time was taken after every ± 5 kPa pressure drop for at least eight intervals or 6 hours. After the tests were completed, the data was exported from the connected computer and used to perform the following calculations.

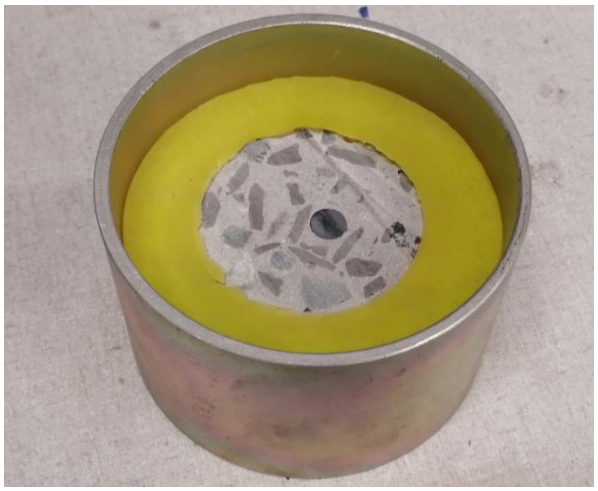

Figure 3.28 Concrete specimen inside the rubber collar, placed in the rigid sleeve

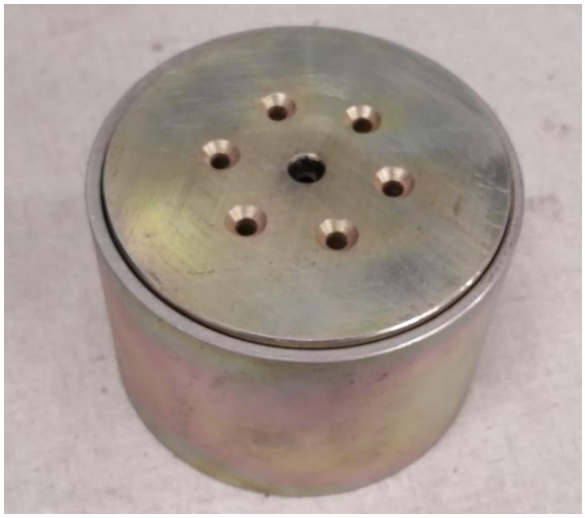

Figure 3.29 All the apparatus assembled, with the solid ring and coverplate in place

Figure 3.30 The specimen and housing placed on the permeability cell, with the coverplate tightened

3.7.4 Calculations

The pressure decay was measured with time increments to obtain a logarithmic relationship between pressure and time. The D'arcy coefficient of permeability may be calculated from Equation 3.1.

$$k = \frac{\omega \cdot V \cdot g \cdot d \cdot z}{R \cdot A \cdot T} \tag{3.1}$$

Where

k is the coefficient of permeability in metres per second [m/s]

ω is the molecular mass of oxygen [i.e. 0.032 kg/mol]

V is the volume of permeability cell to the nearest 0.01 litre or 0.00001 m^3 [i.e. 4.89 l]

g is the gravitational acceleration [m/s^2]

d is the average specimen thickness to the nearest 0.02 mm

z is the slope of linear regression line = $\frac{\Sigma\left[\ln\left(\frac{P_0}{P_t}\right)\right]^2}{\Sigma\left[\ln\left(\frac{P_0}{P_t}\right)\cdot t\right]}$

R is the universal gas constant [8.313 Nm/Kmol]

A is the cross-sectional area of the specimen [m^2]

T is the absolute temperature in Kelvin [K]

Using the coefficient, k, the OPI can then be determined using Equation 3.2.

$$OPI = -log_{10}(k) \tag{3.2}$$

3.8 Crack severity test (modified OPI test)

Plastic settlement cracks are not always visible at the surface of the concrete, therefore, to test the crack severity around the reinforcing rod, cores were drilled from the side of the beam, parallel to the rod. It was assumed that a more rapid pressure decay would indicate a higher crack severity, since cracks would allow more oxygen to permeate through the concrete at a higher rate.

An illustration of how the beam was drilled from the side to capture the behaviour of the plastic settlement cracking is shown in Figure 3.31. The core was placed to ensure that the rod was at the centre, which allowed sufficient area to capture the surrounding plastic settlement cracks, caused by the rod.

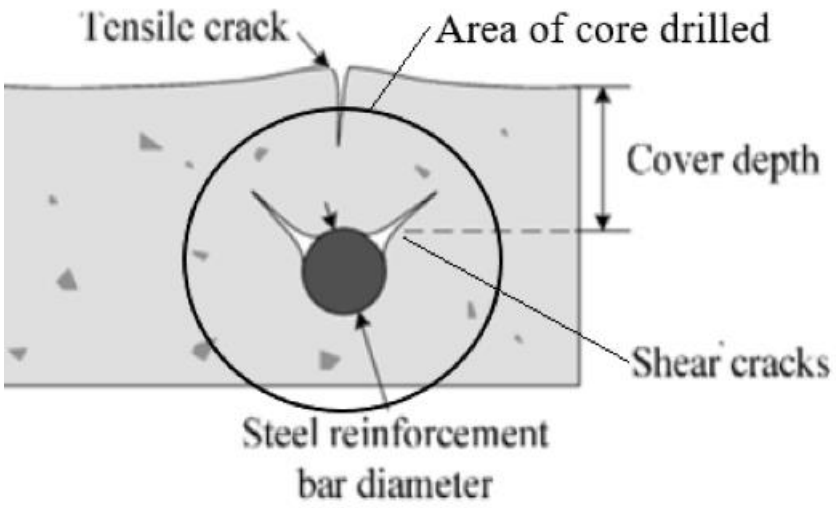

Figure 3.31 Crack severity test illustration

The crack severity testing procedure was similar to the OPI testing procedure. The only difference was with the specimen conditions and the duration of the test. The crack severity of concrete samples was also measured in the permeability cells as shown in Figure 3.22, where the rate of pressure decay was

measured, from 100 kPa to 0 kPa. This test was conducted at least 28 days after casting since the concrete age can have a significant effect on the results.

3.8.1 Apparatus

The apparatus used for the crack severity test was exactly the same as discussed for the OPI test, in Section 3.7.1.

3.8.2 Specimen conditions

As mentioned, for this test the concrete beams were drilled from the side, parallel to the plastic rod, as shown in Figure 3.34 and Figure 3.35. A visual representation of the drilling direction for the crack severity cores is shown in Figure 3.32 and Figure 3.33. The locations of the O-rings were then marked on the core with a marker, as to have the O-rings in the centre of the specimens. To obtain a single specimen, the core was then cut 15 mm on each side of an O-ring mark, as seen in Figure 3.36. This produced four specimens per core.

The specimens were oven dried at 50 ± 2ºC for 24 hours. After the drying period, the specimens were placed in a temperature-controlled room, controlled at 23 ± 2ºC and 60% relative humidity, to cool down for 2 to 4 hours. After the cooling period the test was started. For the crack severity test four specimens were cut from each core, therefore four specimens were tested at each cover depth.

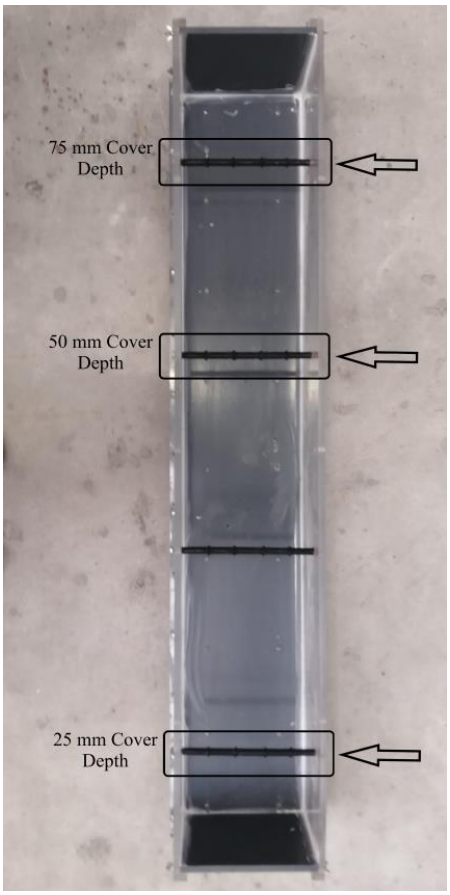

Figure 3.32 Crack severity cores drilled from the side represented by the rectangles and arrow direction

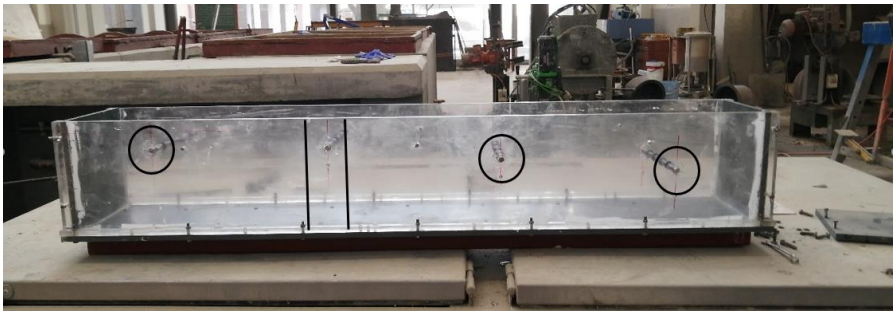

Figure 3.33 Crack severity cores drilled from the sides, represented by the circles

Figure 3.34 Crack severity core, drilled from the side of the beam over the reinforcing rod

Figure 3.35 Top view of crack severity core

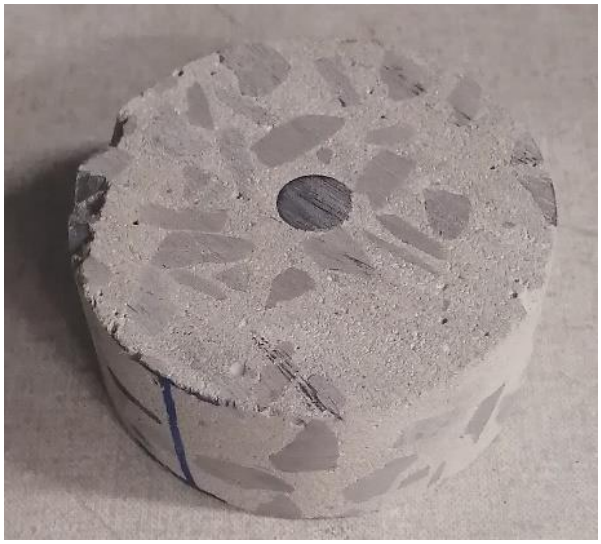

Figure 3.36 Crack severity concrete specimen

3.8.3 Testing procedure

The testing procedure was the same as the OPI testing procedure. The only difference was, the durability samples were tested for 8 intervals, or at least 6 hours, whereas the crack severity samples were tested to find a complete pressure decay curve over time, so the pressure was allowed to drop from 100 kPa to 0 kPa, irrespective of the time it takes.

3.9 Water sorptivity test

The water sorptivity test was briefly described in Section 2.6.2.2. This test method determines the water sorptivity index of concrete as well as the water-penetrable porosity of the specimen. This test should be conducted at least 28 days after casting since the concrete age can have a significant effect on the results. The water sorptivity tests were conducted as described in the Durability Index Testing Procedure Manual, by the University of Cape Town (UCT, 2017).

Cracks in the concrete are likely to influence the sorptivity rate since it acts as pathways for the water solution to travel through the concrete. Therefore, it was assumed that the concrete with a higher sorptivity rate has more severe cracks, in the case of the crack severity samples and a lower durability in the case of the OPI samples. In literature it was stated that concrete with a higher porosity typically has a lower durability. Therefore, it was assumed that the concrete with a higher percentage of pores has a lower durability. The sorptivity, combined with the porosity gave a good indication of the crack severity of the concrete and how it correlates with the concrete durability.

3.9.1 Apparatus

The apparatus used to conduct the water sorptivity tests were an oven, capable of maintaining a temperature of 50 ± 2^{o}C, where the concrete specimens were placed after being obtained from the beams. Plastic or stainless-steel trays with a minimum depth of 20 mm were used where the concrete samples were placed to conduct the tests. These trays were large enough to hold seven specimens at a

time. Ten layers of absorbent paper towel were used to support the specimens. Alternatively, two small rollers or four pins could have been used.

A vernier calliper, capable of reading to 0.01 mm accuracy was used to measure the exact dimensions of each concrete sample. The measurements were used in the calculations. A measuring scale was also needed with an accuracy reading to 0.01 g. Calcium hydroxide was mixed with tap water, with a concentration of 5 grams of $Ca(OH)_2$ per 1 litre of water. The mixture was maintained at 23 ± 2ºC. To measure the timing increments a stopwatch was required.

Packaging tape was used to seal the curved edges of the specimens watertight, as seen in Figure 3.37. Other forms of seals could have also been used. Before the specimens was tested it cooled down in a temperature-controlled room at ± 23ºC and 60% relative humidity. A desiccator could also be used. A vacuum saturation facility was also used for the second part of the experiment to determine the porosity of the concrete specimens (UCT, 2017).

Figure 3.37 Prepared concrete specimen with packaging tape to seal the sides

3.9.2 Building the vacuum saturation facility

To perform the second part of the water sorptivity test, a sealed vacuum saturation facility was needed. This was used to isolate the specimens from any influence of air on the results of the test.

At first a 25-litre metal bin was used. However, the bin could not withstand the required -80 kPa pressure to conduct the experiment. Thus, a square PVC mould, as seen in Figure 3.38, was used. It has the same dimensions as the mould shown in Figure 3.2. A flat PVC piece was used to create the lid of the container. A groove of 3 – 4 mm was cut from the lid to allow it to fit tightly into the square mould, and provide additional stability and seal, as seen in Figure 3.39.

Figure 3.38 Mould used to build the vacuum saturation facility

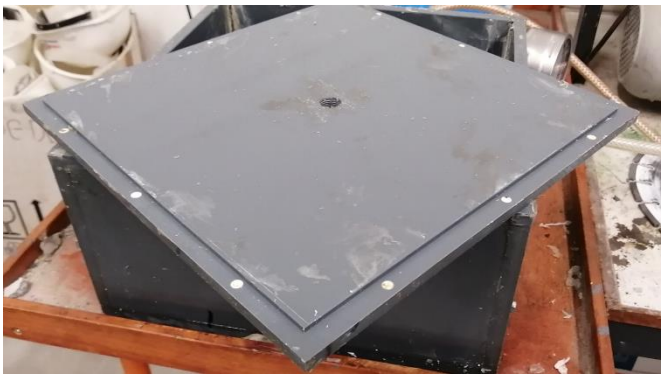

Figure 3.39 Lid of vacuum facility with inserted groove

A controllable valve was fitted and sealed to the lid to allow the vacuum pump to be attached to the container, as seen in Figure 3.40. The lid was sealed to the body using a strong bond type silicone, as well as metal brackets specifically made to fit over and tighten around the container using bolts and rods. The final container is shown in Figure 3.41. The container was not exactly designed as shown in the manual, however, it served the same purpose and could conduct the experiment as needed.

Figure 3.40 Valve inserted in the lid to connect the vacuum pump

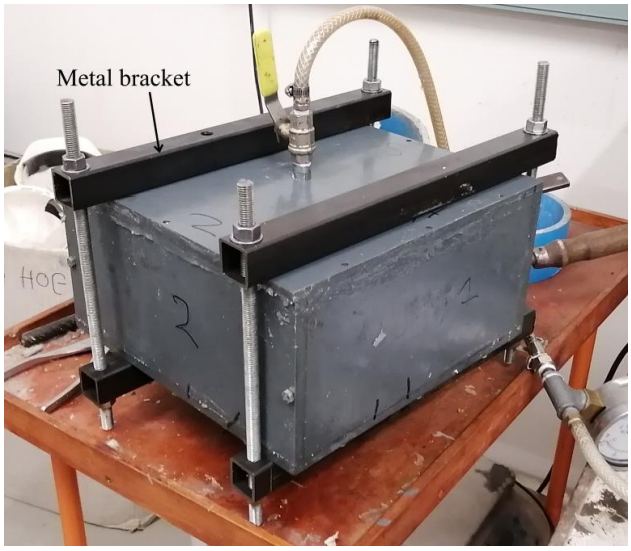

Figure 3.41 Complete assembled vacuum facility connected to the vacuum pump

3.9.3 Specimen conditions

The water sorptivity test was conducted using the oxygen permeability or crack severity test samples. It was also performed as soon as possible after conducting the OPI or crack severity tests. For the OPI samples, that already underwent a 7-day drying period, another drying period was not needed. However, if the water sorptivity test was not conducted within 3 hours after the oxygen permeability test or only conducted the next day, the samples were placed in the oven again overnight. The crack severity specimens were placed in the oven at 50 ± 2ºC for only six days after performing the oxygen permeability test, since it was already placed in the oven for 24 hours before the crack severity test. After the six-day period, the specimens underwent the standard water sorptivity test procedure.

In both cases the specimens were placed in a temperature-controlled room, 23 ± 2ºC and 60% relative humidity, for two to four hours to cool down after being removed from the oven.

The specimens were measured to the nearest 0.01 mm, using a vernier calliper, at four points to obtain the average thickness of each specimen. The curved sides of the specimens were sealed using a sealant, such as insulation tape or thick packaging tape, as seen in Figure 3.37.

3.9.4 Test procedure

The water sorptivity test was conducted in a temperature-controlled room, at 23 ± 2ºC and 60% relative humidity. The specimens were first set in the temperature-controlled room for two to four hours, after being removed from the oven, before the test was performed. Ten layers of paper towel were placed in a plastic tray. The calcium hydroxide solution was then poured into the tray, until the water was visible on top of the paper towels. Air bubble were removed from the paper towels by smoothing the paper towards the edges.

The specimens were weighed to obtain the mass at time 0, and then added onto the paper towel after the stopwatch was started. It was ensured that the water level remained at around 2 - 3 mm up the side of the specimens, as seen in Figure 3.42. The specimens were weighed to the nearest 0.01 grams, within ten second of removal, at various time intervals, namely, 3, 5, 7, 9, 12, 16, 20 and 25 minutes. When the specimens were picked up to be weighed, they were rubbed with a paper towel to remove any running water from the surface. It was also ensured that excess water did not drip from the picked-up specimen onto the remaining specimens.

Figure 3.42 Water sorptivity test being performed

After the weighing period, the vacuum chamber test was performed. It was important to perform the test no later than 24 hours after the weighing was complete. The specimens were placed in the vacuum saturation tank, as seen in Figure 3.43. They were arranged to balance on their curved edges as to maximise the exposed surface area. The lid of the tank/chamber was sealed with a strong-bond silicon to ensure an air-tight seal.

Figure 3.43 Specimens placed in vacuum facility

The tank was evacuated to between -75 and -80 kPa (-0.75 to -0.8 bar), as seen in Figure 3.44, for two hours. After two hours ± 15 minutes the tank was filled with the calcium hydroxide solution, through the opening in the lid, as seen in Figure 3.45. The exact amount of solution was calculated in order to cover about 40 mm above the top edge of the specimens.

Figure 3.44 Pressure gauge reading

Figure 3.45 Calcium hydroxide solution added to in the chamber through the lid

The vacuum was re-established to between -75 and -80 kPa for one hour ± 15 minutes. After one hour the vacuum was released and the specimens were allowed to soak for a further 18 hours ± 1 hours. After 18 hours the specimens were removed and tapped dry, whereafter it was weighed to an accuracy of 0.01 grams. This was recorded as the vacuum saturated mass, M_{sv}, of the specimen.

3.9.5 Calculations

The sorptivity and porosity was determined by performing the following calculations. Note: all the mass measurements were taken to the nearest 0.01 grams, and the time measurements were taken to the nearest 0.001 hours.

The porosity (n) was determined using Equation 3.3.

$$n = \frac{M_{sv} - M_{s0}}{Ad\rho_w} \times 100 \tag{3.3}$$

Where,

M_{sv} is the vacuum saturated mass of the specimen [g].

M_{s0} is the mass of the specimen at the start of the experiment, at time 0 [g].

A is the cross-sectional area of the flat face of the specimen [mm^2].

d is the average specimen thickness taken from four different measurements [mm].

ρ_w is the density of water in grams per millimetres cubed [g/mm^3].

The results were plotted of the mass gain (M_{wt}) versus the square root of time, using Equation 3.4.

$$M_{wt} = F\sqrt{t} \tag{3.4}$$

Where,

F is the slope of the best fit line from plotting M_{wt} against the square root of time [g].

t is the time in hours after the specimen was first exposed to water, at time 0 [h].

The mass gain (M_{wti}) was determined using Equation 3.5.

$$M_{wti} = M_{st} - M_{s0} \tag{3.5}$$

Where,

M_{st} is the mass of the specimen at any particular point in time t [g].

M_{s0} is the mass of the specimen at the initial time (t_0) [g].

The correlation coefficient, r^2, was determined using Equation 3.6.

$$r^2 = \left[\frac{\sum\left(\sqrt{t_i} - T\right)(M_{wti} - \bar{M}_{wt})}{\sqrt{\sum\left(\sqrt{t_i} - T\right)^2 \sum(M_{wti} - \bar{M}_{wt})^2}}\right]^2 \tag{3.6}$$

Where,

M_{wti} is the mass gain as determined using Equation 3.5.

t_i is the corresponding time of the mass gain reading [h].

and

$$\bar{M}_{wt} = \frac{\sum M_{wti}}{n} \tag{3.7}$$

and

$$T = \frac{\sum \sqrt{t_i}}{n} \tag{3.8}$$

Where,

n is the number of data points.

Note the following:

- If a coefficient of correlation (r^2) of less than 0.98 was achieved, the last value (25 min) was disregarded and r^2 was re-calculated, while adjusting the number of data points (n) as needed.
- If r^2 is still less than 0.98,
- If r^2 was still less than 0.98, r^2 was re-calculate by disregarding the next value, i.e. 20 min. from the analysis, and adjusting n as needed.
- If the problem still persisted, the above procedure was repeated until a value of 0.98 was achieved, or less than 5 data points remained.
- If after the above procedure was followed, a value of 0.98 could not be achieved, with a set of five or more data points, the specimen was disregarded.

After a value of larger than 0.98 was achieved within the steps given above, the slope of the line of best fit was determined by linear regression, using Equation 3.9.

$$F = \frac{\sum\left(\sqrt{t_i} - T\right)\left(M_{wti} - \bar{M}_{wt}\right)}{\sum\left(\sqrt{t_i} - T\right)^2} \tag{3.9}$$

Where,

F is the slope of the line of best fit [g/h$^{0.5}$].

M_{wti} is the mass gained as calculated with Equation (.

t_i is the corresponding time of the mass gain reading [h].

$\bar{M}_{wt}$ and T were determined as shown in Equation 3.7 and 3.8, respectively.

The water sorptivity, measured in mm/√h, of the specimen was determined using Equation 3.10.

$$S = \frac{Fd}{M_{sv} - M_{s0}} \tag{3.10}$$

Where,

F is the slope of the line of best fit [g/h$^{0.5}$].

d is the average thickness of the specimen [mm].

M_{sv} is the vacuum saturated mass of the specimen [g].

M_{s0} is the mass of the specimen at the initial time (t_0) [g].

3.10 CT scans

After performing the crack severity, OPI, and water sorptivity tests, a good understand could be drawn regarding the cracks in the concrete. However, since the plastic settlement cracks of interest to the study are usually not visible, CT scans were performed to visualise the cracks and compare it to the results of the mentioned tests. For each beam one crack severity specimen at the 50 mm cover depth was used for the CT scans, except for Beam 2 of Experiment 4, where a 25 mm cover depth sample were also used to compare the cover depth results between the 25 mm and 50 mm rods. The re-vibration experiment also showed interesting results, as discussed in Section 4.4, with its 75 mm cover sample. Thus, one 75 mm cover sample from that beam was also scanned. The CT scans were not used for a detailed analysis on the volume of the cracks or porosity calculations, but rather to visualise the near invisible cracks in the beam around the reinforcement.

3.11 Experiments

This section discusses the experiments conducted in the study. Experiments 1 to 3 was the preliminary experiments and Experiments 4 to 7 was the main experiments that was used to draw the final conclusions of the study. A summary of the experiments, the mix used, phenomenon tested as well as the tests performed is shown in Table 3.4.

Table 3.4 Summary of experiments performed during this study

Experiment	Beam name	Mix Used	Phenomenon tested	Tests performed
1	-	Mix A	Preliminary experiment testing the OPI procedure.	OPI test.
2	15 MPa, 30 MPa and 45 MPa Beam	Mixes A, B and C	Preliminary experiment testing the effect of cover depth on plastic settlement cracking, using three different strength mixes and steel rods.	Crack severity test.
3	-	Mix A	Preliminary experiment testing the effect of different types of rods and how it influences the crack severity of the concrete.	Crack severity test.
4	Beam 1, Beam 2	Mixes 1 and 2	Testing the influence of cover depth on plastic settlement cracking, using two different strength mixes and plastic rods with O-rings.	OPI test, crack severity test, water sorptivity test and CT scan.

5	Beam 3	Mix 2	Testing the influence of re-vibration of concrete after a period of time on plastic settlement cracking	OPI test, crack severity test, water sorptivity test and CT scan.
6	Beam 4	Mix 3	Testing how a liquid VMA influences the plastic viscosity of a concrete mix and how that influences plastic settlement cracking.	OPI test, crack severity test, water sorptivity test and CT scan.
7	Beam 4	Mix 2	Testing the influence of plastic shrinkage cracking combined with plastic settlement cracking on concrete.	OPI test, crack severity test, water sorptivity test and CT scan.

3.11.1 Preliminary experiments

3.11.1.1 Preliminary cylindrical concrete moulds (Experiment 1)

For the first practical experiment of the study, PVC pipes were used to create individual concrete moulds. The PVC pipes were 110 mm in diameter and 300 mm in height each. The pipes were glued to a 150x150x10 mm piece of flat PVC.

Holes on both sides of the pipe were drilled, each mould at a different depth, to allow the reinforcing rods to be inserted through the sides of the PVC pipe to act as the restraining factor. Each had a different cover depth, namely, 20 mm, 60 mm, and 100 mm cover. Each sample was drilled from the top, cut on both sides of the reinforcement and then tested according to the standard OPI test procedure.

3.11.1.2 The influence of cover depth on plastic settlement cracking (Experiment 2)

This experiment was designed to determine the effect of concrete cover depth on plastic settlement cracking. The beam mould used in this experiment had slightly adjusted cover depths for the rods compared to the standard beam mould shown in Section 3.2. The rods were placed at different cover depths throughout the length of the beam, 30 mm, 60 mm, 90 mm, and 140 mm, respectively, as seen in Figure 3.46. Also, three different concrete mixes were used, each with a different design strength, as discussed in Section 3.1, to correlate the influence of concrete strength and viscosity to the crack severity of the concrete.

Each beam underwent the same casting procedure. However, this was not the standard procedure as described in Section 3.3 and 3.4, but it was very similar. The main difference with this experiment was that the beams were not constantly cured after being cast, therefore, these results were not used to draw any final conclusions. It did, however, provide insight into how to perform the main experiments to follow. Only the crack severity test was performed for this experiment.

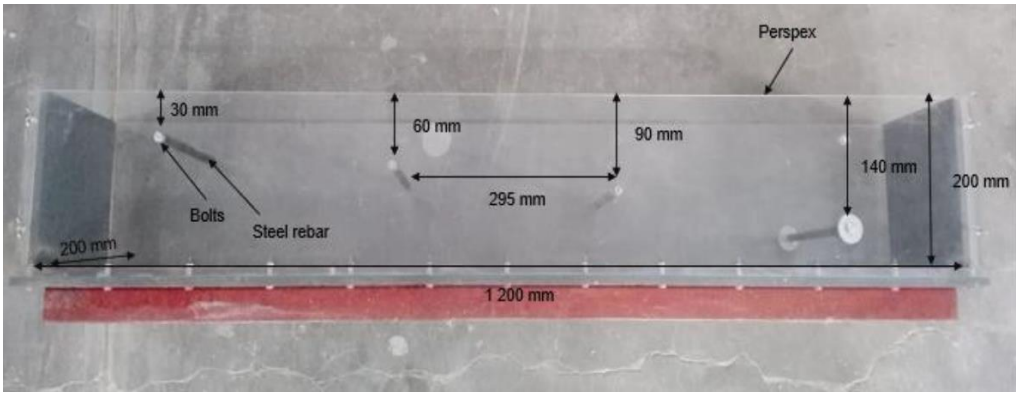

Figure 3.46 Mould and spacing used (Sukhnandan, 2019)

3.11.1.3 The influence of different reinforcement types on plastic settlement cracking (Experiment 3)

After conducting the experiments discussed in the previous sections, it was discovered that the steel reinforcement damaged the concrete when cutting through it, which may cause additional cracks or voids in the samples, as seen in Figure 3.47. It was also discovered that when cutting through the samples the steel rod vibrated loose inside the sample, and thus the crack severity tests only lasted a few seconds each, which was not ideal.

In an attempt to lower the rate to a more realistic value, it was decided to investigate other possibilities of rod materials or adjustments to the rod, which would still simulate the same effect of steel rods in terms of plastic settlement cracking in the concrete.

Different materials and conditions for rods, each 10 mm diameter, were tested; clean plastic, plastic with tightly fitted O-rings of 15 mm outer diameter, plastic with tightly fitted rubber-washers with an outside diameter of 20 mm, also a standard steel rebar.

To prevent a straight path between the rod and the concrete for the air to follow, O-rings were added to the rod to be a form of resistance to slow down the rate of pressure decay and make the readings more interpretable. The washers and O-rings were added in an attempt to lower the rate of pressure decay through the sample during the crack severity tests to a few minutes, instead of a few seconds. It was found difficult to interpret the data of the pressure decay if it did not at least last a few minutes. It was also important that the washer/O-ring did not have an intrusive influence on the settlement cracking, but still lowered the rate of pressure decay to an interpretable rate.

To test the difference in materials, a sample mould was built with the different rods, as seen in Figure 3.48. The left reinforcement was the clean plastic and plastic with the O-rings, the middle was the plastic with rubber washers and on the right was the standard steel rebar.

Figure 3.47 Effect of standard steel reinforcement on concrete sample

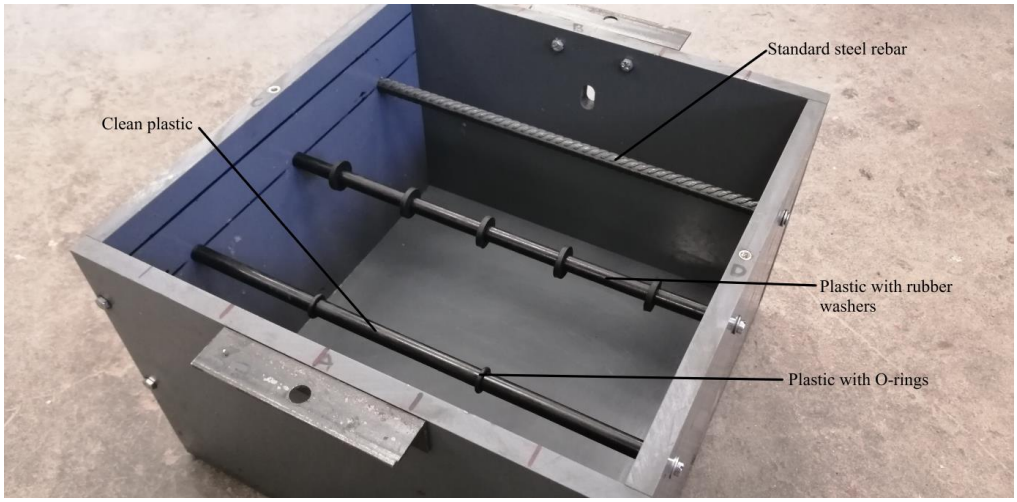

Figure 3.48 Different types of reinforcements

After the concrete block was cast, the post-cast procedure was followed as mentioned in Section 3.4. However, in this case, two samples with O-rings were obtained, and two with clean plastic, whereas three samples of the plastic with washers and steel rods were obtained. The crack severity test was then performed on the respective samples.

3.11.2 The influence of cover depth on plastic settlement cracking (Experiment 4)

After the results of the previous experiment, as discussed in Section 4.2.3, it was decided to use plastic rods with tightly fitted O-rings, instead of steel rods to simulate plastic settlement cracking. This was purely from a practical standpoint and not to suggest that plastic reinforcement would supply a superior strength capacity to the concrete. However, it was assumed to serve the same purpose in this experiment as a steel rod.

The standard beam mould, as shown in Section 3.2, was used for this experiment. The first two rods were placed at the same cover depth of 25 mm. This allowed one rod to be tested using standard OPI

testing procedure, whereas the other rod was tested according to the crack severity testing procedure, which allowed the crack severity results to be compared to the OPI value and durability results. The other two rods were placed at cover depths of 50 mm and 75 mm, respectively, and was also tested according to the crack severity testing procedure. Two concrete mixes were used for this experiment, as shown in Table 3.2.

It is well-known, as described in the literature study, that the cover depth of concrete greatly influences the plastic settlement cracking. This experiment tested the theory by determining the crack severity at the different cover depths and relating it to the OPI and water sorptivity results. The water sorptivity test was also performed to determine if there was more evidence of a correlation between the cover depth and crack severity to the durability of the concrete. Since two beams of different strengths were used in this experiment, the influence of concrete strength on these factors could also be determined.

3.11.3 The influence of re-vibration of concrete on plastic settlement cracking (Experiment 5)

As concrete settles, it creates voids and plastic cracks at points of restraint. However, if the concrete could be compacted again, while still in its plastic state, these voids and cracks might close. Re-vibration of concrete is known to improve the concrete strength and mitigate plastic settlement cracks, as discussed in Section 2.2.3.

Therefore, to test the impact of re-vibration on plastic settlement cracking and the crack severity, a beam was cast following the standard procedures described. Using the initial setting time of the concrete, as described in Section 3.5 and 4.1, as a guide, the re-vibration was applied after 3 hours. The beam was re-vibrated for 1 minute. After the re-vibration, the beam was immediately placed back into the climate-controlled room and the rest of the standard post-cast procedure was followed.

The beam also had rods at various cover depths in order to determine how re-vibration affects the concrete at different depths. The crack severity testing of the 25 mm specimen could also be directly compared to the OPI of the 25 mm durability sample, to find a possible correlation between crack severity and concrete durability. This correlation was further investigated by performing the water sorptivity test. Mix 2 was used for this beam to compare the results of the re-vibration to the results of the previous experiment that used Mix 2 for a beam. Thereby the re-vibration was the only variable.

3.11.4 The influence of plastic viscosity of concrete on plastic settlement cracking (Experiment 6)

The plastic viscosity of concrete has a large impact on the flow and workability thereof. Therefore, a liquid viscosity modifying admixture (VMA) was added on Mix 2 to modify the viscosity. This was done to determine the effect of plastic viscosity on plastic settlement cracking, compared to the standard Mix 2 beam. Thus, the viscosity of the concrete was the only variable.

Even though the viscosity of Mix 1 and Mix 2 may be different, other factors such as w/c ratio, amount of aggregate etc. can influence the results. Therefore, a liquid VMA was added to Mix 2, forming Mix 3, to determine the sole effect of plastic viscosity on the concrete and settlement cracking.

The VMA used was CHRYSO quad 20, with a recommended usage of 0.2 – 0.6 kg per 100 kg of cement. For this experiment, a dosage of 0.23 kg VMA per 100 kg of cement was used. The slump cone test result of the standard Mix 2 was 108 mm, and for Mix 3 it was 145 mm.

The standard casting and testing procedures were followed as described in the previous sections.

3.11.5 The influence of plastic shrinkage cracks on plastic settlement cracking (Experiment 7)

In Section 2.4 the interaction between plastic shrinkage and plastic settlement cracking is discussed and it was discovered that plastic shrinkage cracking negatively impacts plastic settlement cracking by amplifying the severity of the settlement crack.

With the previous experiments the beams were placed in a temperature-controlled room directly after being cast to ensured that only plastic settlement cracks formed in the concrete. However, in practice it is not always possible to protect the concrete against environmental factors that will cause plastic shrinkage cracking. Plastic shrinkage cracking might also influence the plastic settlement cracking and the overall durability of the concrete.

A beam, using Mix 2, was exposed to some well-identified factors that cause plastic shrinkage cracking, such as heat, wind, and humidity. However, the beam was only exposed to these conditions for 6 hours, thereafter it was cured and placed in the temperature-controlled environment, as explained in Section 3.4. This ensured that the only variable was plastic shrinkage cracking.

To force plastic shrinkage cracks to occur, the entire beam was placed in a controllable heat box with a specific air temperature, relative humidity, and wind speed. The air temperature was set to 30^{o}C, the relative humidity set to 30 % and the wind speed set as 7 Hz or 2.17 m/s. Uno's equation, as discussed in Section 2.1.9, was then be used to determine the evaporation rate due to the specific parameters, depending on the concrete temperature. The concrete temperature of the beam after cast was 17^{o}C. The initial evaporation rate was determined to be 0.145 kg/m^{2}/hr.

Since Mix 2 was used for this beam, the results can be compared to the standard beam using Mix 2, in Section 3.11.2. Thereby, the only variable was the factors applied for the first 6 hours that caused plastic shrinkage cracking. This allowed the determination of the influence of plastic shrinkage cracks on plastic settlement cracks. The crack severity, OPI, and water sorptivity results was compared to find a correlation between the crack severity and durability of concrete, caused by plastic settlement cracking.

4 Results and discussion

This chapter discusses the results obtained from the experiments conducted in Chapter 3.

It is important to note with regards to the water sorptivity results discussed in Chapter 4: the point plotted at 30 minutes on the graphs were not actually after 30 minutes. This point represented the vacuum saturated mass of the specimen after performing the second part of the sorptivity tests. However, to visually simplify the results, the points were plotted at 30 minutes, instead of 21 hours.

It is also important to note for the CT scans, the sample used in each case was the sample with the result closest to the average result to that specific cover depth. Also, the figures shown of the CT scans, in the results chapter, are sections through the height and depth of a specimen. In each case the figures show the most severe cracks found from the front, top or side, thus, it is not assumed that the crack shown were present throughout the whole length or depth of the rod or specimen.

4.1 Concrete properties results

Various experiments were performed to test the rheological properties of the different concrete mixes, namely the slump tests, rheology tests, setting time tests and cube strength tests.

Mix 1 and 2 were designed to have different strengths, therefore, different w/c ratios were used. However, the other parameters were adjusted to modify the slump of the mixes to be the same, at around 100 – 110 mm. This was to keep the slump and possibly the viscosity constant and to isolate the effect of the w/c ratio, and thereby, the concrete strength. Three different slump cone tests were performed to find an average slump value.

A large factor considered for this study was the viscosity of concrete. However, Mix 1 and 2 had many differing factors in terms of mix design proportions, therefore, a mix was needed to isolate the effect of plastic viscosity alone. A liquid viscosity modifying agent (VMA) was used to adjust the viscosity of Mix 2, forming Mix 3. The plastic viscosity of each mix was then determined, as discussed in Section 3.6, using the ICAR rheometer. Three different mixtures were tested for each mix to determine the average plastic viscosity.

The concrete strength of the different mixes was determined by conducting a 28-day cube strength tests on three samples and applying Equation 4.1. Four different cubes were tested for each mix to determine the average 28-day cube strength.

$$Calibrated\ load = 1.018 \cdot Load + 4.9\ [kN] \tag{4.1}$$

The initial setting times of Mix 1 and 2 were also determined as discussed in Section 3.5. Mix 1 had a set time of 2 hours and 45 minutes to 3 hours, whereas mix 2 had an initial setting time of 3 hours and

15 minutes to 3 hours and 30 minutes. Three different conical rings were used for each mix to determine the average initial setting time.

The results of these tests are shown in Table 4.1.

Table 4.1 Concrete properties results of Mix 1, 2 and 3

Property	Mix 1	Mix 2	Mix 3 - VMA
Average slump (mm)	110	108	145
Average plastic viscosity (Pa.s)	123.9	173.6	107.2
Average cube strength (MPa)	21.92	33.75	32.21
Average initial setting time (h:m)	2:45 – 3:00	3:15 – 3:30	-

As seen, Mix 1 and 2 had a very similar slump, however, the cube strength and plastic viscosity differs significantly, due to the difference in water/cement ratio. Mix 3 had a much higher slump value and a much lower plastic viscosity, compared to the other mixes, due to the effect of the added VMA. Since the water/cement ratio and all other mix proportions stayed the same, the cube strength of Mix 3 was similar to that of Mix 2.

4.2 Preliminary experiments results

4.2.1 Cylindrical concrete moulds

As discussed in Section 3.11.1.1, this experiment used cylindrical PVC pipes as concrete moulds. Due to the nature of this experiment, the results were not used to draw any final conclusions on the topic of the study, but the results are still discussed, since it confirmed initial assumptions and thereby influenced the development of the final experiments. It also gave a good understanding of what to expect and how to perform the OPI tests.

The samples did have visible voids and cracks from the side, but no surface cracks. The OPI procedure was performed as standard, where the samples were drilled from the top. The concrete was not vibrated properly and contained several large, entrapped air bubbles, as seen in Figure 4.1. Some settlement cracks were still visible from the sides around the area of the reinforcement, as seen in Figure 4.2.

Figure 4.1 Demoulded Cylindrical Concrete Samples

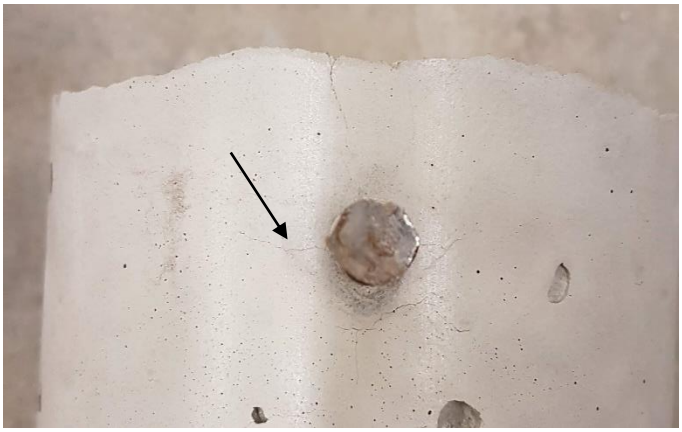

Figure 4.2 Slightly visible tensile and shear cracks

The larger cover depths showed a lower rate of pressure decay and a higher OPI value, as seen in Figure 4.3 and Table 4.2.

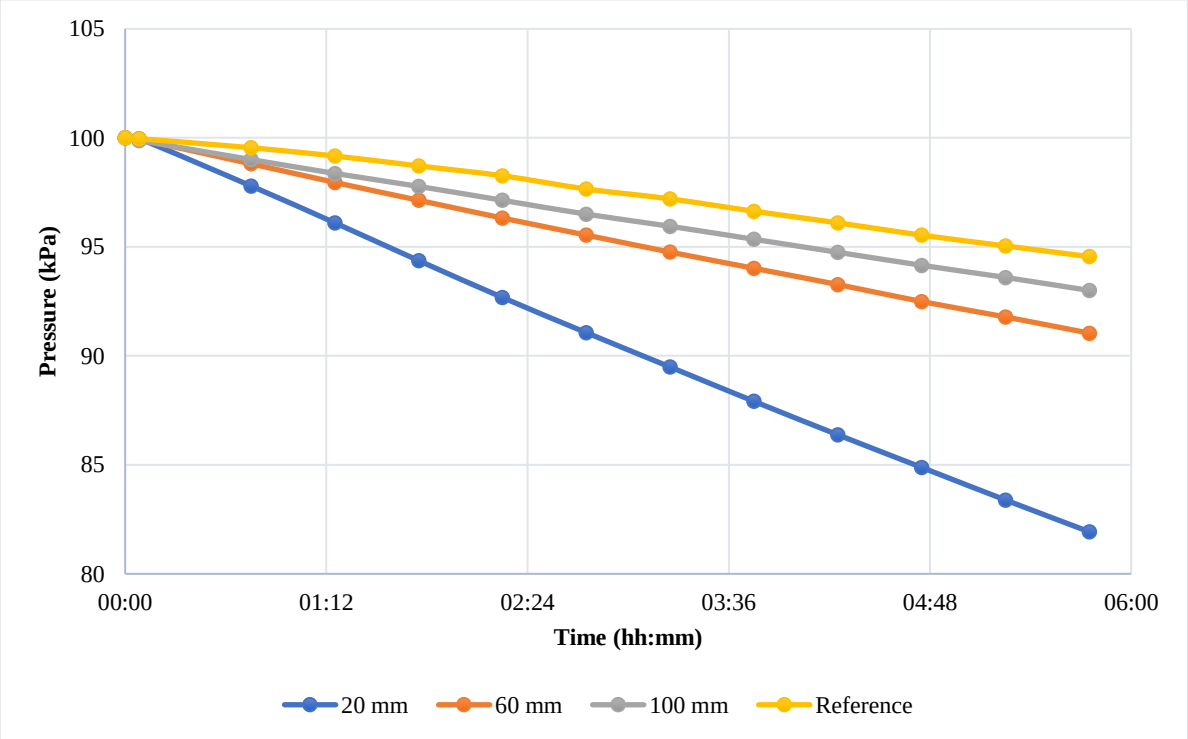

Figure 4.3 Pressure decay results for preliminary experiment 1

Table 4.2 Experiment 1: OPI results

Cover Depth	OPI
20 mm	10.30
60 mm	10.62
100 mm	10.73
Reference	10.86

The cover depth of the steel rods significantly impacted the pressure decay and OPI results, confirming the assumption that cover depth plays a role in the durability of concrete. If the settlement of concrete

is obstructed, as with a steel rod, the concrete on top of the rod settles less than the concrete on the sides of the rod. This difference in settlement is known as differential settlement. A smaller cover depth would cause more differential settlement, since the concrete settles less above the steel rod compared to a steel rod at a larger cover depth.

This test indicated that the durability may be impacted more negatively with smaller cover depths in the concrete than with larger cover depths and inspired the design of the later experiments.

4.2.2 Influence of cover depth on plastic settlement cracking

Three large beams were cast using the beam mould discussed in Section 3.11.1.2. Each beam consisted of concrete with a different w/c ratio, as shown in Section 3.1. The completed and demoulded beams are shown in Figure 4.4.

Figure 4.4 Demoulded beams

Each beam contained a steel rod at 30 mm, 60 mm, 90 mm, and 140 mm cover depths. The concrete mix designs were aimed to be 15, 30 and 45 MPa, respectively. An example of a tensile crack that formed at the steel reinforcement is shown in Figure 4.5. With the increased cover depth, the voids around the reinforcements were less visible and the tensile cracks decreased to barely visible. However, the absence of visible cracks and voids at the larger cover depth did not mean micro cracks and voids were not present.

Figure 4.5 Slightly visible voids and tensile cracks at the reinforcement

After the beams were demoulded, cores were drilled from the sides of the beam and samples were cut, as explained in Section 3.8, as seen in Figure 4.6 and Figure 4.7. Each beam contained four steel rods which allowed 4 samples to be cut from it. With the added four reference samples per beam, there were a total of 60 samples between the three beams.

Figure 4.6 Core-drilled concrete core samples

Figure 4.7 Cut 70 mm x 30 mm samples

After testing a few samples, it was found that by cutting through the steel reinforcement, the steel vibrated and loosened which could cause additional damage and voids to the sample (This issue is further discussed and solved in Experiment 3. Therefore, the rate of pressure decay was extremely high through the samples, at around 10 seconds. An epoxy was added on each side of the specimens, in a 15 mm diameter over the steel rods to temporarily solve this issue, as seen in Figure 4.8. The rate of pressure decay was slowed down slightly, which allowed it to be measured more accurately.

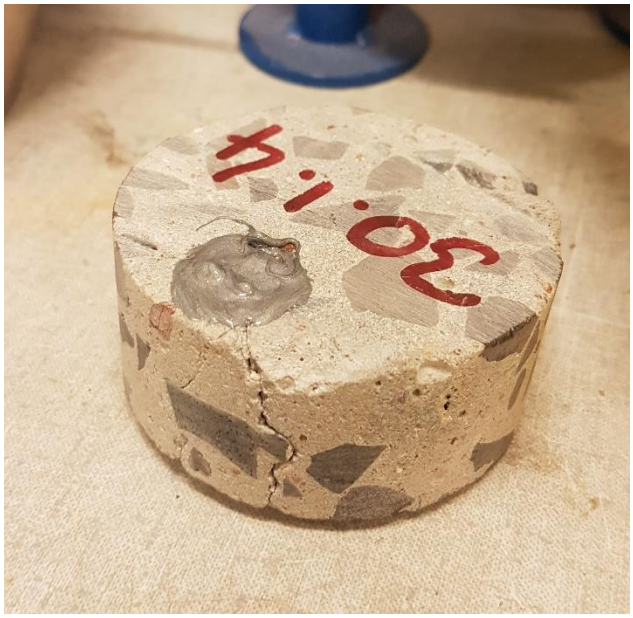

Figure 4.8 Epoxy covering reinforcement

The results of the 15, 30 and 45 MPa beams are shown in Figure 4.9 to Figure 4.13. These results show the same phenomenon. The crack severity increases with the decrease of cover depth, as seen in Figure 4.9 to Figure 4.11, since it is assumed that a faster pressure decay indicates more severe cracks. However, this effect is not consistent in all cases throughout the experiment, as seen in the figures mentioned. In the case of the 45 MPa beam, the 90 mm cover depth showed a lower rate of pressure decay than the 140 mm. However, in all the cases the lower cover depths – 30 mm, and 60 mm – showed a higher rate of pressure decay than the 90 mm and 140 mm cases.

This indicates that the rate of pressure decay increases as the cover depth decreases, and it is therefore assumed that the crack severity increases as the cover depth decreases. Thus, for a lower cover depth there is a higher crack severity, as indicated by the rate of pressure decay in the figures.

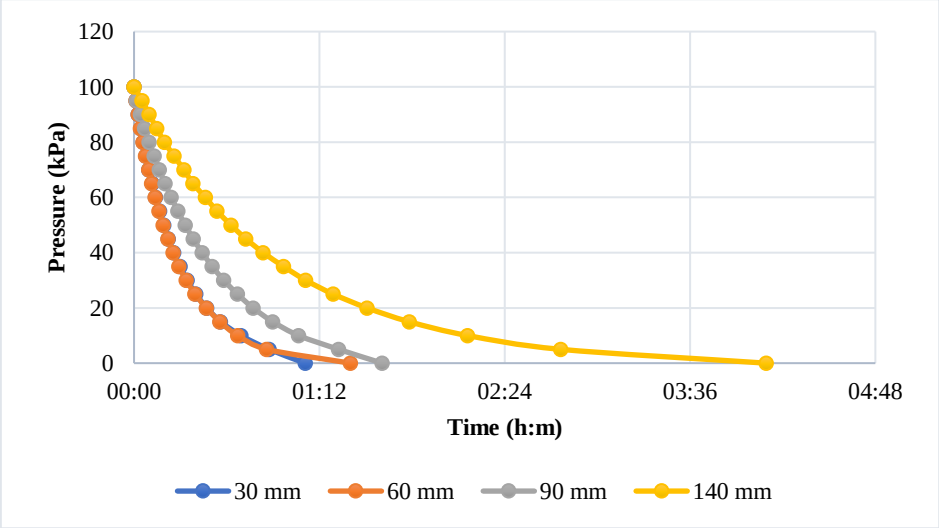

Figure 4.9 15 MPa Pressure decay over time between different cover depths

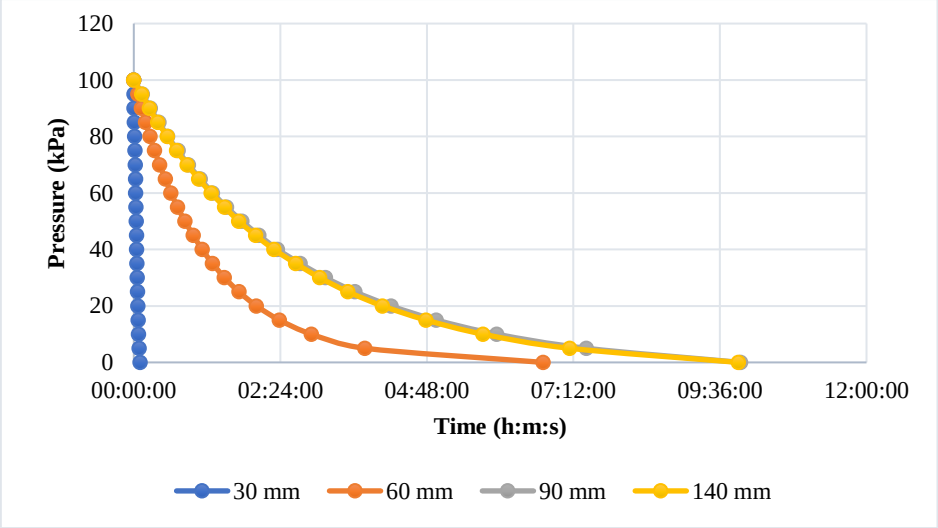

Figure 4.10 30 MPa Pressure decay over time between different cover depths

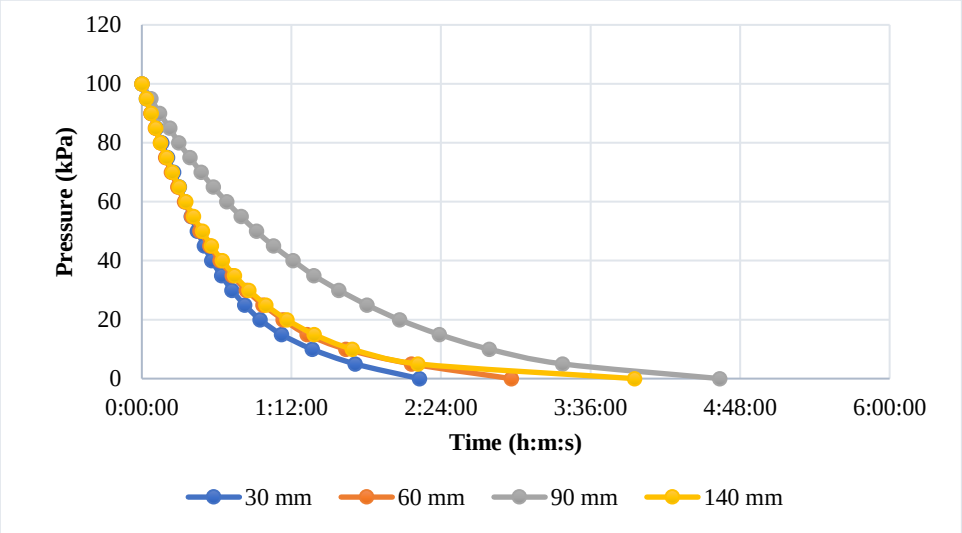

Figure 4.11 45 MPa Pressure decay over time between different cover depths

Although the rate of pressure decay was not as high at the 140 mm cover depth, there is still assumed to be voids and cracks present. Since, if it is compared to the reference sample, the pressure decay rate is much higher. This indicates that even when the settlement cracks and voids were not visible, it was still present.

As seen in Figure 4.12 and Figure 4.13, there is also a significant difference between the results of the different beams. Firstly, the 90 mm cover depth samples are compared between each beam and there is a significant difference. The reference samples of each beam are compared to each other and according to both results, the 30 MPa beam showed the lowest rate of pressure decay, followed by 45 MPa and 15 MPa. This may be due to the difference in concrete strength, or rather, the water/cement ratio.

It is usually assumed that a higher strength concrete has a higher durability or are less likely to crack, however, these tests show that at the high strengths, this might not be the case. The high strength

concrete had the lowest w/c ratio at 0.42. A w/c this low may result in less workable concrete, and therefore, it was not sufficiently compacted around the reinforcement or even in general. This may have resulted in the formation of more severe cracks and voids in the concrete.

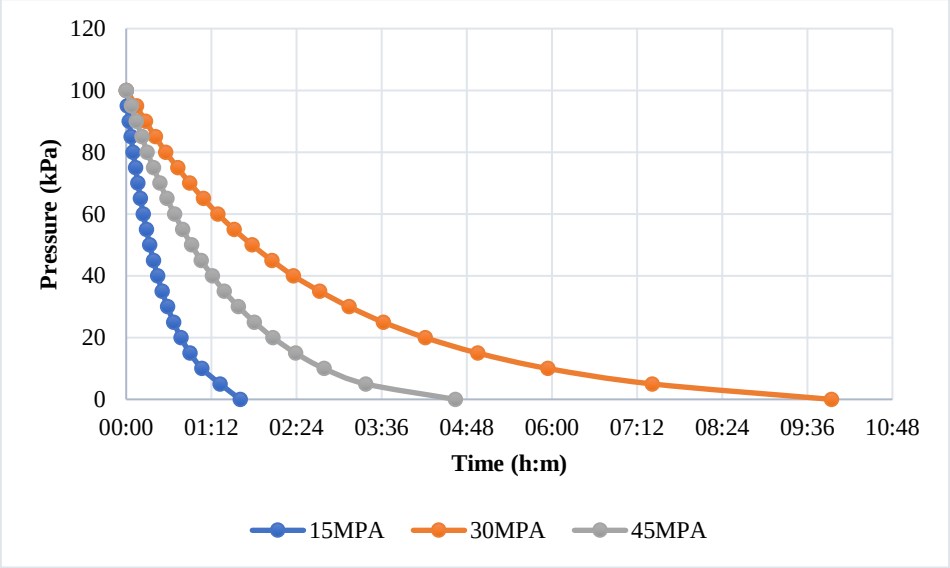

Figure 4.12 Pressure decay over time of different beams at the same cover depth

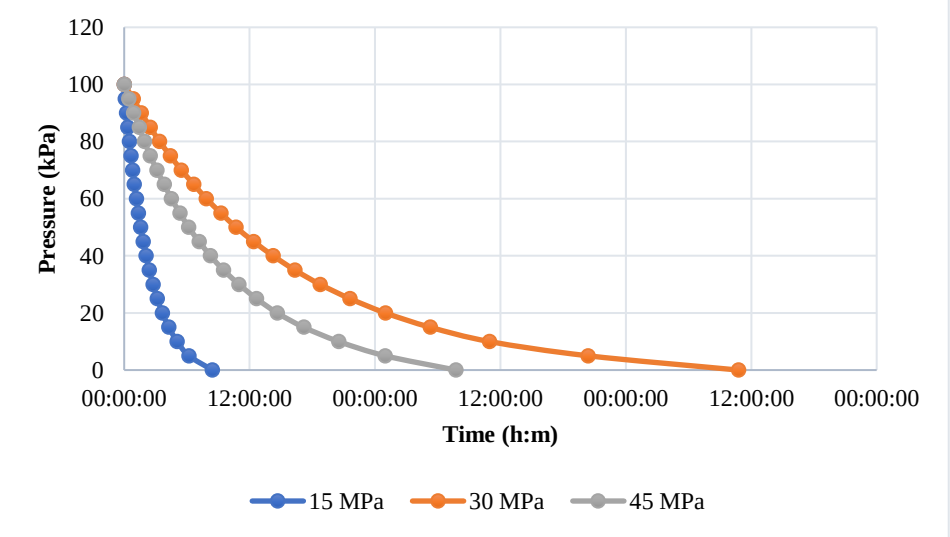

Figure 4.13 Pressure decay over time of different beams at the same cover depth

These experiments are not used to derive any final conclusions for this study, since each beam did not undergo proper and constant curing procedures after being cast, and thus resulted in surface cracks which is not wanted. Also, the steel reinforcement caused some unwanted issues and affected the voids and cracks of the samples while being cut. However, this experiment did confirm the initial assumptions and assisted in developing and improving the following experiments.

4.2.3 The effect of different reinforcing rod types on plastic settlement cracking

As explained, this experiment was conducted due to the nature of the previous experiment, Experiment 2, where the steel showed a negative impact on the test samples and the crack severity results. The voids of the rods in the concrete block are shown in Figure 4.14. The left rod contained the samples of the clean plastic as well as the plastic with O-rings. After extracting and testing the samples, the results were obtained as shown in Figure 4.15. The reinforcement on the right was the steel, middle was the plastic rod with washers and left was the clean plastic rod with rubber O-rings. The concrete specimen of each rod type is also shown in Figure 4.16. As seen in Figure 4.16 (a), the steel rod caused the most severe voids in the concrete, followed by the clean plastic rod, Figure 4.16 (b). The plastic rods with the washer and O-ring had no visible voids or cracks, as shown in Figure 4.16 (c) and (d).

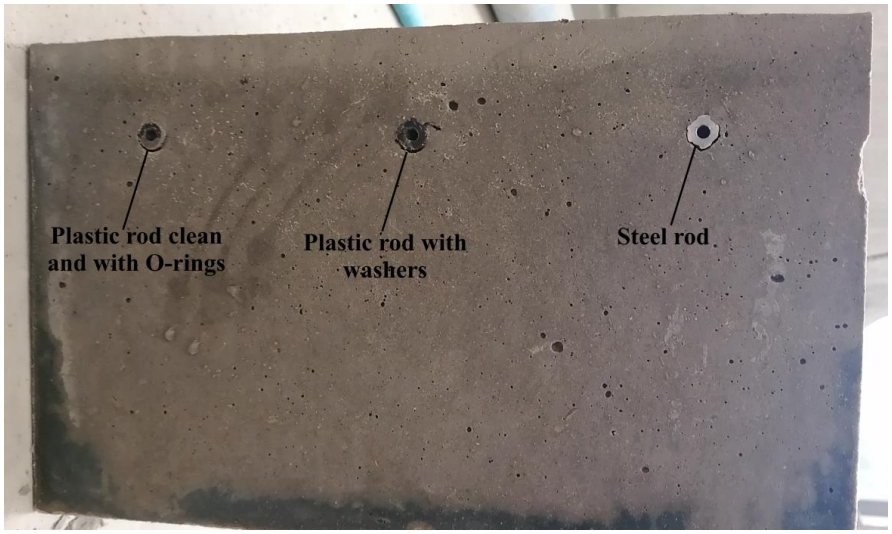

Figure 4.14 Void comparison of each rod

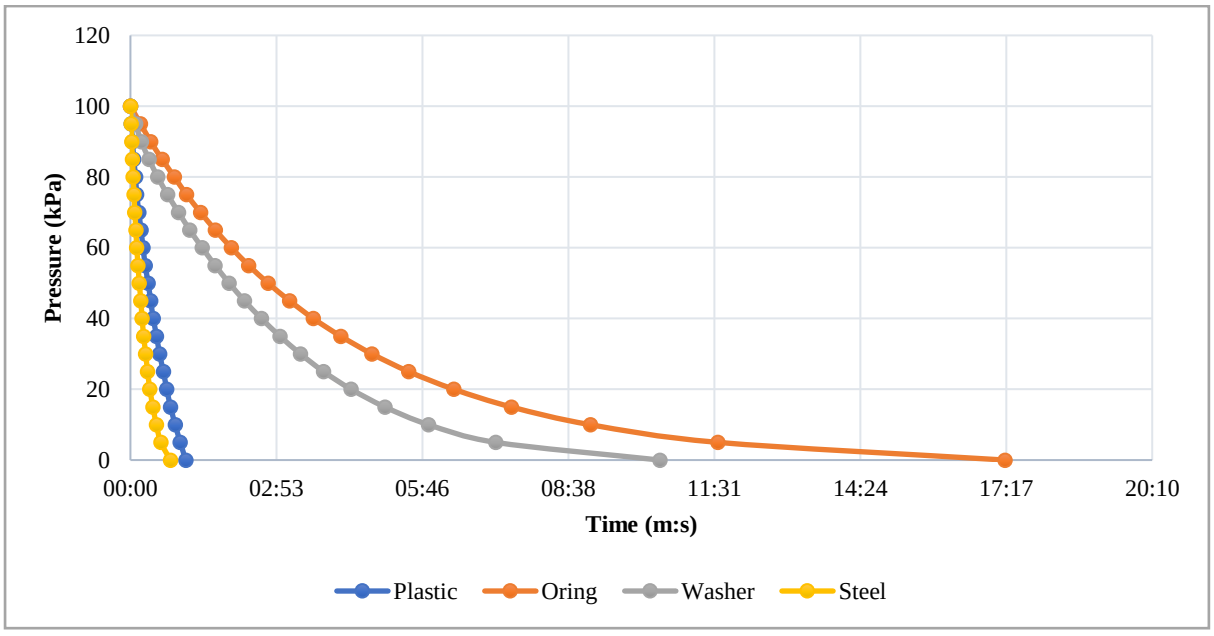

Figure 4.15 Pressure decay curve of the different reinforcement types

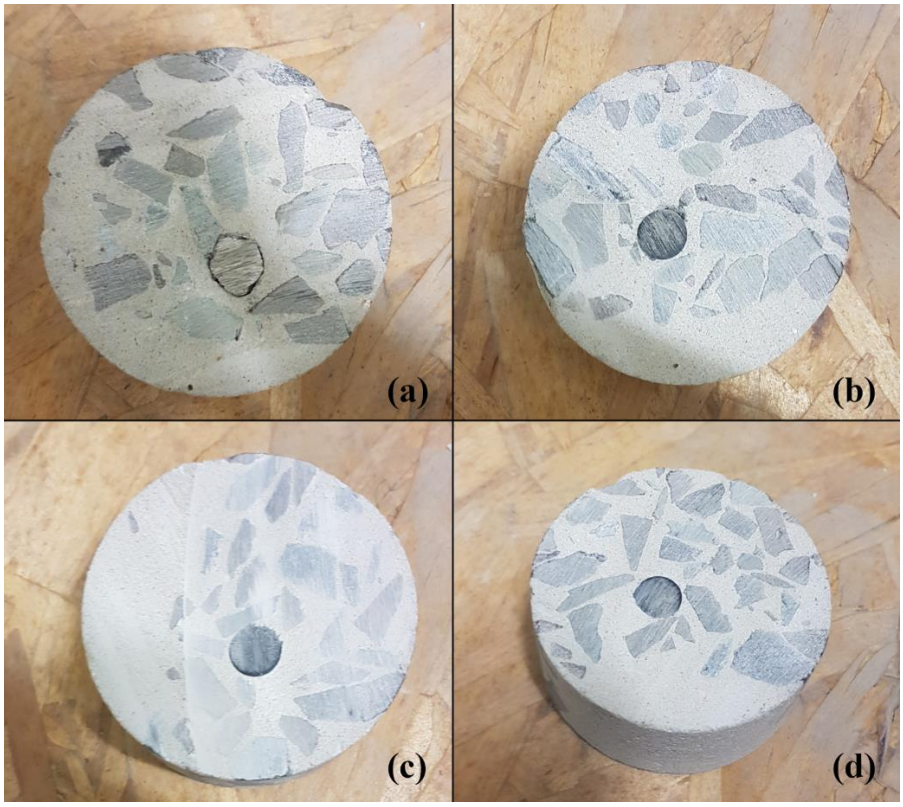

Figure 4.16 Concrete samples of different rods, namely (a) steel rod, (b) clean plastic rod, (c) plastic rod with washer and (d) plastic rod with O-ring

It is assumed that the duration of pressure decay is directly correlated to the number of voids present and the crack severity of the sample, as concluded in previous experiments. Although the washers were bigger than the O-rings, it showed a more rapid pressure decay rate. It is argued that the size of the washer has been too intrusive in the settlement of the concrete and may have caused additional or larger voids and cracks, not present with the standard plastic rod or O-rings.

After analysing the results, it was decided that plastic rods were going to be used in all the further experiments. The plastic rods allow the cores to be cut seamlessly, since the blade cuts through the plastic with ease and does not cause any significant vibrations, cracking or loosening of the rods.

It was also decided to use the plastic rods with tightly fitted O-rings, which was sealed to the rod with silicone to provide additional resistance to the applied air pressure in the OPI chamber. The O-rings were strictly added to prevent a straight path between the rod and the concrete for the oxygen to follow and force the oxygen to rather travel through the cracks or voids.

The plastic rods with O-rings may have an intrusive effect on the concrete, in terms of creating voids or influencing the bond with the concrete and might not accurately portray the real-life events of concrete with steel reinforcement. However, all the factors mentioned were considered as well as all previous experiments, and it was found to be the best to test it with plastic rods and O-rings. Also, the

plastic rods do not influence the settlement effect of the concrete, and it does cause the same differential settlement as with a steel rod, therefore the plastic rods were used.

4.3 The influence of cover depth and concrete strength on plastic settlement cracking

4.3.1 Crack severity test results

Two beams were used for this experiment so strength characteristics could be compared. Mix 1 had a 28-day cube strength of 21.92 MPa, whereas Mix 2 had a 28-day cube strength of 33.75 MPa. Beam 1 was cast using Mix 1 and Beam 2 was cast using Mix 2.

Cores were drilled as mentioned in Section 3.8 when performing the crack severity test. Reference cores were also drilled through the concrete in areas with no rods present.

After conducting the crack severity test, the following results were obtained. As seen in Table 4.3 and Figure 4.17, it is clear that the cover depth of the rod has a significant impact on the rate of pressure decay. With both beams the rate decreases with the increase in cover depth. For Beam 1, the 25 mm cover depth showed a pressure decay of 43 minutes, followed by 5 hours and 31 minutes for the 50 mm cover depth and finally 8 hours and 23 minutes for the 75 mm cover depth. For Beam 2, the 25 mm cover depth showed a pressure decay of 1 hour and 4 minutes, followed by 28 hours and 40 minutes for the 50 mm cover depth and finally 50 hours and 50 minutes for the 75 mm cover depth. There was a large time difference between the results of the beams. In addition, Beam 2 showed an overall much slower pressure decay compared to that of Beam 1.

Table 4.3 Pressure decay final times of Beam 1 and 2

	Pressure decay time from 100 kPa to 0 kPa (hh:mm)	
Cover depth	**Beam 1**	**Beam 2**
25 mm	00:43	01:04
50 mm	05:31	28:40
75 mm	08:23	50:50
Reference	19:38	56:52

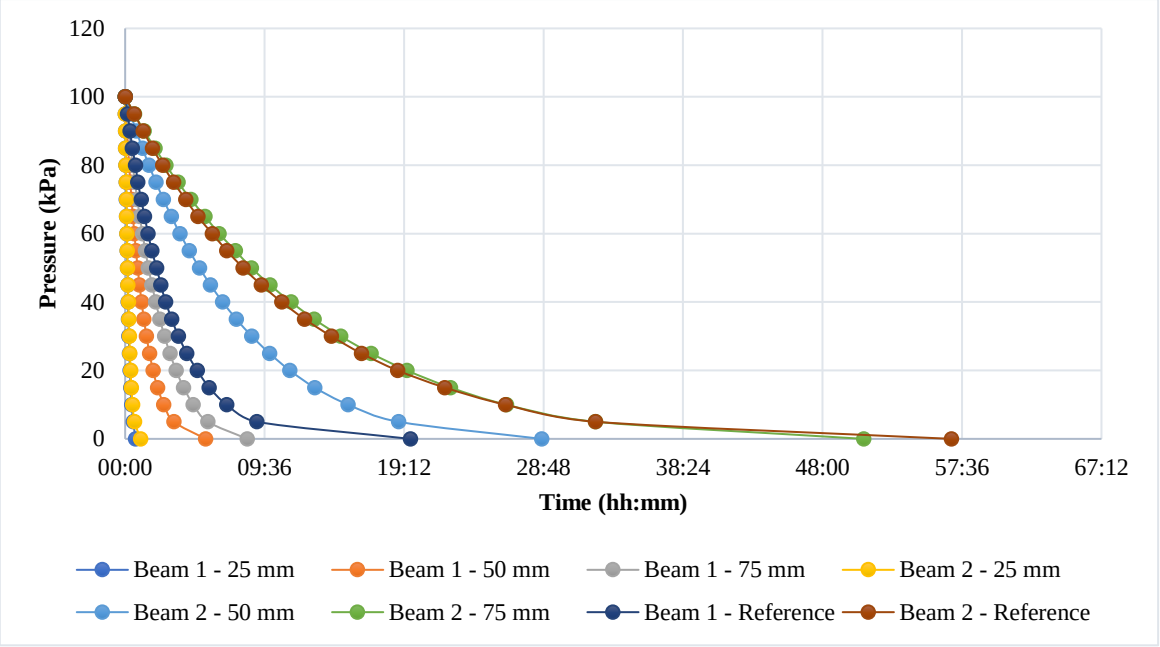

Figure 4.17 Beam 1 vs 2 pressure decay over time

The plastic viscosity of the mixes could have also played a role; however, this phenomenon was discussed in more detail in Section 4.5. The reference samples were also compared to each other, as seen in Figure 4.18. It is clear between the cover samples as well as the reference samples that Beam 2 had a much slower rate of pressure decay compared to Beam 1. The results were assumed to be due to the difference in strength and possibly viscosity.

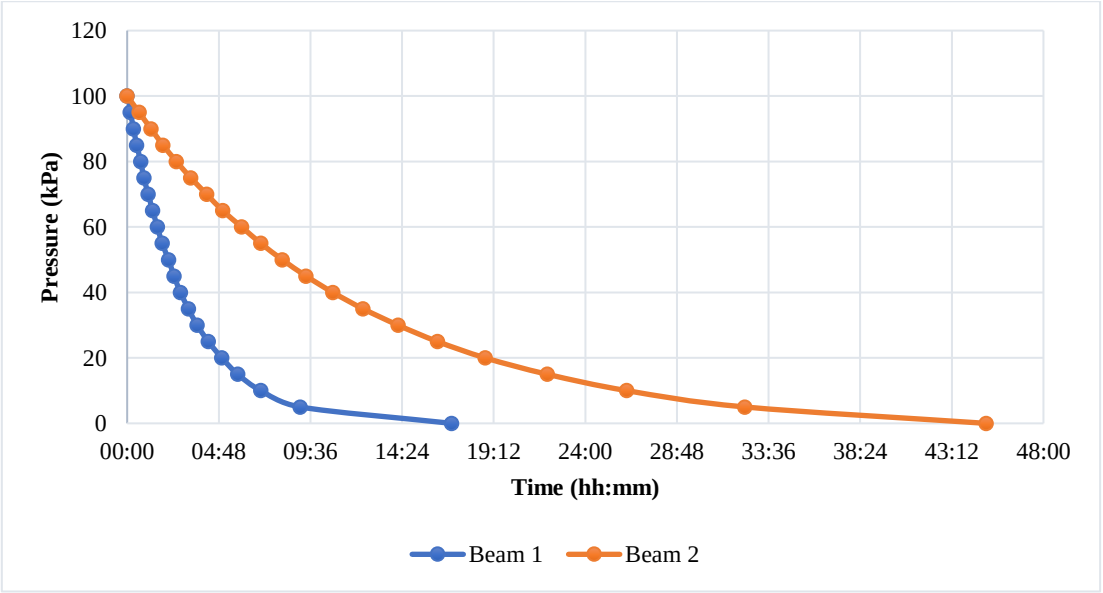

Figure 4.18 Beam 1 and 2 reference samples pressure decay over time

One sample of each cover depth from Beam 1 and 2 are shown in Figure 4.19 (a) to (c) and (d) to (f), respectively. As seen, there are no visible cracks or voids present in the samples around the reinforcements. However, even with no visible cracks or voids the results still show the phenomenon

that cover depth influenced the crack severity. The samples shown indicate no clear plastic settlement cracking. However, just because the cracks are not visible to the naked eye, does not mean they are not present. Microcracks can still be present. That is why CT scans were also performed and discussed in a later section.

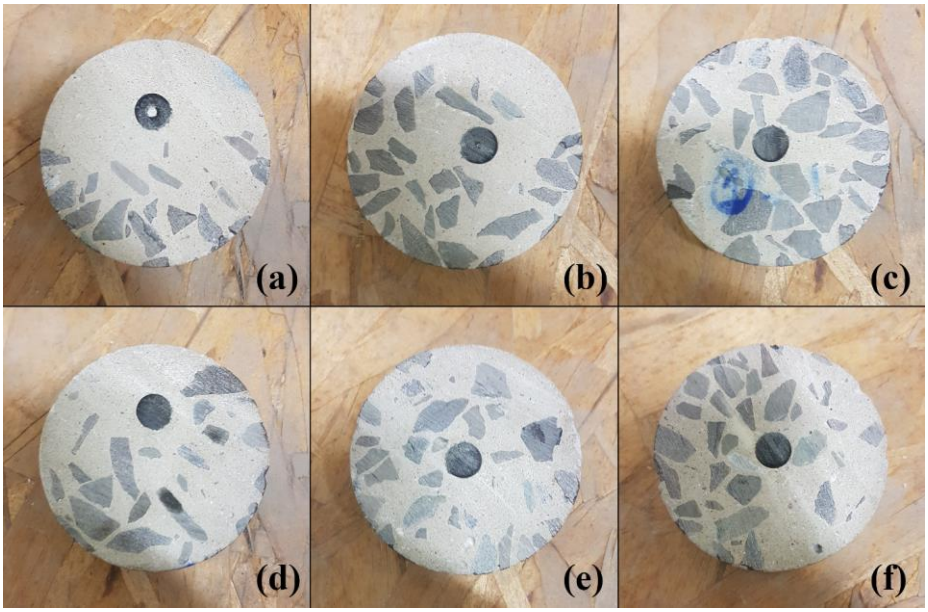

Figure 4.19 The crack severity concrete specimens of (a) Beam 1 - 25 mm cover depth, (b) Beam 1 - 50 mm cover depth, (c) Beam 1 - 75 mm cover depth, (d) Beam 2 - 25 mm cover depth, (e) Beam 2 - 50 mm cover depth and (f) Beam 2 - 75 mm cover depth

4.3.2 OPI test results

The Oxygen Permeability Index (OPI) test results shows how the crack severity of the 25 mm cover depth relates to the permeability of the concrete at that depth. For Beams 1 and 2 the OPI results are given in Table 4.4. As shown the OPI results correlate with the crack severity results. Beam 2 shows a higher OPI value of 8.49, compared to 7.97 of Beam 1, which is a similar result to the rate of pressure decay shown in Table 4.3. Although both OPI values are low, it still indicated a higher durability for Beam 2, which had a higher strength and higher plastic viscosity.

Table 4.4 OPI results of Beam 1 and 2

	OPI	
Cover Depth	**Beam 1**	**Beam 2**
25 mm (OPI)	7.97	8.49
Reference	9.33	9.90

One durability sample of Beams 1 and 2 are shown in Figure 4.20 to Figure 4.21 and Figure 4.22, respectively. As seen, both samples had visible voids and tensile cracks that lead to the surface of the concrete from the plastic rod. This reflects typical crack behaviour of plastic settlement cracking. Although the crack present with Beam 2 seems more severe, the presence of invisible voids or cracks may still have influenced the results of the durability test.

The results of the reference samples indicate that Beam 2 shows a higher durability compared to Beam 1. This may also indicate that regardless of the influence of a restraint, such as a reinforcing rod, the higher strength concrete still shows improved durability.

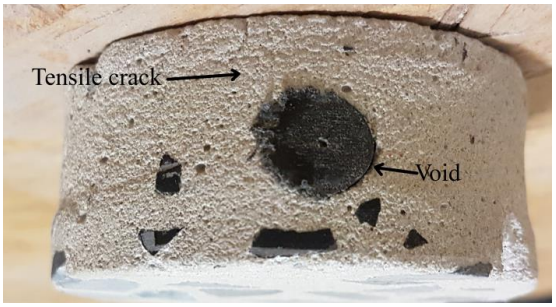

Figure 4.20 Beam 1 OPI sample

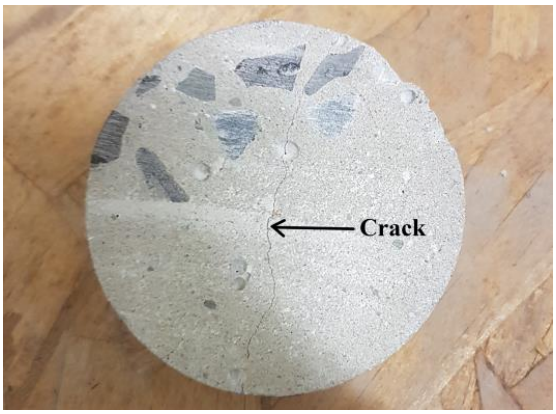

Figure 4.21 Beam 2 OPI sample top crack

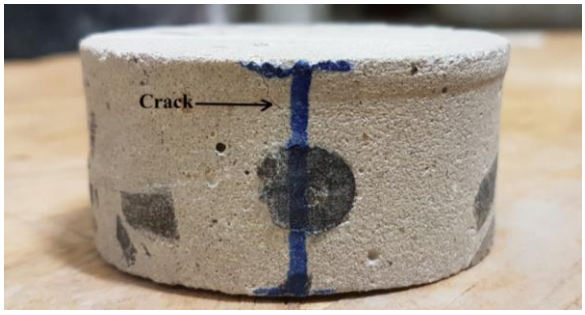

Figure 4.22 Beam 2 OPI sample front crack

4.3.3 Water sorptivity test results

The water sorptivity tests were conducted and the calculations were performed as discussed in Section 3.9. Table 4.5, Figure 4.23 and Figure 4.24, shows the results of the water sorptivity test for Beam 1 and 2, respectively.

The water sorptivity test results also reflect the phenomenon seen with the crack severity test results, where the cover depth has an influence on the plastic settlement cracking of the concrete. It is assumed that a higher sorptivity and porosity would indicate more severe cracks.

Table 4.5 Water sorptivity results for Beam 1 and 2

	Beam 1			Beam 2		
Cover Depth	**R^2**	**Sorptivity ($mm/hr^{0.5}$)**	**Porosity (%)**	**R^2**	**Sorptivity ($mm/hr^{0.5}$)**	**Porosity (%)**
25 mm	0,9942	10,05	17,59	0,9943	11,90	14,04
50 mm	0,9934	9,70	14,82	0,9908	9,55	13,22
75 mm	0,9894	9,27	12,86	0,9923	8,56	12,29
Reference	0,9880	8,65	13,33	0,9858	9,08	13,22
25 mm (OPI)	0,9977	12,54	20,35	0,9960	12,02	16,62

Overall the sorptivity rate and porosity percentage increased with a decrease in cover depth. Where, the 25 mm cover depth showed the highest sorptivity and porosity, followed by the 50 mm cover depth, and with the 75 mm having the lowest sorptivity and porosity.

Between the two beams, the 50 mm cover depth showed a relatively similar sorptivity rate, with that of Beam 1 sligtly higher. The 25 mm cover depth of Beam 2 showed a higher sorptivity, and the 75 mm a lower sortptivity, compared to Beam 1. Overall, the porosity of all the samples of Beam 1 are higher than that of Beam 2.

The sorptivity rate and porosity of Beam 2 is mostly lower than that of Beam 1, except for the sorptivity of the 25 mm and reference sample.

The results of the 25, 50 and 75 mm samples also indicate that cover depth directly influences crack severity, with both beams. The results of the 25 mm OPI sample, show that Beam 2 has an improved durability compared to that of Beam 1.

Figure 4.23 and Figure 4.24 shows the mass gain over time with performing the sorptivity tests of Beam 1 and 2, respectively.

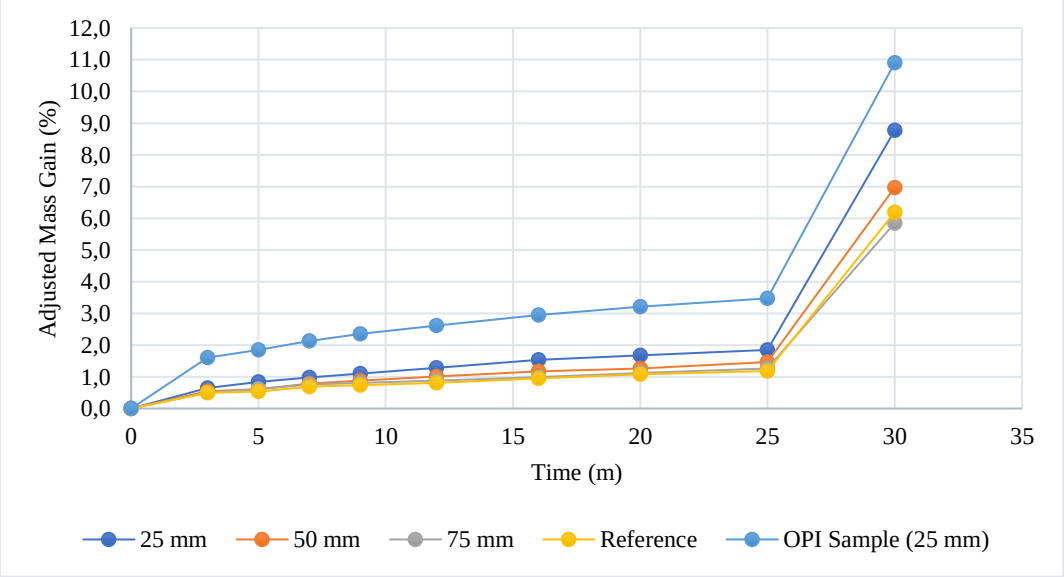

Figure 4.23 Beam 1 Sorptivity results: percentage mass gain over time

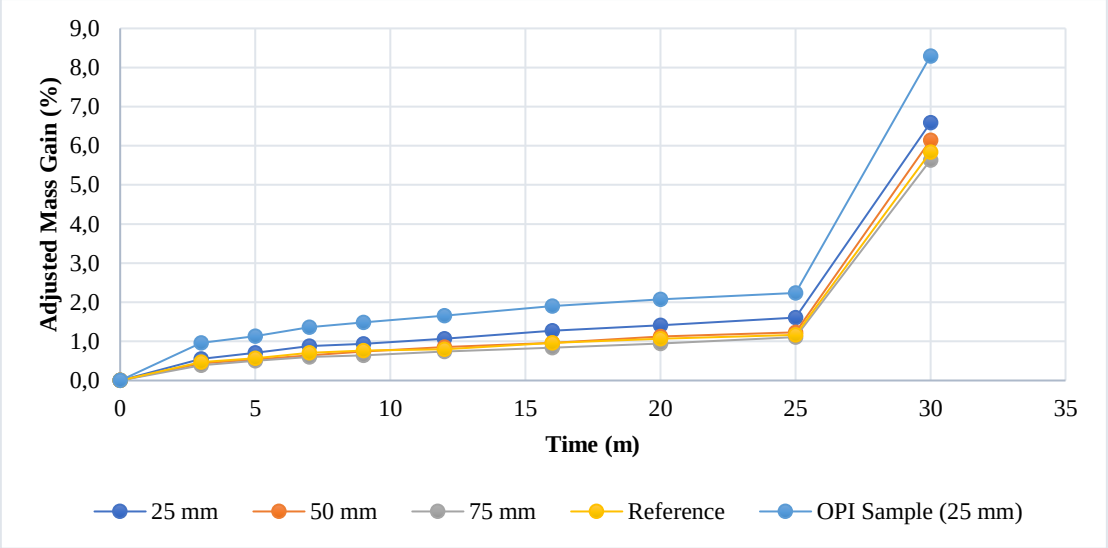

Figure 4.24 Beam 2 Sorptivity results: percentage mass gain over time

4.3.4 CT Scan

This section discusses the CT scans of the 50 mm cover sample of Beam 1 and the 25 mm and 50 mm cover sample from Beam 2, as shown in Figure 4.25. Firstly, compare the 50 mm cover samples of each beam, shown in Figure 4.25 (a), (c), (d) and (f). Beam 1 has more visible cracks than Beam 2. There are visible shear cracks around the rod of Beam 1, as indicated with the arrows. Beam 2 on the other hand has slightly visible shear cracks in one region of the sample, as shown in Figure 4.25 (c).

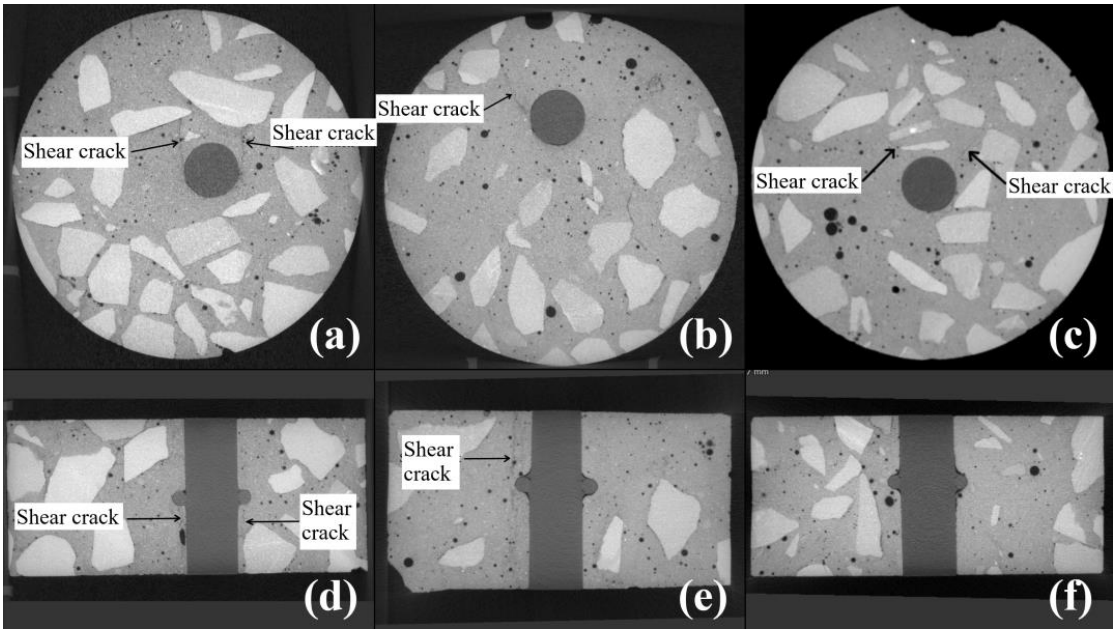

Figure 4.25 CT scans of (a) Beam 1 - 50 mm cover front section view, (b) Beam 2 – 25 mm cover front section view, (c) Beam 2 – 50 mm cover front section view, (d) Beam 1 – 50 mm cover top section view, (e) Beam 2 – 25 mm cover top section view and (f) Beam 2 – 50 mm cover top section view

There was a major difference in plastic settlement cracking severity between the two different cover depths of Beam 2, as shown in Figure 4.25 (b), (c), (e) and (f). The 25 mm cover sample has a clearly

visible shear crack at the rod, whereas the 50 mm sample has slightly visible shear cracks, which are not as severe as the cracks present with the 25 mm cover. The 50 mm cover sample of Beam 2 also indicates more severe voids than that of the 25 mm cover sample. The voids might also have influenced the results of the durability tests. However, the void volume was not calculated to make a direct correlation between the sizes of the voids and durability results could not be made.

4.3.5 Discussion

The results obtained from Beam 1 and 2 clearly indicate that the cover depth of a reinforcement effects the plastic settlement crack severity and possibly the durability of the concrete. The crack severity results showed a clear difference between the cover depths. For both beams, the smaller cover depths have a more rapid rate of pressure decay, and presumably more severe plastic settlement cracks.

It is also clear that the strength or w/c ratio has an impact on the crack severity. The higher strength concrete showed an overall slower rate of pressure decay, which indicates a lower crack severity. However, due to the lower w/c ratio, the higher strength concrete has a denser microstructure. This may have also caused a slower rate of pressure decay.

The OPI results indicate that the higher strength concrete has an improved permeability index, compared to the lower strength concrete, which may indicate a higher durability according to the test parameters.

The water sorptivity results are more mixed and does not provide a clear distinction between the two beams. The 50 mm and 75 mm samples of Beam 1 has a higher sorptivity rate, indicating more severe cracks, whereas the 25 mm sample has a lower sorptivity, which indicates less severe cracks. With the OPI samples, Beam 1 has a higher sorptivity, indicating a lower durability rating. Overall, the porosity of Beam 2 was lower compared to Beam 1.

The results from the CT scans indicate that the higher strength concrete has less severe plastic settlement cracks, compared to the lower strength concrete. It also indicates more severe cracking with the smaller cover depth sample compared to the larger cover depth sample.

Therefore, considering all the results, it is clear that the lower strength concrete has more severe cracks at the same cover depths. The durability testing shows a lower permeability and mixed water sorptivity, which may indicate a lower durability rating. It was also clear that a higher crack severity occurs with smaller cover depths, compared to larger cover depths.

However, this experiment only used two beams of different strengths, which concluded the higher strength concrete has a lower crack severity and improved durability. However, the impact of concrete strength on crack severity should also be tested with higher strength concrete, such as 45 MPa or higher. The preliminary experiment indicated that at a very high strength and low w/c ratio, such as 45 MPa and 0.42, respectively, the crack severity results may be worse. Therefore, more study is still required

in this area with a higher variety of concrete strengths. As mentioned, the higher strength concrete has a denser microstructure, therefore, the results were not necessarily just due to the plastic settlement cracks present. The results may not be as straightforward as relating single differing factors between two mixes since the different w/c ratio's changes the microstructure of the concrete.

4.4 The influence of re-vibration of concrete on plastic settlement cracking

Re-vibration of concrete is a well-known phenomenon used to limit the effects of plastic settlement cracking. When concrete is re-vibrated after a certain period during the plastic state, the voids and cracks may close due to the additional compaction. This experiment put the theory to the test to measure how re-vibration would influence plastic settlement cracking in concrete. Beam 3 was cast using Mix 2. The beam was re-vibrated on a vibrating table, for one minute, at about three hours after being cast. The initial setting time of the concrete was about three hours and 30 minutes.

4.4.1 Crack severity test results

The results are summarised in Table 4.6 and the pressure decay curve is shown in Figure 4.26. The results are compared to that of Beam 2 from the cover depth experiment.

Table 4.6 Pressure decay final times of Beam 2 and 3

	Pressure decay time (hh:mm)	
Cover Depth	**Beam 2**	**Beam 3**
25 mm	01:04	00:25
50 mm	28:40	08:08
75 mm	50:50	00:23
Reference	56:52	71:30

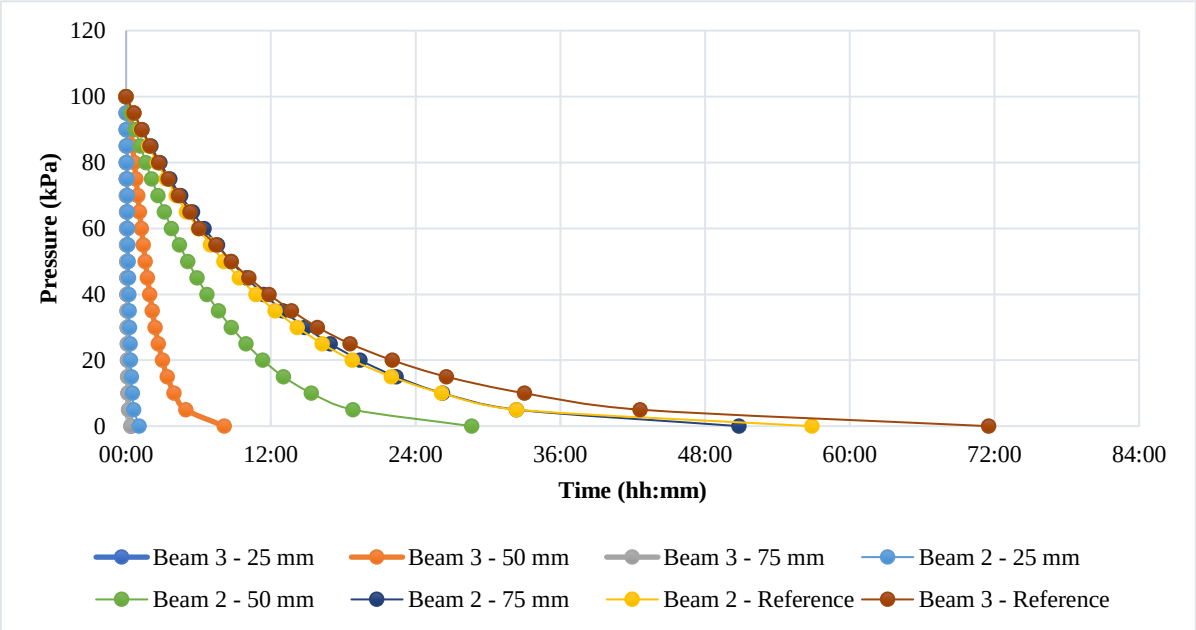

Figure 4.26 Beam 2 vs 3 pressure decay over time

As seen, the results are inconsistent for this experiment. The 75 mm cover depth has a rapid pressure decay curve, at around 23 minutes. This is not the norm if related to the cover depth experiment. Also, the results have not improved by re-vibrating the concrete after three hours. The re-vibration may have been applied too late.

The 25 mm, 50 mm, as well as the 75 mm cover depths has a more rapid pressure decay compared to that of Beam 2 from Experiment 4. However, as also shown in Figure 4.27, the reference has an improved pressure decay rate, at around 71 hours and 30 minutes, compared to the 56 hours and 52 minutes of the standard Beam 2.

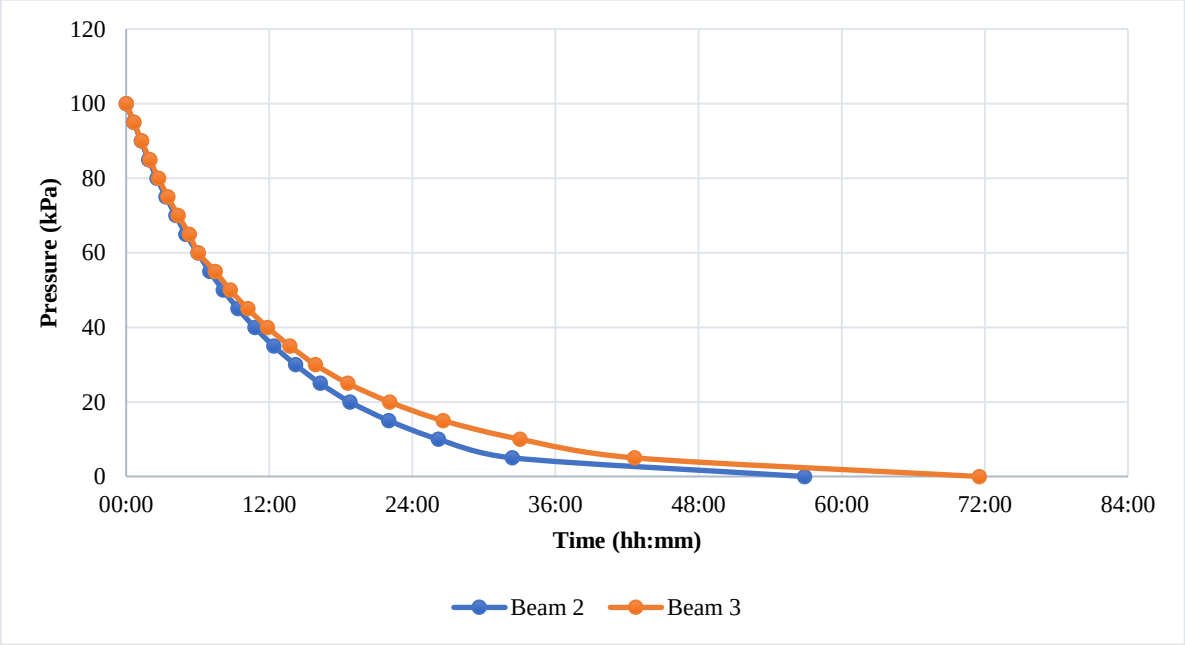

Figure 4.27 Beam 2 vs 3 reference sample pressure decay over time

One sample of each cover depth from Beam 3 are shown in Figure 4.28 (a) to (e). The results of Beam 2 are also shown in Figure 4.28 (f) to (h) to compare to Beam 3. As seen for Beam 3, at the 25 mm cover depth sample there was a tensile crack from the rod to the top of the sample, and it shows on the curved side of the specimen as well. This type of crack was not present with the standard Beam 2 at the 25 mm cover depth, which may indicate that the re-vibration of the concrete may have had a negative influence on plastic settlement cracking, rather than a positive one, specifically at such a low cover depth. No cracks were visible with the 50 mm cover depth. The 75 mm cover sample also has a visible tensile crack on the curved edge of the sample. This again indicate the negative effect of re-vibration not seen with the standard Beam 2.

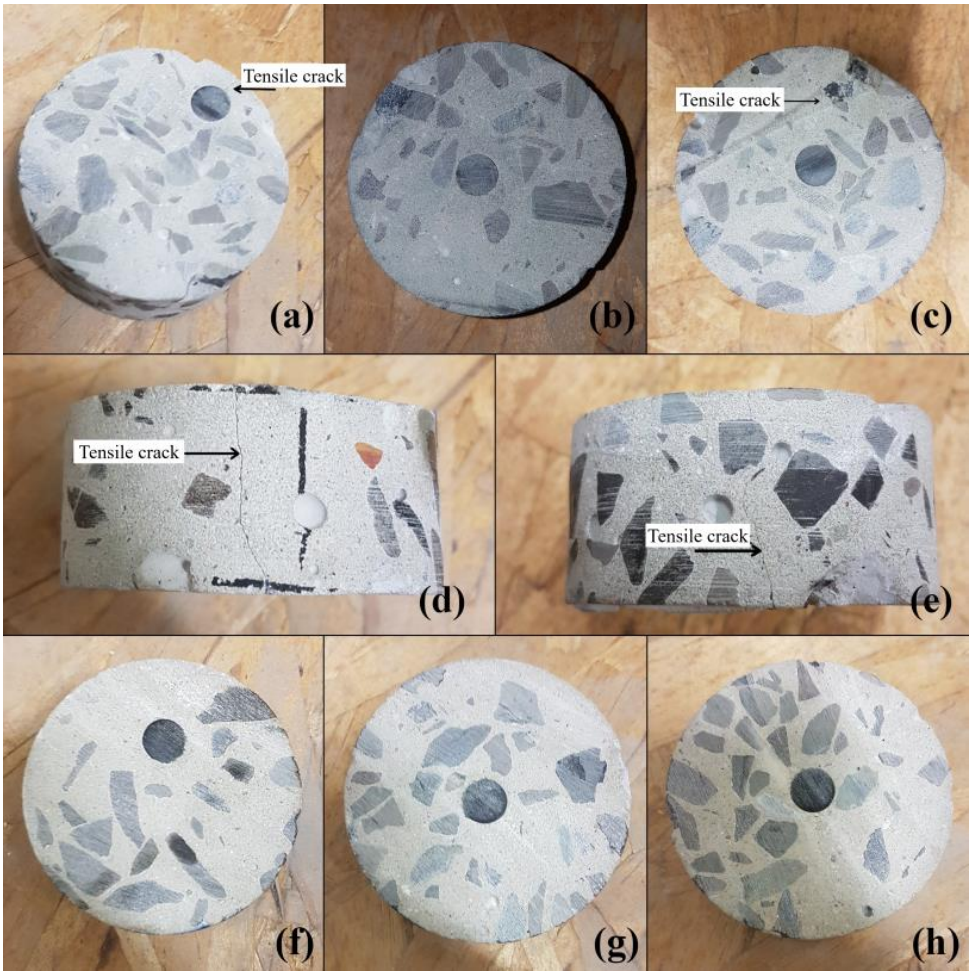

Figure 4.28 The crack severity concrete specimens of (a) Beam 3 - 25 mm cover depth, (b) Beam 3 - 50 mm cover depth, (c) Beam 3 - 75 mm cover depth, (d) Beam 3 - 25 mm cover depth top view, (e) Beam 3 - 75 mm cover depth top view, (f) Beam 2 - 25 mm cover depth, (g) Beam 2 - 50 mm cover depth and (h) Beam 2 - 75 mm cover depth

4.4.2 OPI test results

The OPI results for this experiment are shown in Table 4.7. In this case the results of the 25 mm cover depth do not correlate with the crack severity results shown in Table 4.6. Beam 3 has a higher permeability rating, with an OPI value of 9.32 compared to the 8.49 of Beam 2. As seen with the OPI sample of Beam 3, shown in Figure 4.29, no visible voids or cracks were present, which may be because of re-vibration, especially when compared to the cracks present with the Beam 2 sample shown in Figure 4.21 and Figure 4.22.

Comparing the reference samples of Beam 2 and 3, re-vibration has a slightly improved impact on the permeability of the concrete. This in contrast to the previous section may indicate the positive effect of re-vibration, even when just used on normal concrete.

Table 4.7 OPI results of Beam 2 and 3

Cover Depth	Beam 2	Beam 3
25 mm (OPI)	8.49	9.32
Reference	9.90	9.93

Figure 4.29 Beam 3 OPI sample

4.4.3 Water sorptivity test results

The water sorptivity tests were conducted and the calculations were performed as discussed in Section 3.9. The results of the Beam 3, compared to the results of Beam 2, are shown in Table 4.8. The absorption over time of Beam 3 is shown in Figure 4.30.

For Beam 3, the 75 mm cover depth has a higher sorptivity rate than the 50 mm cover depth, but lower than the 25 mm, which is also reflected in the crack severity results. Overall, Beam 3 has a lower porosity than Beam 2, which may be due to the re-vibration. The reference sample, 50 mm and the OPI sample has a lower sorptivity rate than the corresponding cover depths from Beam 2, whereas the 25 mm and 75 mm samples has a higher sorptivity rate.

Table 4.8 Water sorptivity results for Beam 2 and 3

	Beam 2			Beam 3		
Cover Depth	**R^2**	**Sorptivity ($mm/hr^{0.5}$)**	**Porosity (%)**	**R^2**	**Sorptivity ($mm/hr^{0.5}$)**	**Porosity (%)**
25 mm	0,9943	11,90	14,04	0,9909	14,20	11,53
50 mm	0,9908	9,55	13,22	0,9894	9,22	12,27
75 mm	0,9923	8,56	12,29	0,9881	12,26	10,93
Reference	0,9858	9,08	13,22	0,9872	8,97	11,76
25 mm (OPI)	0,9960	12,02	16,62	0,9864	9,03	14,60

The inconsistencies with the 25 mm and 75 mm cover depths may be an indication that even if re-vibration improves the concrete permeability, the effect of plastic settlement cracking on concrete is still relatively unpredictable.

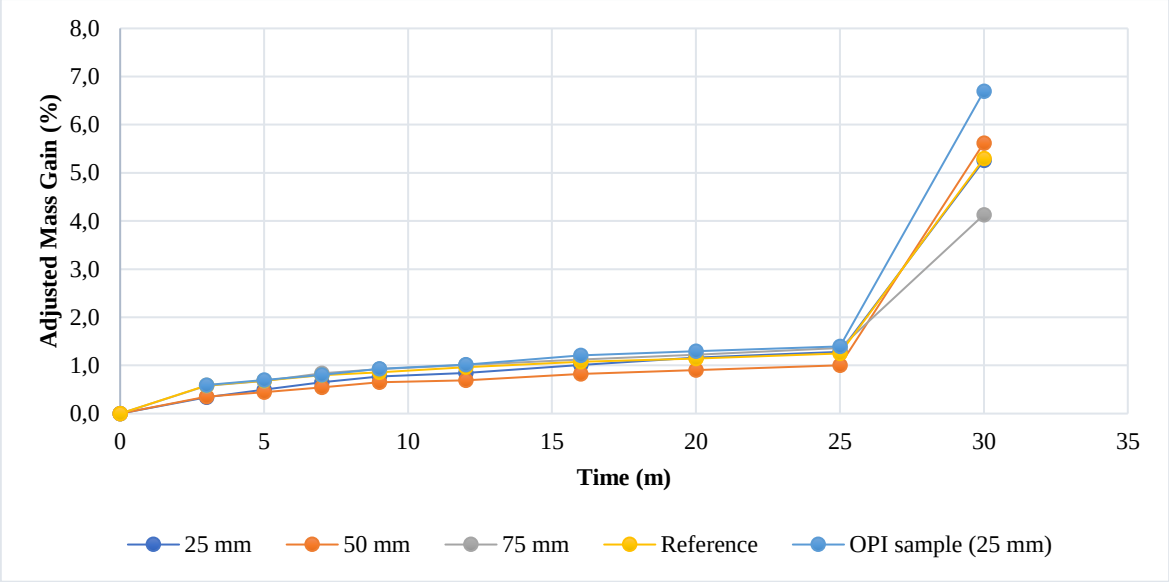

Figure 4.30 Beam 3 Sorptivity results: percentage mass gain over time

4.4.4 CT scans

This section discusses the CT scans of the re-vibrated beam, Beam 3, at 50 mm and 75 mm cover depths. The 50 mm cover of Beam 3 is shown in Figure 3.33 (a) and (d), and the 75 mm cover of Beam 3 is shown Figure 3.33 (b) and (e). The 50 mm cover sample of Beam 3 is compared to that of Beam 2, which is shown in Figure 3.33 (c) and (f).

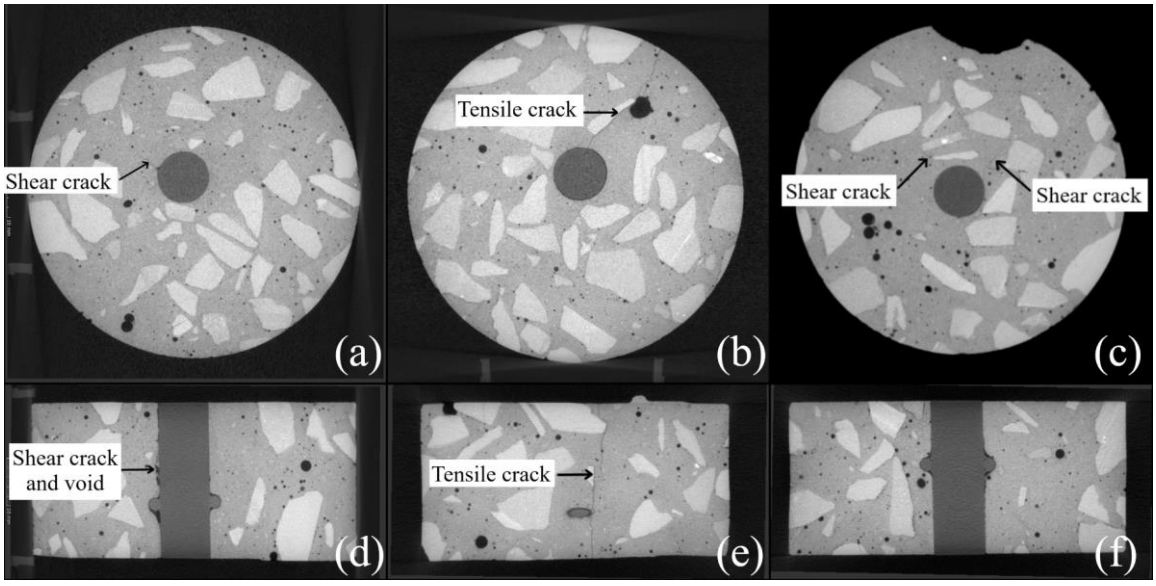

Figure 4.31 CT scans of (a) Beam 3 – 50 mm cover front section view, (b) Beam 3 – 75 mm cover front section view, (c) Beam 2 – 50 mm cover front section view, (d) Beam 3 – 50 mm cover top section view, (e) Beam 3 – 75 mm cover top section view and (f) Beam 2 – 50 mm cover top section view

For the 50 mm cover samples of Beam 2 and 3, Beam 3 has less severe cracks present, in terms of crack length, however, there were more severe voids around the rod, which induced a slight crack. In the top

view the void is clearly shown which formed around the rod. At the Beam 2 sample there are slightly visible shear cracks, however, this does not occur throughout the whole length of the sample.

The 75 mm cover sample of Beam 3 shows a severe tensile crack from the rod to the edge of the sample, as seen in Figure 3.33 (b) and (e). This crack, as also shown in Figure 4.28 (c) and (e), was visible with all four specimens for that cover depth.

4.4.5 Discussion

The inconsistent crack severity results could be for many reasons. Only one re-vibration test was performed, therefore it was not determined what the most efficient time for re-vibration would be. Rather, it was assumed that the beam should be re-vibrated near initial setting time. Although this assumption was made because it was mentioned in literature, this could have easily needed more experimentation. The time of re-vibration could play a large role in the outcome of the results. However, the results for the reference samples indicated that re-vibration could improve the concrete durability if there was no object of restraint.

The results indicate that an object of restraint could increase the plastic settlement cracking severity if the timing of the re-vibration is incorrect. Therefore, it can also indicate that re-vibration was applied too late and damaged the microstructure of the concrete. Re-vibration can, however, allow concrete without restraint to be further compacted and also close possible voids present in the concrete and thereby improve the permeability.

The OPI test results did not reflect the crack severity test results. Beam 3 has an improved permeability index on both the 25 mm OPI, and reference samples. This may indicate that the crack severity does not reflect the permeability of the concrete. It also indicates that re-vibration may impact the crack severity negatively but has a positive influence on the permeability of the concrete. The cracks or voids caused by re-vibration that negatively influenced the crack severity results may not negatively influence the permeability.

With the water sorptivity test, the sorptivity of the 25-, 50- and 75 mm cover samples of Beam 3 is similar to the crack severity test results, where the 25 mm and 75 mm has more rapid pressure decay rates compared to the 50 mm cover.

With the exception of the water sorptivity of the 25 and 75 mm cover depths of Beam 3, the results do indicate that re-vibration did improve the sorptivity of the concrete. However, the results are still mixed and not 100% conclusive. Overall the porosity of Beam 3 is lower than that of Beam 2, even with more severe plastic settlement cracks. Thus, re-vibration may reduce the porosity in the concrete, even though it does not reduce the sorptivity or crack severity, as seen with the crack severity and sorptivity results.

The CT scans show that the re-vibration caused more severe voids around the reinforcement at 50 mm cover depth, compared to the standard Beam 2. However, the length of the cracks seem to be shorter

than the tensile cracks of Beam 2. The 75 mm cover of Beam 3 has a very severe tensile crack, which may explain the crack severity results.

Therefore, re-vibration did not decrease the crack severity of plastic settlement cracking, however, it did have a positive impact on the permeability and sorptivity of the concrete in most cases. This indicates that: a) crack severity of plastic settlement cracks does not necessarily influence the concrete permeability, b) plastic settlement cracking does not form all the way to the surface of the concrete, according to the tests performed. The re-vibration could have worsened the cracks directly surrounding the rod but closed some of the cracks closer to the concrete surface.

The 75 mm cover sample, however, showed strange results. It was not clear why the rod with the most concrete cover almost has the worst crack severity and second highest sorptivity rate. The cause of the crack remains uncertain. It may be due to the time of re-vibration or the cover depth. Since the re-vibration was applied at the bottom of the beam, the highest impact may have been on the lowest cover depth, resulting in such a severe crack.

This experiment could be improved by casting various beams and re-vibrating it at different times to determine the most effective time to apply re-vibration. Since re-vibration is a well-known method used to reduce plastic settlement cracking it would not be discarded based on this experiment. More study is definitely needed in this area. Different forms of re-vibration should also be tested, e.g. a poker, to measure how the cover depth influences re-vibration.

4.5 The influence of plastic viscosity of concrete on plastic settlement cracking

The ICAR Rheometer test was performed as described in Section 3.6. A total of three rheology tests were performed for each mix and the average of the three results were used, as shown in Table 4.9.

The plastic viscosity for all the mixes were different. Mix 2 has the highest plastic viscosity of 173.6 Pa.s, whereas Mix 3, which was Mix 2 with added VMA, has the lowest plastic viscosity of 107.2 Pa.s and Mix 1 somewhere in between with 123.9 Pa.s.

Table 4.9 Yield stress and Plastic viscosity of Mix 1, 2 and 3

Parameters	Mix 1	Mix 2	Mix 3
Yield Stress (Pa)	318.2	311.9	365.8
Plastic Viscosity (Pa.s)	123.9	173.6	107.2

As shown in Table 4.9, there was a significant difference between the mix viscosities of Mix 2 and Mix 3. While the components of the mix were the same, namely the water-cement ratio and aggregate content, the added VMA adjusted the plastic viscosity. The strength difference was also minimal, as discussed in Section 4.1, with both mixes having a 28-day cube strength of around 33 MPa.

It was strange that the addition of the VMA decreased the viscosity of the concrete, since it was expected to increase the viscosity. Therefore, the lower viscosity achieved with Mix 3 was then used to perform the test instead of a mix with a higher viscosity.

4.5.1 Crack severity test results

The results of the crack severity tests are shown in Table 4.10 and Figure 4.32. Table 4.10 compares the pressure decay time for the standard Beam 2 to that of Beam 4. The pressure decay rate of the 75 mm cover depth was the sample with the closest results to that of the standard Beam 2, at 39 hours and 35 minutes, compared to 50 hours and 50 minutes, whereas the other cover depths has completely different results. The 50 mm cover depth has a decay rate of only 1 hour and 11 minutes, compared to 28 hours and 40 minutes of Beam 2 and the 25 mm cover depth has a decay rate of only 7 minutes compared to the 1 hour and 4 minutes of Beam 2.

Comparing the results of Beam 1 to Beam 4, Beam 1 shows a slower pressure decay at the 25 mm and 50 mm cover depths, but a faster pressure decay at the 75 mm and reference cover depth. However, due to the difference in strength and water/cement ratio, the results of Beam 1 were not fully considered to draw final conclusions, but it still shows the behaviour of concrete at different plastic viscosities.

Table 4.10 Pressure decay final times of Beam 2 and 4

	Pressure decay time (hh:mm)		
Cover Depth	**Beam 1**	**Beam 2**	**Beam 4**
25 mm	00:43	01:04	00:07
50 mm	05:31	28:40	01:11
75 mm	08:23	50:50	39:35
Reference	19:38	56:52	175:00

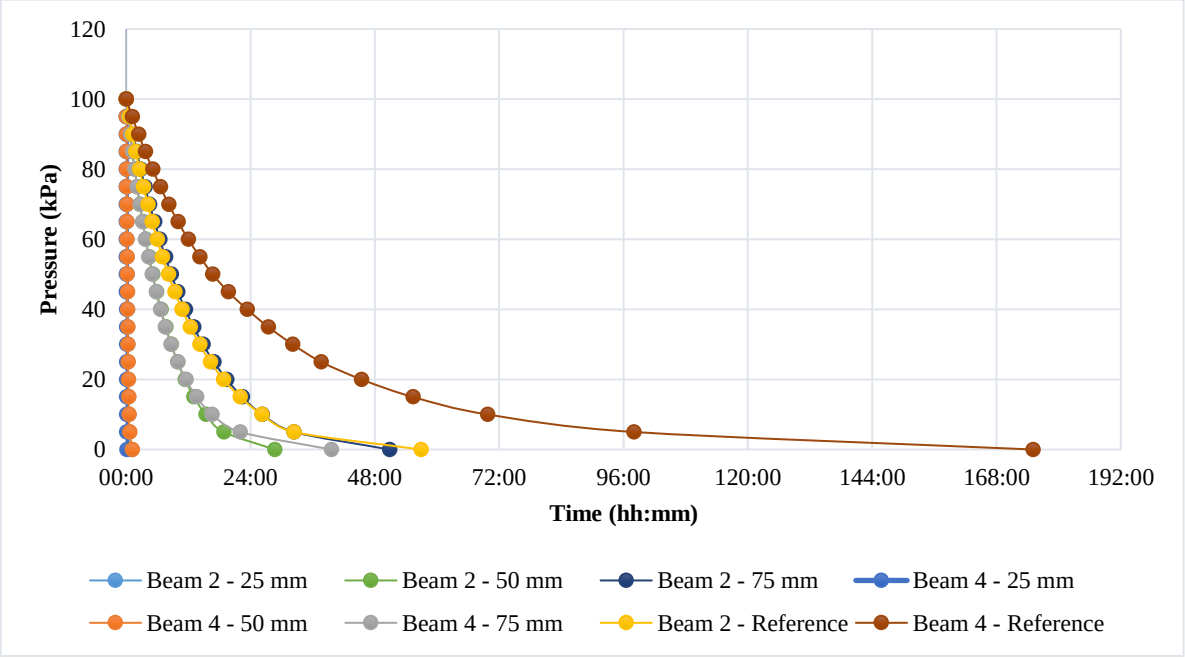

Figure 4.32 Beam 2 vs 4 pressure decay over time

The reference samples again have an opposite effect compared to the crack severity results. The reference sample of Beam 4 has a much slower rate of pressure decay, at 175 hours, compared to the 56 hours and 52 minutes of Beam 2, as seen in Figure 4.33. This may indicate that a lower plastic viscosity may not have a negative impact on the concrete itself but does have a negative effect on the severity of plastic settlement cracks.

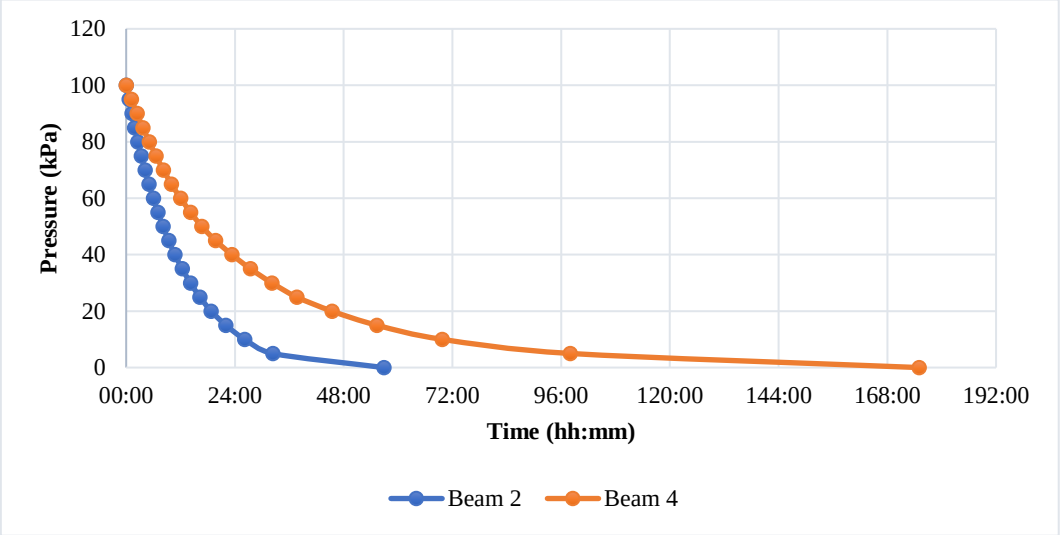

Figure 4.33 Beam 2 vs 4 reference sample pressure decay over time

One sample of each cover depth is shown in Figure 4.34. The samples of Beam 4, Figure 4.34 (a) to (c) can be compared to that of Beam 2, Figure 4.34 (d) to (f). As seen, there were no visible voids or cracks present in the samples. However, even with no visible cracks or voids the results were still worse than that of Beam 2.

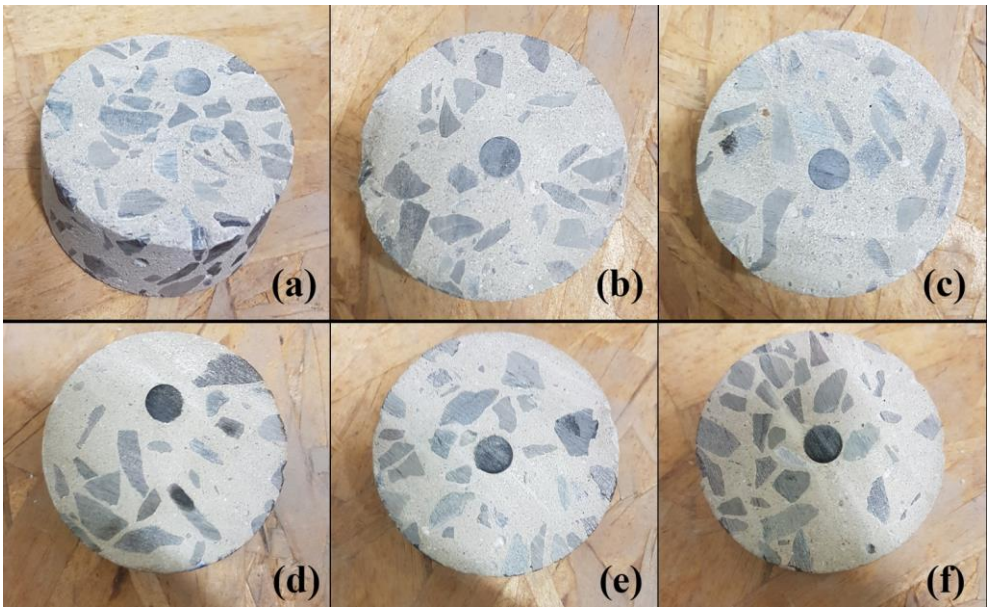

Figure 4.34 Crack severity concrete samples of (a) Beam 4 - 25 mm cover depth, (b) Beam 4 - 50 mm cover depth, (c) Beam 4 - 75 mm cover depth, (d) Beam 2 - 25 mm cover depth, (e) Beam 2 - 50 mm cover depth and (f) Beam 2 - 75 mm cover depth

4.5.2 OPI test results

The OPI results for this experiment are shown in Table 4.11. Again, the results of the 25 mm (OPI) cover do not reflect the crack severity results shown in the previous section. Beam 4 has a higher durability rating, with an OPI value of 9.40 compared to the 8.49 of Beam 2.

A sample from Beam 4 is shown in Figure 4.35 and Figure 4.36. As seen, a single shear crack was visible, starting from the reinforcement to the surface of the concrete sample. The reference sample of Beam 4 shows a greatly improved permeability over Beam 2. Although the cube strength of Beam 2 and 4 were relatively similar, the permeability was not. This may indicate that a lower plastic viscosity may improve the permeability of concrete.

Table 4.11 OPI results of Beam 2 and 4

Cover Depth	Beam 2	Beam 4
25 mm	8.49	9.40
Reference	9.90	10.21

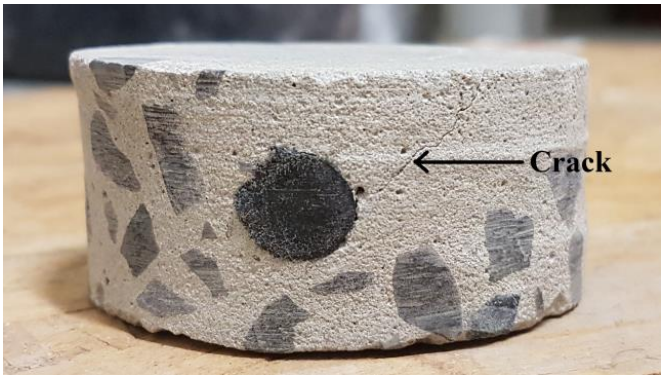

Figure 4.35 Beam 4 OPI sample front crack

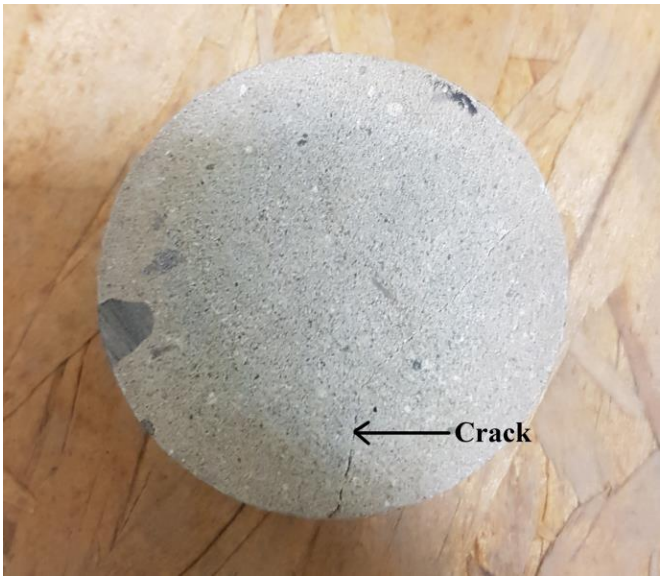

Figure 4.36 Beam 4 OPI sample top crack

4.5.3 Water sorptivity test results

The water sorptivity test results of Beam 4, compared to Beam 2, are shown in Table 4.12. The absorption over time of Beam 4 is shown in Figure 4.37.

The decrease in water sorptivty and porosity of Beam 4, with the increase in cover depth, reflects the results of the crack severity test. Overall, the sorptivity of Beam 4 was higher than Beam 2, and the porosity of Beam 4 was lower than Beam 2, when the cover depth of each beam is compared. The results indicate that concrete with a lower plastic viscosity has a lower porosity. This is because a lower viscosity means that less air is entrapped in the concrete. However, a lower plastic viscosity does seem to negatively impact the sorptivity of the concrete.

Table 4.12 Water sorptivity results for Beam 2 and 4

	Beam 2			Beam 4		
Cover Depth	**R^2**	**Sorptivity ($mm/hr^{0.5}$)**	**Porosity (%)**	**R^2**	**Sorptivity ($mm/hr^{0.5}$)**	**Porosity (%)**
25 mm	0,9943	11,90	14,04	0,9919	14,35	12,42
50 mm	0,9908	9,55	13,22	0,9921	12,24	12,03
75 mm	0,9923	8,56	12,29	0,9904	10,49	11,58
Reference	0,9858	9,08	13,22	0,9888	10,38	11,76
25 mm (OPI)	0,9960	12,02	16,62	0,9911	15,67	14,29

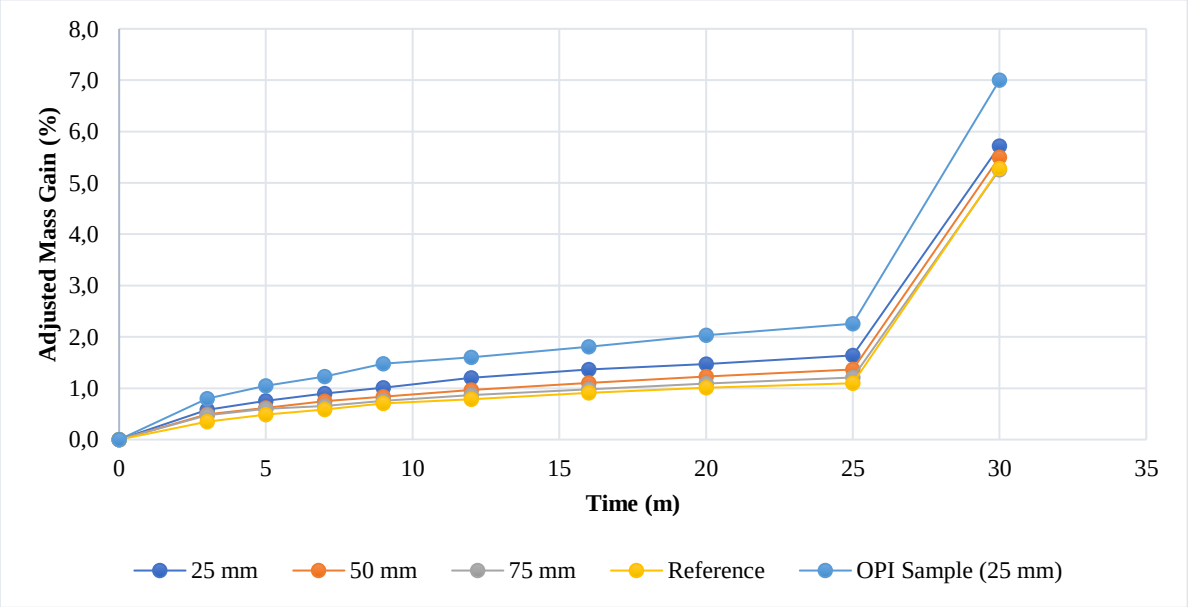

Figure 4.37 Beam 4 Sorptivity results: percentage mass gain over time

4.5.4 CT scans

This section shows the CT scans of the lower plastic viscosity beam, Beam 4, in Figure 4.38. The 50 mm cover samples of Beam 4, shown in Figure 4.38 (a) and (c), is compared to that of Beam 2 in Figure 4.38 (b) and (d). Beam 4 has a void around the rod, with a clear tensile crack from the rod to the edge

of the sample. Compared to Beam 2, the crack and void present were more severe. This may be due to the lower viscosity.

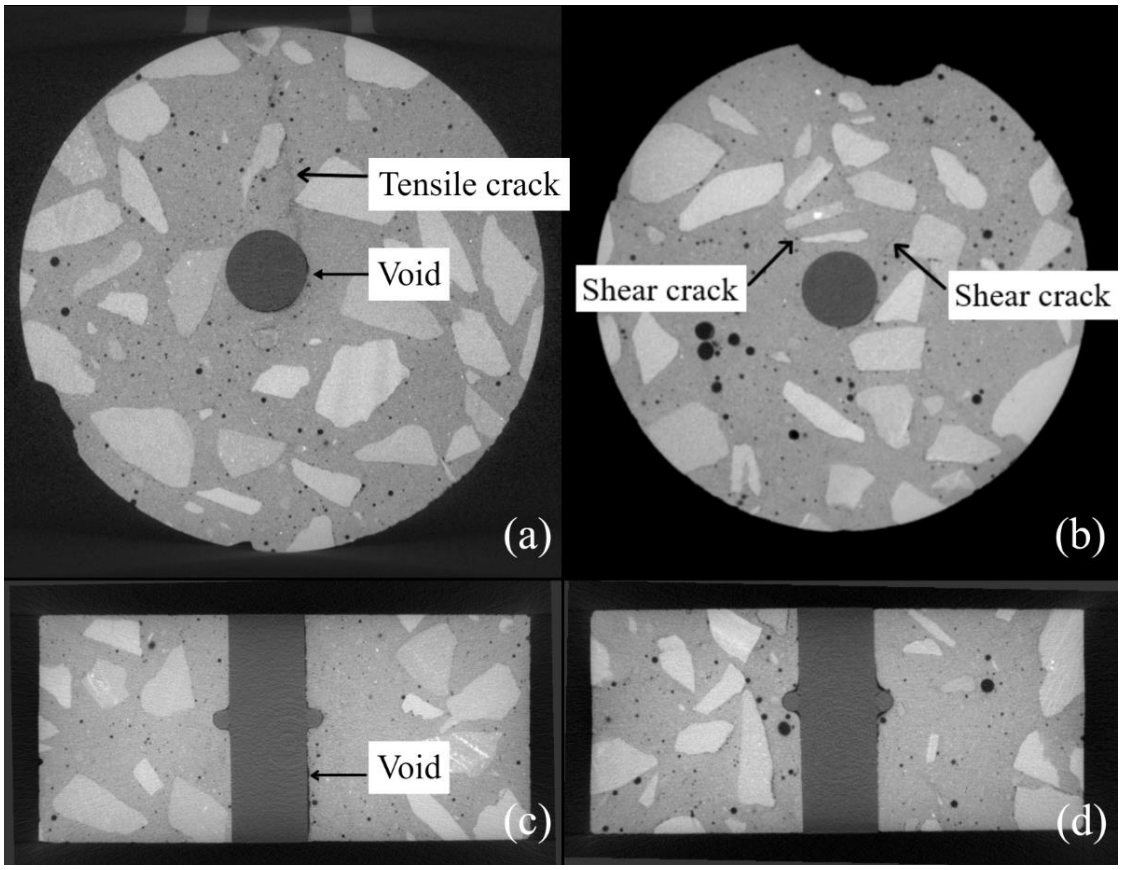

Figure 4.38 CT scans of (a) Beam 4 – 50 mm cover front section view, (b) Beam 2 – 50 mm cover front section view, (c) Beam 4 – 50 mm cover top section view and (d) Beam 2 – 50 mm cover top section view)

4.5.5 Discussion

For the crack severity results the lower plastic viscosity has a negative influence on the plastic settlement cracking of the concrete. This was not expected and it was assumed that a lower plastic viscosity would reduce the severity of plastic settlement cracking.

The results of the reference samples may indicate that a lower viscosity provides better compaction, and therefore, a lower permeability, since the reference of Beam 4 has a slower pressure decay than Beam 2. According to this, it can be assumed that a lower plastic viscosity may lower the permeability of the concrete, except when there is a restraint present.

The OPI results did not reflect the results from the cracks severity test, where Beam 4 with the lower viscosity has an improved permeability index compared to Beam 2. This again indicated that the plastic settlement crack severity may not affect the permeability of the concrete. The voids present in the concrete may have also influenced the results.

The water sorptivity results were fairly consistent. It reflected the phenomenon that the sorptivity of concrete increases with a smaller cover depth. The overall sorptivity of Beam 4 was higher compared to Beam 2, and the porosity was lower. Thus, the crack severity samples indicate that Beam 4 did have more severe plastic settlement cracks, but still a lower porosity. The OPI and reference samples also indicate more severe cracks, with the higher sorptivity compared to Beam 2.

The CT scans confirm the crack severity results and show more severe plastic settlement cracking in Beam 4. This may be a direct result of the lower plastic viscosity.

According to this experiment a lower plastic viscosity does not decrease the crack severity of plastic settlement cracking; however, it did have a positive influence on the permeability index and porosity, of the concrete. However, the sorptivity was not improved with a lower plastic viscosity. This again indicates that plastic settlement cracking and crack severity does not necessarily influence the durability parameters of the concrete. Since many factors influence the durability of the concrete, more consistent results would be needed to determine exactly if a lower plastic viscosity has a positive influence on the concrete durability.

The results indicate that a low plastic viscosity may negatively influence plastic settlement cracking, depending on the cover depth. This phenomenon should be researched further to determine the effect of plastic viscosity on plastic settlement cracking. However, at least three or more beams should be compared with different plastic viscosities. This will allow a better understanding of the behaviour of the concrete at different plastic viscosities and more tangible conclusions could be drawn.

4.6 The influence of plastic shrinkage cracks on plastic settlement cracking

The evaporation rate of 0.145 kg/m^2/h was not enough to cause clear plastic shrinkage cracks. Therefore, this experiment tested a low potential for plastic shrinkage cracking.

4.6.1 Crack severity test results

To initiate the effect of plastic shrinkage cracking, Beam 5 was cast, using Mix 2, and was placed in a climate box where the humidity, air temperature and wind speed was controlled.

The pressure decay results of the beam are shown in Table 4.13 and Figure 4.39. As seen, the 25 mm cover depth has a more rapid pressure decay rate of 16 minutes, compared to the results of the standard Beam 2 of around 1 hour and 4 minutes. The 50 mm cover depth results are also more rapid at around 11 hours and 10 minutes, compared to 28 hours and 40 minutes, and the 75 mm cover depth rate only 15 hours and 55 minutes, compared to 50 hours and 50 minutes, which is also significantly faster.

Table 4.13 Pressure decay final times of Beam 2 and 5

	Pressure decay time (hh:mm)	
Cover Depth	**Beam 2**	**Beam 5**
25 mm	01:04	00:16
50 mm	28:40	11:10
75 mm	50:50	15:55
Reference	56:52	135:06

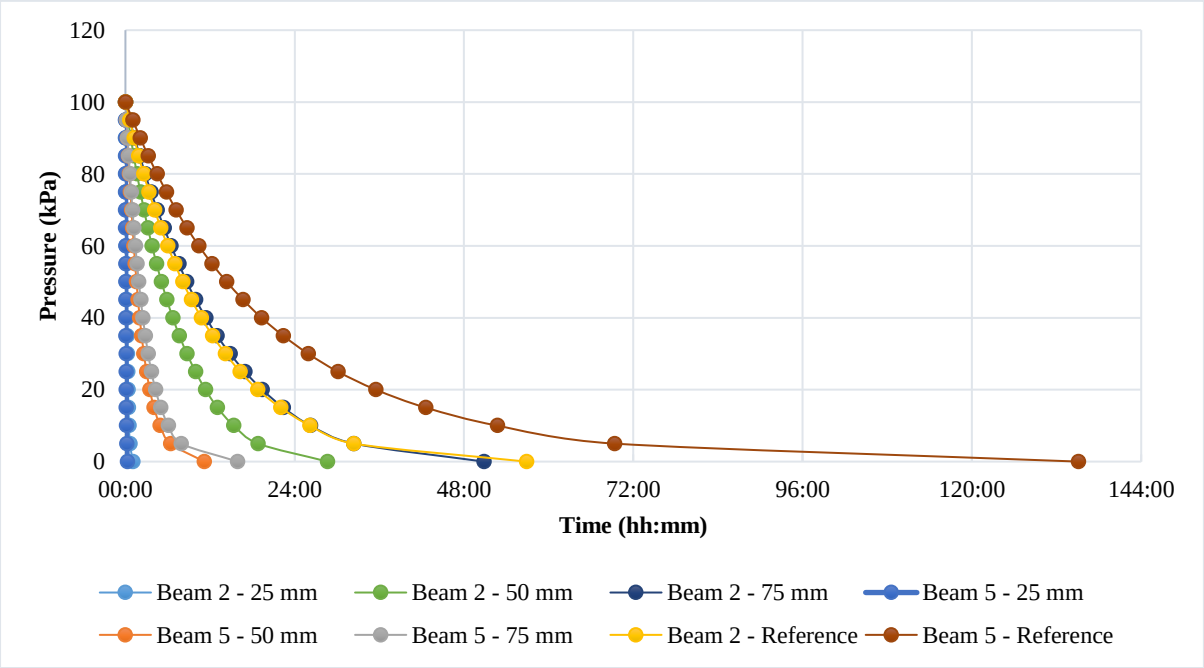

Figure 4.39 Beam 2 vs 5 pressure decay over time

These results may be because of plastic shrinkage cracking, especially the 25 mm cover depth, which show a significant difference in pressure decay time and a severe visible crack and void, as seen in Figure 4.41 (a), which was not present with the standard Beam 2. The reference sample of Beam 5 again showed a much slower rate of pressure decay compared to that of Beam 2, as seen in Figure 4.39 and Figure 4.40. This was not expected. It was assumed to have the same pressure decay time, or at least more rapid than that of Beam 2. However, the results still indicate that the climate conditions negatively influenced the severity of the plastic settlement cracks at the different cover depths.

It is clear that the plastic shrinkage crack at the 25 mm cover depth has an influence on the crack severity of the concrete. Although there were no visible cracks present at the other cover depths, it can be assumed, according to the results, that the induced environment has an effect on the concrete. According to these results it does show that a low potential plastic shrinkage can negatively affect plastic settlement cracking and crack severity.

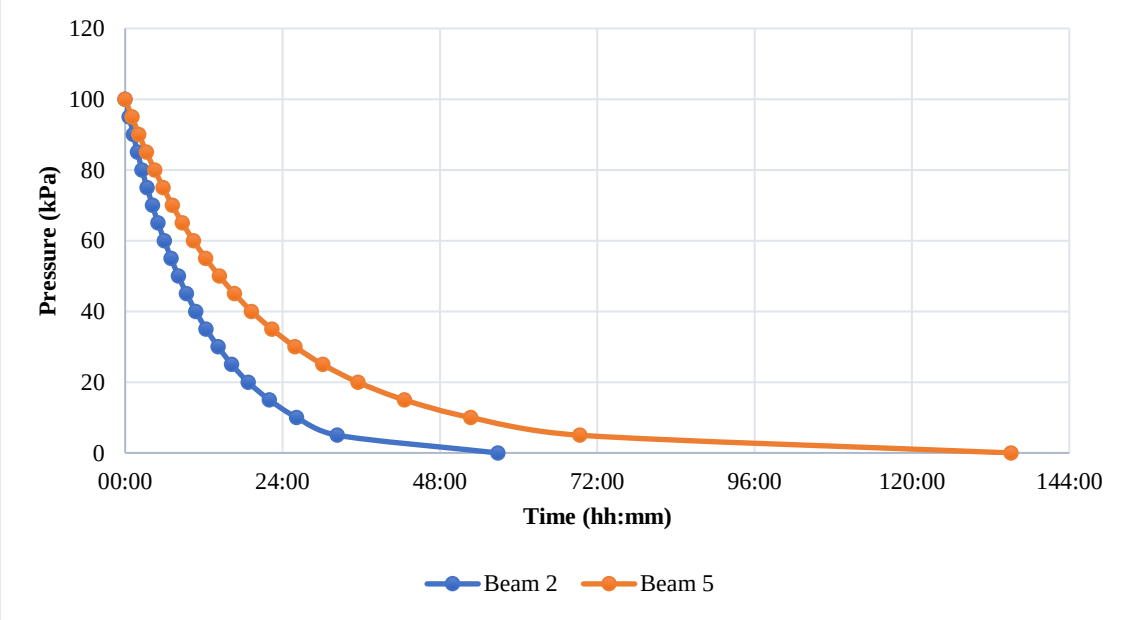

Figure 4.40 Beam 2 vs 5 reference sample pressure decay over time

One sample of each cover depth is shown in Figure 4.41. The 25-, 50- and 75 mm samples, shown in Figure 4.41 (a) to (c), can be compared to that of Beam 2, shown in Figure 4.41 (d) to (f). As seen, there is a large crack and void present in the 25 mm cover sample. This may be due to the influence of plastic shrinkage cracking. The 50 mm and 75 mm cover samples show no visible voids or cracks. The samples of Beam 2 (d, e and f) also show no visible voids or cracks.

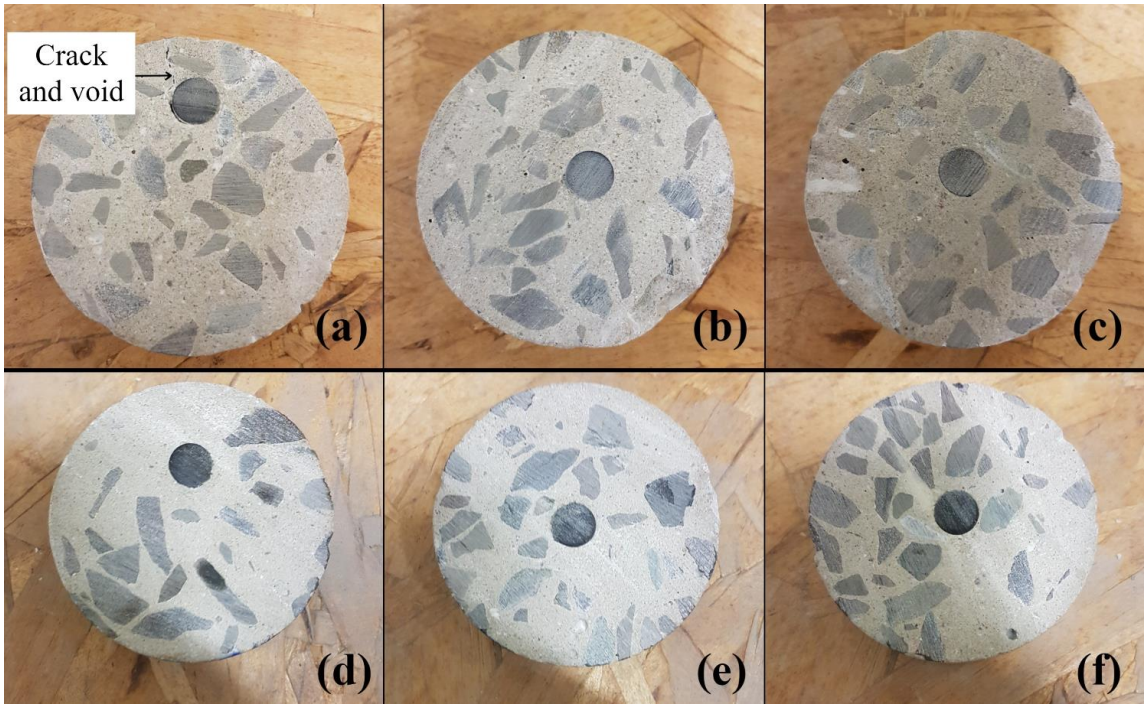

Figure 4.41 Crack severity concrete samples of (a) Beam 5 - 25 mm cover depth, (b) Beam 5 - 50 mm cover depth, (c) Beam 5 - 75 mm cover depth, (d) Beam 2 - 25 mm cover depth, (e) Beam 2 - 50 mm cover depth and (f) Beam 2 - 75 mm cover depth

4.6.2 OPI test results

The OPI results for this experiment are shown in Table 4.14. Again, the results of the 25 mm (OPI) cover depth do not reflect the crack severity results shown in Table 4.13. Beam 5 had a higher durability rating, with an OPI value of 9.36 compared to the 8.49 of Beam 2. This again indicates that the crack severity may not reflect the permeability of the concrete, based on the OPI results.

The reference sample also indicated that the external climate did not severely affect the permeability of concrete without a restraint.

A 25 mm OPI sample is shown in Figure 4.42. As seen, there were visible voids and shear cracks present around the plastic rod, however, there was no crack that resembled a plastic shrinkage crack. With the presence of the cracks and voids, it still performed better than the standard Beam 2 in terms of permeability.

Table 4.14 OPI results of Beam 2 and 5

Cover Depth	Beam 2	Beam 5
25 mm (Top)	8.49	9.36
Reference	9.90	10.15

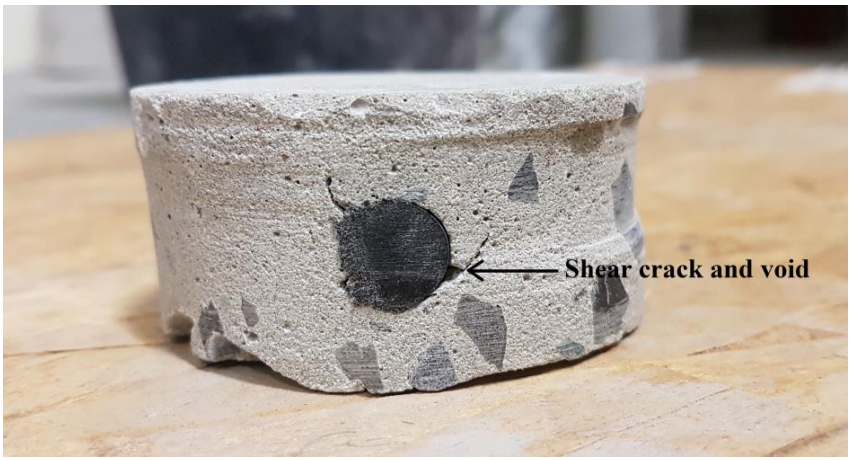

Figure 4.42 Beam 5 OPI sample front crack

4.6.3 Water sorptivity test results

The water sorptivity test results of Beam 5, compared to the results of Beam 2, are shown in Table 4.15. The water sorptivity curve of Beam 5 is shown in Figure 4.43.

Table 4.15 shows that the water sorptivity test results for Beam 5 also reflect the phenomenon seen with the crack severity test results, where the cover depth has an influence on cracking of the concrete. As seen the sorptivity and porosity decreases with an increase in cover depth. The sorptivity of Beam 5 was higher than that of Beam 2, and the porosity of Beam 5 was lower than Beam 2, at each cover depth.

Table 4.15 Water sorptivity results for Beam 2 and 5

	Beam 2			Beam 5		
Cover Depth	**R^2**	**Sorptivity ($mm/hr^{0.5}$)**	**Porosity (%)**	**R^2**	**Sorptivity ($mm/hr^{0.5}$)**	**Porosity (%)**
25 mm	0,9943	11,90	14,04	0,9954	13,89	13,04
50 mm	0,9908	9,55	13,22	0,9895	10,85	12,75
75 mm	0,9923	8,56	12,29	0,9898	10,30	11,79
Reference	0,9858	9,08	13,22	0,9908	10,53	12,07
25 mm (OPI)	0,9960	12,02	16,62	0,9911	20,15	15,31

The sorptivity results reflect the crack severity results, where the presence of plastic shrinkage cracks negatively influence the plastic settlement cracking, when compared to Beam 2. However, the porosity reflected the OPI test results, in that regardless of the crack severity, or in this case the sorptivity, the porosity was less severe than that of Beam 2.

The sorptivity rate does seem to very closely resemble the crack severity results, whereas the porosity more accurately protrays the permeability results achieved with the OPI test.

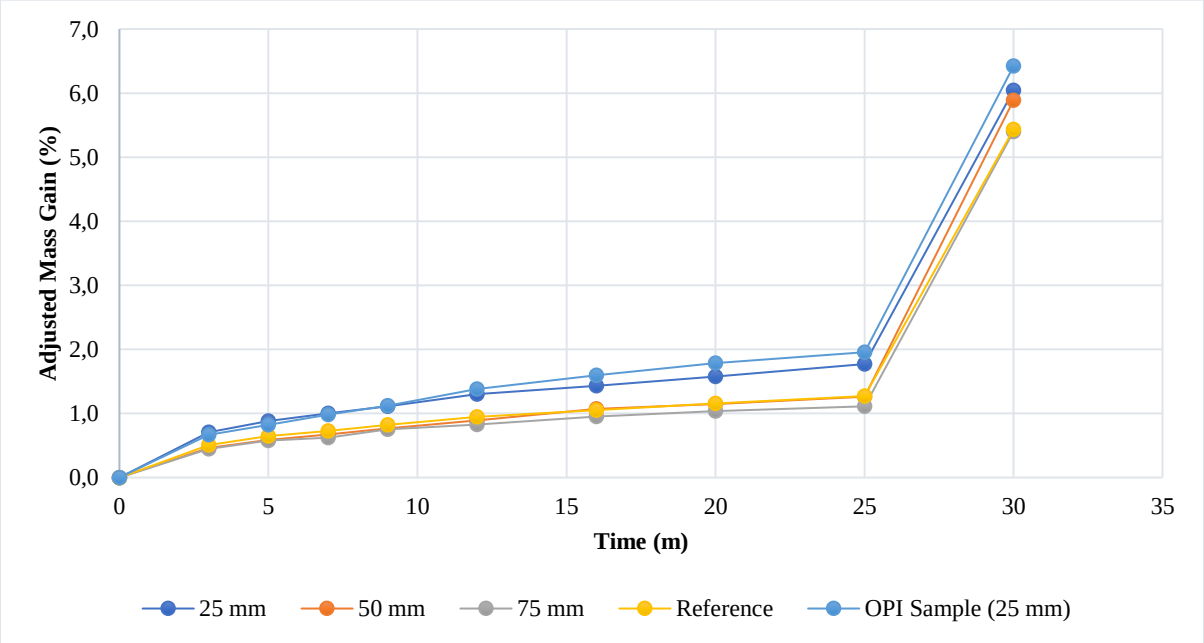

Figure 4.43 Beam 5 Sorptivity results: percentage mass gain over time

4.6.4 CT scans

This section discusses the CT scans of Beam 5 compared to the results of Beam 2. The results of Beam 5 are shown in Figure 4.44 (a) and (c), which is compared to the results of Beam 2, as shown in Figure 4.44 (b) and (d). Beam 5 has much more severe voids and cracks. In the front view there is a clear shear crack on the left of the rod, resulting from the large voids underneath the rod, also visible in the top view. No plastic shrinkage cracks are visible in the scan. This suggests that the results are not directly caused by traditional surface plastic shrinkage cracking. However, plastic shrinkage may still have

widened any possible settlement cracks below the surface. This shows that small settlement cracks could be widened by even a low potential for plastic shrinkage cracking.

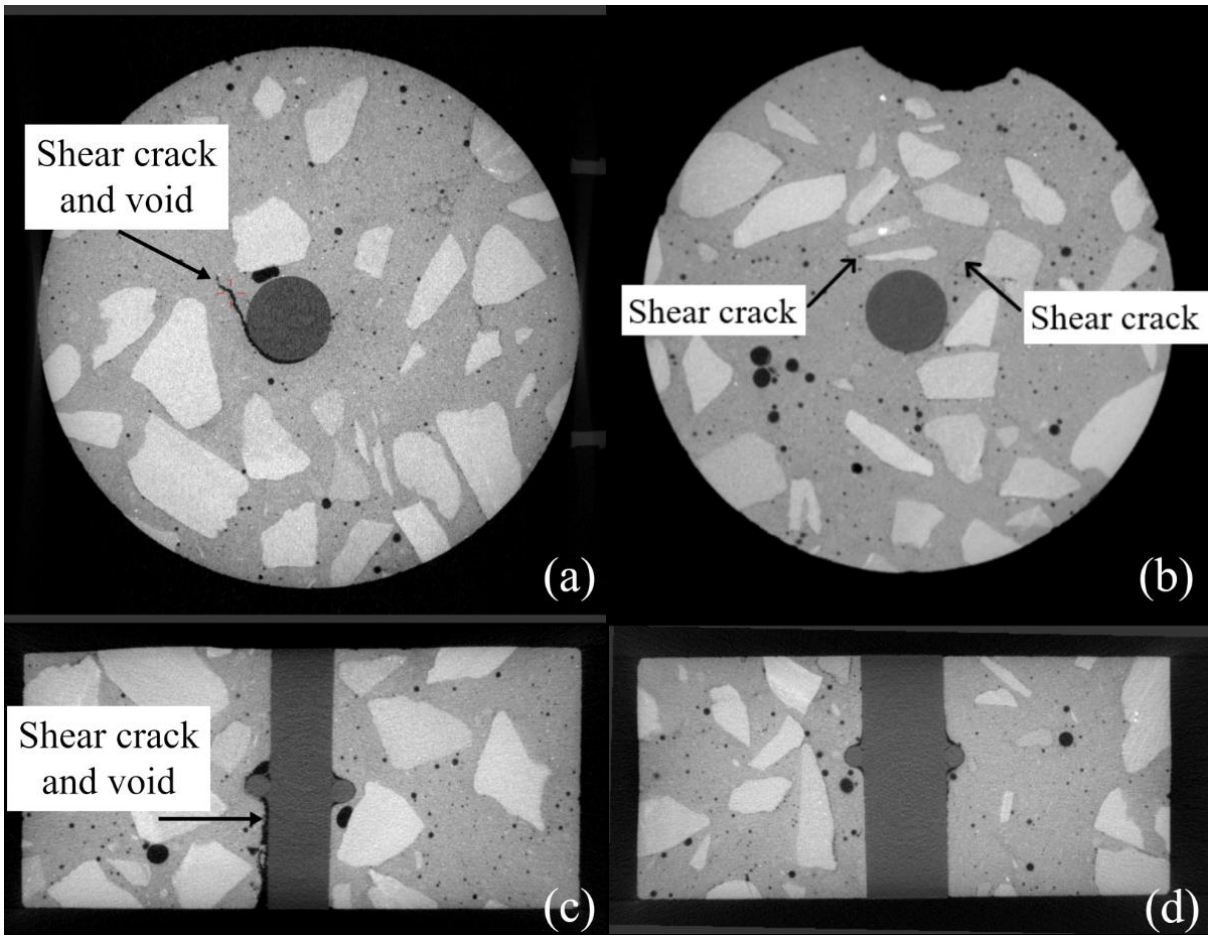

Figure 4.44 CT scans of (a) Beam 5 – 50 mm cover front section view, (b) Beam 2 – 50 mm cover front section view, (c) Beam 5 – 50 mm cover top section view and (d) Beam 2 – 50 mm cover top section view)

4.6.5 Discussion

With the crack severity results, the crack present at the 25 mm cover depth indicated the influence of plastic shrinkage cracking, and how it amplified the plastic settlement crack, since the same cover depth for Beam 2 has no visible cracks present. Overall, Beam 5 showed worse results than Beam 2, in terms of crack severity. The different cover depths also reflected the phenomenon that crack severity increases with a decrease in cover depth.

The OPI results indicate that the permeability of the 25 mm (OPI) cover sample was higher for Beam 5. This does not reflect the results of the crack severity test. If the images of the OPI samples are compared between Beam 2 and 5, Figure 4.21 and Figure 4.42, respectively, the Beam 2 sample showed a distinct tensile crack that leads to the surface of the sample. However, the Beam 5 sample only shows voids around the rod, with some shear cracks. There was no indication of a plastic shrinkage or tensile crack at the surface. The behaviour of the plastic shrinkage cracks was inconsistent when comparing these results. The climate box settings were not severe enough to consistently induce plastic shrinkage

cracks that form at the surface throughout the beam. The 25 mm crack severity sample indicates a crack leading to the surface, but not the 25 mm OPI sample. However, with the absence of visible plastic shrinkage cracks, there were still major differences in the results between the two beams.

The permeability of Beam 5 was better than that of Beam 2, which again indicates that the plastic settlement and possibly plastic shrinkage crack severity does not influence the permeability of the concrete.

The water sorptivity results also reflect the results achieved by the crack severity test and OPI test. The overall sorptivity of Beam 5 was higher than that of Beam 2, of each sample. Thus, indicating possibly more severe cracks present in the concrete. However, the porosity of Beam 5 was lower compared to Beam 2.

The CT scans also reflect the same shear crack and void present with the 25 mm OPI sample of Beam 5, Figure 4.42. At a 50 mm cover depth, Beam 5 shows much more severe voids and cracks, however, no plastic shrinkage cracks are visible. This may indicate that the more severe cracks in Beam 5 may not be due to a result of surface plastic shrinkage cracking. However, the climate conditions may have widened the small plastic settlement crack below the surface, even when there was only a low potential for plastic shrinkage cracks.

The results of this experiment were inconsistent with the logical parameters of the tests. There was no additional factor that would result in an improved durability for the beam exposed to the plastic shrinkage cracks. In the case of the re-vibration and plastic viscosity experiments, logical conclusions could be drawn to the improved durability of the concrete. However, in this case it is a bit more difficult, especially since there are no visible plastic shrinkage cracks, even with the CT scans. However, the crack severity of the concrete does indicate that the potential for plastic shrinkage cracks may amplify plastic settlement cracks and its severity.

Therefore, the influence of the external environmental factors, and presumably plastic shrinkage cracks, negatively influenced the crack severity of the plastic settlement cracks in the concrete. However, the durability parameters tested, such as the permeability, remains unaffected and seems to have improved. This again confirms that high plastic settlement crack severity does not necessarily influence the durability parameters of the concrete negatively, as tested in this study. The durability tests performed for this experiment did not have consistent results which clearly indicate the influence on the concrete durability. More tests would need to be performed and possibly using another method of testing, such as chloride conductivity test.

A factor that needs to be considered is, after the 6-hour period that the beam was placed in the climate box, it was physically removed from the box and moved to the temperature-controlled room. Although much care was taken with the movement, it may still have been disruptive on the concrete, since it has

only reached initial set at that time and not yet final set. The disruption could have caused more severe cracks around the reinforcement than initially present since the concrete was not workable anymore. This could have easily influenced the crack severity around the reinforcement, without affecting the cracks at the surface.

Another factor that may have influenced the results were the contraction and/or expansion of the concrete due to the change in temperature and humidity when the beam was moved from the climate box to the temperature-controlled room. In hindsight only the wind should have been adjusted to induce plastic shrinkage cracking, whereas the air temperature and relative humidity should have been kept constant throughout the entire duration of the test.

However, this is just a speculation about a possible cause of the inconsistent results.

More testing should be done on this phenomenon, where the beam remains undisturbed for at least 24 hours. Also, different climate conditions should be tested to determine the conditions from least to most severe plastic shrinkage cracks, and how that influences plastic settlement cracking and durability.

5 Conclusions and recommendations

The objectives of this study were to provide a fundamental understanding of the behaviour of plastic settlement cracking and to determine the influence of different factors, namely reinforcement cover depth, concrete strength and viscosity, re-vibration of concrete, and plastic shrinkage cracking on the formation and severity of plastic settlement cracking. It was also to relate how the severity of plastic settlement cracking and each specific factor influences the durability of the concrete.

5.1 Conclusions

The following significant conclusions can be drawn from this study

- The severity of plastic settlement cracks in concrete does not directly influence the durability parameters of the concrete, as indicated by the OPI and water sorptivity tests. In three of the four main experiments the results showed higher crack severity, but improved permeability, when compared to the standard beam. This indicates that plastic settlement cracks do not have a significant influence on the permeability of concrete.
- The crack severity, permeability and sorptivity of the concrete can all be considered durability parameters. However, they do not always indicate the same phenomenon in their results and do not necessarily influence each other.
- Plastic settlement cracks start at the object of restraint and does not necessarily form to the surface of the concrete.
- The crack severity testing method was a successful method to determine the crack severity of a concrete sample.
- Even when not visible, plastic settlement cracks are likely to be present. Many samples indicated no or barely visible plastic settlement cracks but showed a great difference in the crack severity when analysing the results.
- The cover depth of concrete has a significant influence on the severity of plastic settlement cracking. All the experiments indicated that a smaller cover depth resulted in more severe plastic settlement cracks.
- The w/c ratio and strength of concrete has an influence on the plastic settlement cracking severity and durability parameters. With a higher strength concrete the plastic settlement cracks are less severe than with a lower strength concrete. The higher strength concrete also had lower permeability. However, the change in w/c ratio's influences the microstructure of the concrete, which may also have influenced the results. Therefore, this phenomenon should be researched further with a very high strength concrete and also with a focus on the microstructural change in the concrete.

- Re-vibration can result in an increase in crack severity of plastic settlement cracking, when applied at the incorrect time. However, it does improve the permeability of the concrete. This conclusion is highly dependent on the time when re-vibration is applied.
- A low plastic viscosity results in more severe plastic settlement cracking. However, it does improve the concrete permeability. This conclusion is highly dependent on the specific plastic viscosity tested. Results may differ at other viscosities.
- The presence of plastic shrinkage cracks results in more severe plastic settlement cracking. The plastic settlement crack acts as a weak point for the formation of the plastic shrinkage crack, which increases the severity of the crack. Small settlement cracks could be widened by an environment with a low potential for plastic shrinkage cracking.

5.2 Recommendations

From the knowledge gained in this study, the following aspects require further investigation:

- In many cases the sorptivity reflected the results of the crack severity tests and did not always reflect the permeability result of the concrete. This indicates the possible correlation between crack severity and sorptivity. However, more testing is needed using another durability test, such as the chloride conductivity test, since the durability of concrete is related to many aspects, and not just permeability and sorptivity.
- The influence of a high strength concrete, such as 45+ MPa with a low w/c ratio, on plastic settlement cracking, compared to medium and low strength concrete still needs investigation.
- The influence of re-vibration at different times before initial setting time. The re-vibration experiment did not deliver the expected results. However, it was assumed to be highly dependent on the time of re-vibration. More than one beam, at least three, should be re-vibrated, each at a different time to determine the optimal time to apply it. This would also give a clear indication on how re-vibration affects plastic settlement cracking, since various results can be compared. The duration of re-vibration should also be investigated, as well as the type of re-vibration e.g., a poker.
- A higher variety of plastic viscosities should be tested, using different beams. This would give a clear indication of the optimal plastic viscosity and how it influences plastic settlement cracking.
- More durability tests should be performed to have a larger amount of data to correlate and find a general consensus on results, not just OPI and water sorptivity, such as the chloride conductivity test.
- The influence of plastic shrinkage cracking on plastic settlement cracks should be researched further. Different degrees of the environmental setting should be tested. Also, the beam should remain undisturbed for at least 24 hours after cast. After the 6-hour period, the beam should be

cured, and the environment of the climate-controlled room should be replicated with the climate box. Also, mainly wind should be used to increase evaporation, to minimise the influence of temperature change on the concrete.

- Other plastic settlement cracking initiating factors should also be considered, such as varying section depth. This study gave the general conclusion that plastic settlement cracking does not influence the concrete permeability or sorptivity, however, other types of plastic settlement cracking should also be studied to confirm or disprove the results, such as plastic settlement cracking at a varying section depth.

6 Reference list

American Society for Testing and Materials (2008) 'ASTM C191-08 Standard Test Methods for Time of Setting of Hydraulic Cement by Vicat Needle', *Annual Book of ASTM Standards 191-04*, i, pp. 1–8. doi: 10.1520/C0191-08.2.

Armaghani, J. M., Larsen, T. J. and Romano, D. C. (1992) 'Aspects of Concrete Strength and Durability', *Transportation Research Records*, (1335), pp. 63–69.

ASTM (2013) 'ASTM C 1579 - The standard test method for Evaluating plastic shrinkage cracking of restrained fiber reinforced concrete'. West Conshohocken: ASTM International.

Banfill, P. F. G. (2006) 'Rheology of fresh cement and concrete', *The british society of Rheology*, (May), pp. 61–130. Available at: http://www.bsr.org.uk.

Barlow, P. *et al.* (1998) 'Causes , Evaluation and Repair of Cracks in Concrete Structures', pp. 1–22.

Bertolini, L. *et al.* (2004) 'Transport Processes in Concrete', *Corrosion of Steel in Concrete*. Weinheim: WILEY-VCH Verlag GmbH & Co. KGaA, Weinheim, pp. 21–48. doi: 10.1002/3527603379.ch2.

Bullard, J. W. *et al.* (2011) 'Mechanisms of cement hydration', *Cement and Concrete Research*. Elsevier B.V., 41(12), pp. 1208–1223. doi: 10.1016/j.cemconres.2010.09.011.

Combrinck, R. (2012) 'Investigation of plastic shrinkage cracking in conventional and low volume fibre reinforced concrete', (March), pp. 1–124.

Combrinck, R. and Boshoff, W. . (2014) 'Fundamentals of Plastic Settlement Cracking in Concrete', *Concrete Materials CONMAT'15 conference*, 4, pp. 65–73.

Combrinck, R. and Boshoff, W. P. (2018) 'The origin of plastic settlement cracking and the effect of re-vibration'.

Combrinck, R., Steyl, L. and Boshoff, W. P. (2018) 'Interaction between settlement and shrinkage cracking in plastic concrete', *Construction and Building Materials*. Elsevier Ltd, 185, pp. 1–11. doi: 10.1016/j.conbuildmat.2018.07.028.

Dhawan, S., Bhalla, S. and Bhattacharjee, B. (2003) 'Reinforcement corrosion in concrete structures, its monitoring and service life prediction - A review', *Cement and Concrete Composites*, 25(4-5 SPEC), pp. 459–471. doi: 10.1016/S0958-9465(02)00086-0.

Faleschini, F. *et al.* (2014) 'Rheology of fresh concretes with recycled aggregates', *Construction and Building Materials*. Elsevier Ltd, 73, pp. 407–416. doi: 10.1016/j.conbuildmat.2014.09.068.

Gagg, C. R. (2014) 'Cement and concrete as an engineering material: An historic appraisal and case study analysis', *Engineering Failure Analysis*. Elsevier Ltd, 40, pp. 114–140. doi:

10.1016/j.engfailanal.2014.02.004.

Ghourchian, S. *et al.* (2019) 'On the mechanism of plastic shrinkage cracking in fresh cementitious materials', *Cement and Concrete Research*. Elsevier, 115(November 2018), pp. 251–263. doi: 10.1016/j.cemconres.2018.10.015.

GI (2016) 'ICAR Rheometer Manual', *German Instruments. Test Smart - Build Right*.

Gjørv, O. E. (2011) 'Durability of concrete structures', *Arabian Journal for Science and Engineering*, 36(2), pp. 151–172. doi: 10.1007/s13369-010-0033-5.

Gouws, A. S. M., Alexander, M. G. and Maritz, G. (2001) 'Use of Durability Index Tests for the Assessment and Control of Concrete Quality on Site', *Concrete Beton*, 98(April), pp. 5–16.

Hansson, C. M., Poursaee, A. and Jaffer, S. J. (2012) 'Corrosion of Reinforcing Steel Bars in Concrete', *The Masterbuilder*, pp. 110–120. doi: 10.3323/jcorr1954.18.3_110.

Hasanain, G. S., Khallaf, T. A. and Mahmood, K. (1989) 'Water Evaporation From Freshly Placed Concrete', *CEMENT and CONCRETE RESEARCH.*, 19, pp. 465–475.

Helmuth, R. A. and Detwiler, R. J. (2006) '2. The Nature of Concrete', *Significance of tests and properties of concrete and concrete-making materials, STP 169B*, (1), pp. 5–15.

Kayondo, M., Combrinck, R. and Boshoff, W. (2019) 'State-of-the-Art Review on Plastic Cracking of Concrete Article type', *Construction and building materials*. doi: 10.1099/00207713-50-2-901.

Kolawole, J. T., Combrinck, R. and Boshoff, W. P. (2019) 'Measuring the thixotropy of conventional concrete: The influence of viscosity modifying agent, superplasticiser and water', *Construction and Building Materials*. Elsevier Ltd, 225, pp. 853–867. doi: 10.1016/j.conbuildmat.2019.07.240.

Kwak, H. *et al.* (2010) 'Experimental and Numerical Quantification of Plastic Settlement in Fresh Cementitious Systems', *JOURNAL OF MATERIALS IN CIVIL ENGINEERING © ASCE*, (October), pp. 951–966.

Leemann, A. and Winnefeld, F. (2007) 'The effect of viscosity modifying agents on mortar and concrete', *Cement and Concrete Composites*, 29(5), pp. 341–349. doi: 10.1016/j.cemconcomp.2007.01.004.

Mackechnie, J. R. and Alexander, M. G. (2002) 'Durability Predictions Using Early-Age Durability Index Testing', (1993), pp. 1–9.

Marques, P. F. and Costa, A. (2010) 'Service life of RC structures : Carbonation induced corrosion . Prescriptive vs . performance-based methodologies', *Construction and Building Materials*. Elsevier Ltd, 24(3), pp. 258–265. doi: 10.1016/j.conbuildmat.2009.08.039.

Mehta, P. and Monteiro, P. (2006) *Concrete: Microstructure, Properties, and Materials*. 3rd edn. New York, USA: McGraw-Hill.

Narayanan, S. (2013) 'Introduction to reinforced concrete', *Design of RC Structures*, (November), pp. 1–44.

Nehdi, M. and Soliman, A. M. (2011) 'Early-age properties of concrete: overview of fundamental concepts and state-of-the-art research', *Proceedings of the Institution of Civil Engineers - Construction Materials*, 164(2), pp. 57–77. doi: 10.1680/coma.900040.

Otieno, M., Beushausen, H. and Alexander, M. (2011) 'Prediction of Corrosion Rate in RC Structures', *RILEM Bookseries*, 5(August 2014), pp. 15–37. doi: 10.1007/978-94-007-0677-4.

Permana, B. N. *et al.* (2017) 'Effect of re-vibration on the compressive strength and surface hardness of concrete Effect of re-vibration on the compressive strength and surface hardness of concrete'. doi: 10.1088/1757-899X/271/1/012057.

Piyasena, R. R. C. *et al.* (2013) 'Evaluation of Initial Setting Time of Fresh Concrete', (June), pp. 47–52.

Ravindrarajah, R. (2003) 'Bleeding of fresh concrete containing cement supplementary materials', *9th East Asia-Pacific Conference on …*, (December), pp. 16–18. Available at: http://services.eng.uts.edu.au/~ravir/bleeding of concrete containing scm.pdf.

Le Roux, B. D. (2016) *Influence of admixtures on the plastic shrinkage cracking of concrete*. Stellenbosch University.

Safiuddin, M. *et al.* (2018) 'Early-age cracking in concrete: Causes, consequences, remedialmeasures, and recommendations', *Applied Sciences (Switzerland)*, 8(10). doi: 10.3390/app8101730.

Sayahi, F. (2016) *Plastic Shrinkage Cracking in Concrete*. Luleå University of Technology.

Sayahi, F., Emborg, M. and Hedlund, H. (2017) 'Plastic Shrinkage Cracking in Concrete – Influence of Test Methods', *2nd International RILEM/COST Conference on Early Age Crackinh and Serviceability in Cement-based Materials and Structures - EAC2*.

Sayahi, F., Hedlund, H. and Emborg, M. (2016) 'Plastic Shrinkage Cracking in Concrete : State of the Art', (January).

Slowik, V., Schmidt, M. and Fritzsch, R. (2008) 'Capillary pressure in fresh cement-based materials and identification of the air entry value', *Cement & Concrete Composites*, 30, pp. 557–565. doi: 10.1016/j.cemconcomp.2008.03.002.

Suhr, S. and Schoner, W. (1990) 'Bleeding of Cement Pastes', *Properties of Fresh Concrete:*

Proceedings of the Colloquium organized on behalf of the Coordinating Committee for Concrete Technology of RILEM, (October), pp. 33–40.

Sukhnandan, J. (2019) *Influence of Plastic Settlement cracks on concrete durability*. Stellenbosch University.

UCT (2017) 'Durability Index Testing Procedure Manual', *University of Cape Town. Engineering and Built Environemnt*, Ver 4.2.

Uddin, F. and Shaikh, A. (2018) 'Effect of Cracking on Corrosion of Steel in Concrete', *International Journal of Concrete Structures and Materials*. Springer Netherlands. doi: 10.1186/s40069-018-0234-y.

Uno, P. J. (1998) 'Plastic shrinkage cracking and evaporation formulas', *ACI Materials Journal*, 95(4), pp. 365–375. doi: 10.14359/379.

Wittmann, F. H. (1976) 'Capillary Pressure in Fresh Concrete', 6, pp. 49–56.

Zemajtis, J. Z. (2019) 'Role of curing concrete', *Portland Cement Association*, 1.